Optimization of Operating Conditions of a Mixed Liquor Fermenter for Enhanced Biological Phosphorus Removal

By

Chelsea Q Linvill

Submitted to the graduate degree program in Civil, Environmental and Architectural Engineering and the Graduate Faculty of the University of Kansas in partial fulfillment of the requirements for the degree of Master of Science.

_____

Chairperson: Belinda S.M. Sturm

_____

Committee Member: Stephen J. Randtke

_____

Committee Member: Justin Hutchison

Date Defended: 7 May 2020

The Thesis Committee for **Chelsea Q Linvill**

certifies that this is the approved version of the following thesis:

Optimization of Operating Conditions of a Mixed Liquor Fermenter for Enhanced Biological Phosphorus Removal

_____

Chairperson: Belinda S.M. Sturm

Date Approved: 7 May 2020

Abstract

Enhanced biological phosphorus removal (EBPR) has been used for the past 40 years in municipal wastewater treatment to meet declining effluent total phosphorus (TP) limits. While primary fermentation is not new to EBPR, the use of a sidestream fermentation in the Bardenpho configuration of a wastewater treatment plant (WWTP) is a relatively new design that has proven difficult to model (Barnard et al. 2017, Houweling et al. 2010). Sidestream fermentation involves diverting a portion of the return activated sludge (RAS) or anaerobic mixed liquor to a sidestream bioreactor, which allows activated sludge time to settle and collect, allowing volatile fatty acids (VFA) production to take place (Houweling et al. 2010). This configuration is favored over primary fermentation because it helps overcome shortcomings of primary fermentation to allow for consistently high TP removal despite low or fluctuating VFA:TP ratio of the plant's influent (Barnard et al. 2017). Polyphosphate accumulating organisms (PAOs) and denitrifying polyphosphate accumulating organisms (dPAOs) are responsible for the removal of phosphate from wastewater in the EBPR process. The sidestream fermenter with its increased VFA:TP ratio should select for dPAOs, which are preferred over PAOs because of their ability to remove P and nitrogen from wastewater simultaneously. An enriched dPAO population has the potential to reduce operational costs of plants because of the savings on oxygen and carbon sources as compared to EBPR plants with only a PAO community.

The objective of this study was the optimization of a full-scale sidestream fermenter EBPR WWTP to select for dPAOs. The WWTP is a 2.5 annual MGD three-stage Bardenpho plant with a mixed liquor suspended solids (MLSS) sidestream fermenter. The WWTP operates without effluent filtration or the addition of carbon or ferric chloride to assist with biological nutrient removal (Kobylinski et al. 2019). Based on preliminary correlations of operating data, it

is hypothesized there are four contributing factors to the optimization of an EBPR WWTP with sidestream fermentation: 1) the readily biodegradable chemical oxygen demand (rbCOD):TP ratio, 2) oxidation-reduction potential (ORP), 3) volatile fatty acids (VFA) concentration, and 4) the solids retention time (SRT) of the fermenter. Of these four parameters, only SRT can be easily affected by WWTP operators. Over the 15 weeks of this experiment, the SRT of the WWTP was stepwise increased every three weeks to test SRTs from ~1.1 days to ~2.4 days. The SRT of the fermenter was held at approximately 1.1 days, 1.3 days, 1.5 days, 2.0 days, and 2.4 days for three weeks each to reach stabilization and conduct batch sludge activity tests for specific oxygen uptake rate (SOUR), max nitrification rate, dPAO activity, and sludge volume index (SVI). Operational data was collected for the duration of the experiment from both inline probes and daily and weekly lab tests. Finally, microbial analysis (flourescent in situ hybridization (FISH), qPCR, and Neisser staining) was conducted on grab samples collected throughout the 15-week experiment to investigate community shifts in PAOs and GAOs.

All three types of data collected in this experiment showed a positive correlation with increased SRT. The operational data showed a statistically significant correlation between the formation of VFAs and the fermenter SRT between 1.1 and 2.4 days. The activity data was the least correlated with the change in fermenter SRT. The microbial data from fluorescent in situ hybridization (FISH) and quantitative polymerase chain reaction (qPCR) showed very promising results with a strong correlation to the increase in PAOs in the WWTP and the increasing SRT of the fermenter. Based on the results of this study, a sidestream fermenter should be operated around an SRT of 2.0 days to optimize VFA creation to select for PAOs that complete EBPR. These results are at the higher end of previous work by Barnard et al. in 2017, which put the ideal SRT between 1.5 and 2 days (Barnard et al. 2017). This study confirmed that a WWTP

with low influent rbCOD:TP ratio could still reach low P effluent levels through EBPR without the added expense of supplemental carbon by adjusting the SRT of the sidestream fermenter to create the VFAs necessary to select for organisms that remove phosphorous from wastewater (WW).

Acknowledgements

To my advisor, Dr. Belinda Sturm, for teaching me not only about the world of wastewater research but also for mentoring me and showing me how to be a successful researcher, teacher, and advisor all while being a mom.

To Dr. Justin Hutchison and Dr. Stephen J. Randtke, for sitting on my committee and providing guidance on my research.

To Yasawantha Hiripitiyage (Dev), for helping me with method development, teaching me lab technique, and being a sounding board for me these past two years.

To my husband, Josh Linvill, for completely embracing my passion for this topic with constant questions and eagerness to attend field trips to WWTPs, for supporting me in applying for this Army scholarship, and being a source of constant encouragement while pursuing this degree, I love you.

To the members of the Sturm Lab group, thank you for all of your support, thoughtful insights, and companionship over the past two years.

To my parents, for valuing education above all else and teaching me from a young age how important a love of learning is.

Contents:

List of Figures:

List of Tables:

1.0 Introduction

Phosphorus is a non-renewable resource essential for farming to feed the growing world population. Current agriculture practices use mineral fertilizers containing phosphorus to sustain crop yields from season to season (Cordell et al. 2009, Egle et al. 2016). Phosphorus used in agriculture is mined from rock phosphate. During the mid-20th century, the use of mineral fertilizers helped to increase agricultural output across the world, including developing nations. Now countries can support their growing populations and decrease the number of under and malnourished people. The success of mineral phosphorus fertilizers caused a dependence of the world population on phosphate (Cordell et al. 2009). The problem with this method is existing reserves are estimated to be depleted in the next 50 to 100 years (Cordell et al. 2009, Yuan et al. 2012). These estimates jeopardize the future of agriculture and the ability to feed the increasing world population.

The overuse of phosphorous as a mineral fertilizer has not been without drawbacks, besides its non-renewability. After land application in agriculture, runoff of phosphorus ends up in lakes and rivers, which, even at minor concentrations, can have devastating consequences to the aquatic body. Phosphorous causes eutrophication, promotes algal growth, and causes conditions that lead to hypoxia (Cordell et al. 2009, Melia et al. 2017, Zhang et al. 2009). Because of these threats to ecology from phosphorus in water, many countries limit the amount of phosphorus in wastewater effluent to below 1 to 2 mg L^{-1} (Melia et al. 2017).

Municipal wastewater, influenced by surrounding agricultural areas, is a possible source of phosphorus recovery to replace the rapidly declining phosphate rocks (Cordell et al. 2009, Egle et al. 2016). Estimates show 15-50% of the world's agriculture needs for phosphate rock could be fulfilled through recovery from municipal wastewater treatment plants (Cordell et al.

2009, Yuan et al. 2012). Recovering phosphorus from wastewater benefits many interested and invested parties. First, it helps municipalities achieve effluent P limits set by lawmakers. Secondly, it lowers the chance of eutrophication in receiving water bodies, benefiting the surrounding ecology. Finally, it is a potential source of revenue for wastewater treatment when fertilizer products are generated (Melia et al. 2017). For these reasons, countries in Europe, including Austria, Germany, and Switzerland, have made it mandatory to recover phosphorous from municipal sewage sludge (Melia et al. 2017). Enhanced biological phosphorus removal (EBPR) is used to capture phosphorus that would otherwise be lost from municipal wastewater treatment. EBPR relies on polyphosphate accumulating organisms (PAOs) and denitrifying polyphosphate accumulating organisms (dPAOs) to recover the phosphorus from the water in municipal WWTP (Yuan et al. 2012). WWTPs, with enriched populations of PAOs and dPAOs, can have biosolids with up to 15 or 20% of phosphorus as dry cell weight (Yuan et al. 2012). Optimizing the selection of dPAOs within a WWTP helps to improve the resiliency of phosphorus removal because dPAOs can utilize a wider range of carbon sources under anaerobic conditions compared to PAOs adding stability to the nutrient removal process (Nguyen et al. 2011, Barnard et al. 2017). This will help the plant meet effluent limits and potentially provide a source of revenue for the recovered phosphorus to be reused in mineral fertilizer. A literature review shows operating conditions that can be optimized to select for dPAOs.

2.0 Literature Review

2.1 Introduction to Enhanced Biological Phosphorus Removal

EBPR has been a focus of wastewater treatment for the last four decades. Wastewater P removal without the addition of chemicals through the activated sludge process was first observed and documented in the 1970s (Barnard 1976, Levin 1971). A debate sprang out of the scientific community to explain the reasons for the P removal. The first explanation was a chemical reaction, and the second one was a "luxury uptake model" (Levin 1971). This model states bacteria metabolize the P in the wastewater and use it for cell synthesis (Barnard 1976). In his paper, Barnard et al. 1976 demonstrated how the luxury uptake model became the prevailing theory for phosphate removal by studying wastewater treatment plants,all with the inclusion of an anaerobic zone before the aerobic zone that added lime to treatment to keep the pH above 8.5 in aerated streams. When these treatment trains switched back to only biological treatment without chemical addition, phosphate removal increased to 97% or higher (Barnard 1976). A further discussion of PAOs to include their metabolism, kinetics, physical characteristics, and genetics appears in section 2.2 of this paper.

2.1.1 WWTP Configurations for EBPR

There are a few configurations that all EBPR WWTP are designed to accomplish maximum P removal. This study focuses mainly on the Bardenpho configurations, but others are mentioned at the end of this section. The Bardenpho method of EBPR is the process for denitrification and phosphate removal without the addition of chemicals. It was first employed by Dr. James Barnard in 1975 when he saw a 97% removal rate of P from a wastewater treatment plant (Barnard 1976). This configuration has become the basis for design for many wastewater treatment plants to achieve nutrient removal without the use of additional chemicals.

This design starts with an anoxic basin fed with influent wastewater, mixed liquor recycle from the aerobic basin in a four-to-one ratio with the influent, and sludge return from the final clarifier. The next three basins are fed sequentially from the first anoxic basin, and they are the aerobic basin followed by a second anoxic basin and finally a second aerobic basin. The clarifier is the last step in the treatment train, which consistently sees more than 90% removal of nitrogen and P from the plant's influent (Barnard 1976). Now there are multiple iterations of the Bardenpho configuration to include three, four, and five-stage processes. The number of stages corresponds to the number of zones in the plant configuration. A three-stage process goes from anaerobicanaerobic-anoxic-aerobic (Winter 1989). A four-stage Bardenpho configuration has anoxic-aerobic-anoxic-aerobic zones (Barnard et al. 2017). Finally, a five-stage Bardenpho configuration moves WW through the anaerobic-anoxic-aerobic-anoxic-aerobic basins in series with an internal recycle (Schuler and Xiao 2008). The other configuration for EBPR considered a "classical" process is an anaerobic-anoxic-aerobic (A2O) set up and, like the Bardenpho configuration, A2O is also based on pre-denitrification where the anoxic basin is before the aerobic basin (Oehmen et al. 2007) (Wang et al. 2019). These configurations are set up to accompish both nitrification and denitrification as well as P removal and are also referred to as Phoredox and AO (Barnard et al. 2017).

2.1.2 RAS

EBPR is dependent on the conditions of the influent wastewater to supply readily biodegradable COD (rbCOD) or volatile fatty acids (VFAs) for uptake by the organisms responsible for the removal of phosphate (Kobylinski et al. 2008). The operators cannot control the conditions of the influent wastewater to a municipal treatment plant. The concentrations of nutrients in the influent change daily based on weather (temperature and rainfall) and the

population of the service area. When the ratio of rbCOD:TP falls below a favorable level, 15:1, wastewater treatment plants risk losing EBPR (Barnard et al. 2017). To control the rbCOD:TP or VFA:TP ratios, facility operators can manipulate the RAS volume, add a fermentation unit, or purchase supplemental carbon. RAS takes a portion of the sludge from the clarifier, the final step of biological treatment, and brings it back to the first anaerobic zone (Vollertsen et al. 2006). The RAS undergoes hydrolysis under anaerobic conditions to increase the VFAs and rbCOD in the anaerobic region of EBPR (Andreasen et al. 1997). Hydrolysis breaks down the particulate matter from the clarifier into smaller molecules to include VFAs through the incorporation of water molecules (Houweling et al. 2010). To optimize this process, six percent of the sludge from the clarifier should go through the RAS process with a sludge retention time (SRT) of 1.6 days (Houweling et al. 2010, Vale et al. 2008). There is another option for increasing the rbCOD:TP or VFA:TP ratio in an EBPR WWTP, primary fermentation. In this process, primary sludge is hydrolyzed to readily biodegradable substrates (Moser-Engeler et al. 1998). However, primary fermentation is not always feasible, depending on the configuration of the WWTP (Wang et al. 2019).

2.1.3 Side Stream Fermentation

An option for wastewater treatment plants to improve the rbCOD:TP or VFA:TP ratio necessary for EBPR is fermentation. Sidestream fermentation differs from a mainstream EBPR design because the activated sludge has time to settle and accumulate. The settling and accumulation facilitate the decay, hydrolysis, and fermentation process of the activated sludge to increase the rbCOD and VFAs in the wastewater (Houweling et al. 2010). Dr. James Barnard discovered this phenomenon in the 1970s when he found a "dead zone" in his 100 m^3/day pilot plant. The "dead zone" came to be known as an unmixed inline fermenter, which was taking

<7% of the influent mixed liquor and fermenting it. This fermented sludge then increased the amount of VFAs in the second anoxic zone causing the release and uptake of P in the subsequent anoxic and aeration zones (Barnard et al. 2012, Barnard 1976).

2.2 Introduction to PAOs

Polyphosphate accumulating organisms (PAOs) are responsible for the removal of phosphate from wastewater in the EBPR process. Forty years ago, Dr. James Barnard discovered EBPR, and as recently as 30 years ago, scientists began to explain the biochemical model for how PAOs remove phosphate from wastewater (Comeau et al. 1986). Because culturable methods of studying bacteria have proved futile in developing an understanding of PAOs, discovering the metabolism, kinetics, and physical characteristics of these organisms and the role they play in EBPR has only recently been possible through the use of molecular-based methods (Flowers et al. 2013).

2.2.1 Genetics

The majority of EBPR has been credited to the bacteria *Candidatus Accumulibacter phosphatis* (*Ca. Accumulibacter)*, within the class Betaproteobacteria, because of its high abundance in municipal wastewater treatment plants and lab-scale studies conducted on EBPR (Flowers et al. 2013, Slater et al. 2010). Using the polyphosphate kinase (*ppk*1) gene as a phylogenetic marker, *Ca. Accumulibacter* lineage has been divided into two Types, I and II. Each of these Types has been broken down further into clades with Type I having five clades (IA-IE) and Type II having seven clades (IIA-IIG) (Flowers et al. 2013, Peterson et al. 2008). A two-year study of two different EBPR treatment trains revealed that while *Ca. Accumulibacter* populations remained relatively stable within a treatment train, they were susceptible to seasonal temperature changes and significant rain events (Flowers et al. 2013). These two problems result

in the most change and diversity to an *Ca. Accumulibacter* community within a wastewater treatment plant (Flowers et al. 2013).

2.2.2 Metabolism and Stoichiometry

Scientists have studied the metabolic process of PAOs since the 1980s. PAOs metabolize phosphate from wastewater in two steps, an anaerobic feast phase and an aerobic famine phase. During the first phase, the anaerobic feast phase, the PAOs take up VFAs and transform them into poly-b-hydroxyalkanoate (PHA), releasing orthophosphate (Comeau et al. 1986, Mino et al. 1987, Mino et al. 1998, Slater et al. 2010). The energy source for the conversion of VFAs to PHAs within PAOs is the hydrolysis of intercellularly stored poly-P (Acevedo et al. 2012, Comeau et al. 1986, Pereira et al. 1996, Wentzel et al. 1986). There have been two proposed models for respiration in the anaerobic phase, TCA and glycolytic. The TCA model was first proposed by Comeau et al. and Wentzel et al. in 1986 (Comeau et al. 1986, Wentzel et al. 1986). Mino et al. hypothesized a glycolytic pathway in 1987, stating that both glycogen and poly-P could be used as an energy source for PAOs during anaerobic respiration (Mino et al. 1987). Then in 1996, Pereira et al. published a metabolic pathway for PAOs, which uses a combination of both TCA and glycolytic pathways; this pathway was echoed in 2000 by Hesselmann et al. (Hesselmann et al. 2000, Pereira et al. 1996). In the aerobic famine phase, all the readily biodegradable carbon sources are no longer available to the PAOs. As a consequence, they must use the stored PHA as an energy source (Slater et al. 2010). The PAOs must use the oxygen present to take in the previously released orthophosphate to replace their poly-P storage levels (Acevedo et al. 2012). For this process of phosphate release and uptake by *Ca. Accumulibacter* to be considered biologically favorable, a COD to phosphate (COD:P) mass ratio of 15:1 is required (Acevedo et al. 2012, Barnard et al. 2017, Slater et al. 2010).

2.2.3 P Release/C Uptake Ratio

One indicator of PAO presence is the ratio of phosphorus release to carbon uptake (P release/C uptake) during the anaerobic or feast phase of metabolism. The carbon uptake is measured as the amount of acetate taken up by PAOs and dPAOs in mg acetate. Starting in the 1980's, the ratio of P release/C uptake has been studied to determine the metabolic pathways responsible for PAOs to uptake acetate under anaerobic conditions and store it as poly-β-hydroxybutyrate (PHB) within the cell, and later release phosphate molecules into solution (Comeau et al. 1986). Wentzel et al. 1986, Mino et al. 1987, and Comeau et al. 1987 published P release/C uptake results of 0.24, 0.39, and 0.70-0.75, respectively, which were obtained by dosing known concentrations of acetate as the substrate for bacteria to use in conditions without an external terminal electron acceptor available. All authors concluded the mass of P released appeared to be proportional to the mass of carbon taken up (Comeau et al. 1987, Mino et al. 1987, Wentzel et al. 1986). Since PAOs are known to use both poly-P and stored glycogen during anaerobic respiration, the P release/C uptake ratio has been used as an indicator of the dominant metabolic process PAOs utilize during the anaerobic phase of EBPR (Mino et al. 1998). When P release/C uptake ratios for PAOs are between 0.5 and 0.7, this indicates that there is a low amount of poly-P available, and the glycolytic pathway is needed to make up for the lack of ATP formed from poly-P hydrolysis (Acevedo et al. 2012, Welles et al. 2015, Zhou et al. 2008). By contrast, under conditions where poly-P is not limiting, the PAOs are believed to use the tricarboxylic acid cycle (TCA) cycle as the dominant metabolic process and as a result have a much higher P release/ C uptake ratio of greater than 0.7 (Acevedo et al. 2012, Welles et al. 2015). The ratio of P release/ C uptake is pH dependent and ratios should be considered at a near neutral pH (Comeau et al. 1986). A lower energy is required to uptake acetate at lower pH

(Smolders et al. 1994). This has secondary effects in the next phase of metabolism, aerobic/anoxic phase, where less energy is spent to uptake P at low pH.

The ratio of P release/C uptake has also been correlated throughout literature with a population shift of bacterial communities in EBPR WWTP. By the end of the 1980's, the previously published P release/C uptake ratios were being used to prove the presence of PAOs within a population. Wentzel et. al. (1988) found a P release/C uptake ratio between 0.52 - 0.57 to indicate an enhanced culture of PAOs selected by the addition of acetate to the anaerobic phase of an anaerobic/aerobic SBR (Wentzel et al. 1988). A lower ratio, less than 0.5, indicates the presence of glycogen accumulating organisms (GAOs) as well as PAOs in the sludge (Gu et al. 2008, Schuler and Jenkins 2003). A ratio less than 0.02 indicates a GAO-enriched sludge population (Acevedo et al. 2012). This is because GAOs are competing for acetate uptake and increasing this half of the ratio without contributing to the other half of the ratio, P release (Acevedo et al. 2012, Gu et al. 2008). The ratio of P release/C uptake is, therefore, an indicator of the relative PAO to GAO activity within an EBPR WWTP (Acevedo et al. 2012, Schuler and Jenkins 2003).

2.2.4 Kinetics

Important kinetics for the use of PAOs in EBPR are their rates of orthophosphate released during the anaerobic feast phase and phosphate uptake during the aerobic famine phase. These rates have been studied in PAO activity tests, which have been most commonly adopted from the method developed by Wachtmeister et al. in 1997. In their paper, Wachtmeister et al. described procedures for phosphorus release and uptake batch tests using 1L benchtop reactors and acetate as the VFA substrate fed in the anaerobic. (Wachtmeister et al. 1997). In a 2010 study of a membrane bioreactor pilot plant, Monclús et al. found the P release rate of the sludge increased

from 2.39 to 5.01 mg P g^{-1} VSS h^{-1}, and the P uptake rate increased from 3.62 to 13.60 mg P g^{-1} VSS h^{-1} within the first 150 days of plant operation (Monclús et al. 2010). These P uptake rates were higher than previously published by Romanski et al. in 1997, who stated an uptake rate of 2.4 mg P g^{-1} vss h^{-1} (Romanski et al. 1997). The highest researched P uptake rate was published in 2009 by Zhang et al. at 17.3 mg P g^{-1} VSS h^{-1} for an experiment carried out on pilot membrane bioreactors (Zhang et al. 2009). In the 2006 study of the activity of PAOs obtained from sidestream EBPR with anaerobic return activated sludge under different substrate concentrations, Vollertsen et al. saw a P release rate of 0.2 g P $kgVSS^{-1}h^{-1}$ using acetate as the substrate (Vollertsen et al. 2006). Before the Wachtmeister et al. batch tests, Kuba et al. found PAOs in a benchtop anaerobic-aerobic reactor to have a P release rate of 0.03-0.05 g P VSS^{-1} h^{-1} and a P uptake rate of 0.02-0.03 g $PVSS^{-1}$ h^{-1} (Kuba et al. 1993).

2.2.5 Physical characteristics

Environmental engineers must also consider the physical characteristics of the bacterial community they are designing for to optimize the role of PAOs in EBPR and increase their efficiency. During the 282 day operation of a granular sludge reactor, Winkler et al. found that PAOs, which dominated the bottom of the settled sludge bed, had a higher density, ash content, and surface area causing a higher settling velocity than other competing bacteria in the reactor (Winkler et al. 2011). This plug flow reactor, fed from the bottom, gave the PAOs at the bottom of the sludge bed the most available substrate when compared to granules at the top of the reactor during the anaerobic feast phase of PAO metabolism. The aerobic famine phase was the phase before settling, meaning the PAO granules had taken in large amounts of poly-P, making these granules denser than others within the reactor, which cannot remove phosphorus. This increase in poly-P within PAO granules made them sink faster to the bottom of the sludge bed

before the next anaerobic feeding phase (Winkler et al. 2011). Knowing PAOs can become denser and settle more quickly when the aerobic period follows the anaerobic period can influence future configurations of EBPR reactors such as the Bardenpho configurations.

2.3 Introduction to dPAO

After the discovery of EBPR in the 1970s, scientists continued to research the use of oxygen as an electron acceptor in the famine phase of EBPR to trigger phosphate uptake. However, in the 1990s new terminal electron acceptors were starting to be explored. One of the first to investigate this possibility was Kuba et al., who successfully ran an anaerobic-anoxic sequencing batch reactor to remove phosphorus using nitrate as an electron acceptor (Kuba et al. 1993). Denitrifying polyphosphate accumulating organisms (dPAOs) can use nitrite or nitrate as a terminal electron acceptor to remove P and nitrogen from wastewater simultaneously. EBPR plants with an enriched population of dPAOs have advantages over plants with only PAOs because operating costs of the plant have the potential to be severely reduced without the need to supply excess oxygen (Kishida et al. 2006, Oehmen et al. 2007).

2.3.1 Genetics

As was the case with PAOs, scientists have yet to obtain a pure culture of dPAOs in the lab. Previous studies using fluorescence in situ hybridization (FISH) discovered *Ca. Accumulibacter* is the dominant PAO bacteria responsible for P removal in most EBPR systems (Carvalho et al. 2007). However, the gram-positive *Tetrasphaera* is another bacterial genus with a large abundance in EBPR systems, which can denitrify and accumulate polyphosphate (Kristiansen et al. 2012, Marques et al. 2017, Nguyen et al. 2011). Using FISH analysis on five EBPR plants in 2011, Nguyen et al. found the genus *Tetrasphaera* subdivided into three clades (Nguyen et al. 2011). Both the 2012 study by Kristiansen et al. and the 2017 study by Marques et

al. enriched *Tetrasphaera* from EBPR sludge to study its metabolic pathways and showed how *Ca. Accumulibacter* and *Tetrasphaera* each occupy a slightly different metabolic niche based on the carbon source. Enriching both genera in a system may improve the resiliency of an EBPR system (Kristiansen et al. 2012, Marques et al. 2017). *Tetrasphaera* has the ability to take up glucose and ferment it as well as synthesize glycogen as a storage polymer (Kristiansen et al. 2012). *Tetrasphaera* can also consume amino acids, while *Ca. Accumulibacter* needs fermentation products to survive (Marques et al. 2017).

Besides FISH, qPCR has been used as a genetic analysis tool in wastewater to study dPAO populations. In 2007, He et al. first looked at *Ca. Accumulibacter* populations in EBPR sludges. They designed primer sets to exclusively target the ppk1 gene of each *Ca. Accumulibacter* clade, and these have since been used in numerous studies to understand populations in EBPR wastewaters (He et al. 2007). The ppk1 gene is a single-copy gene specific to *Ca. Accumulibacter* (He et al. 2007). These primers were used in 2013 by Flowers et al. to measure the variation of five phylogenetically-defined clades within the *Ca. Accumulibacter* lineage (Flowers et al. 2013). In 2016, Camejo et al. reevaluated the He et al. primers with newer sequencing data and published a new set of *Ca. Accumulibacter*-ppk1 primers (Camejo et al. 2016). As of this study, there have not been specific dPAO primers published for qPCR.

2.3.2 Metabolism and Stoichiometry

Scientists have tried to understand the metabolic pathway capable of performing nitrogen and P nutrient removal from wastewater since the 1970s. As mentioned above, *Ca. Accumulibacter* and *Tetrasphaera* each occupy a slightly different metabolic niche. *Tetrasphaera* can utilize glucose as well as other carbon sources, while *Ca. Accumulibacter* cannot use glucose (Kristiansen et al. 2012, Marques et al. 2017, Nguyen et al. 2011). During the

first anaerobic phase of EBPR, carbon sources are taken up and stored as PHA through the release of phosphorus (Carvalho et al. 2007). In the second phase of EBPR, dPAOs can utilize nitrate or nitrite (NOx) as an electron acceptor instead of oxygen (Carvalho et al. 2007, Comeau et al. 1986). Therefore, these bacteria are capable of nitrate reduction, or denitrification, as well as P removal (Comeau et al. 1986). The stoichiometry of P release per mmol of the substrate in the anaerobic phase for dPAOs has been consistently low in literature, between 0.48 - 0.30 mmol P/mmol C substrate (Marques et al. 2017, Oehmen et al. 2005). Kuba et al. reported the ratio of phosphate uptake to NO_3-N consumption by dPAOs in 1993 at 2.10 g P/g NO_3^- (Kuba et al. 1993). dPAOs have a 20 to 30% lower cell yield because they are 40% less efficient in generating energy as compared to PAOs, making them appealing for use in EBPR because of the lower COD demand and sludge production along with lower aeration costs (Monclús et al. 2010, Zeng et al. 2003a).

2.3.3 Kinetics

Scientists understand relatively little about dPAOs, and the literature lacks a standardized rate for phosphate uptake by dPAOs. However, there are consistent reports that P uptake under anoxic conditions is lower than P uptake under aerobic conditions (Monclús et al. 2010, Oehmen et al. 2007, Zeng et al. 2003a). The dPAO activity test for phosphate release and uptake rates is determined similarly as the PAO activity test, but the aerobic famine phase is replaced with an anoxic phase, injecting a known concentration of either nitrite or nitrate between 10 to 50 mg NO_3-NL^{-1} and 20 mg NO_2-NL^{-1} (Carvalho et al. 2007, Monclús et al. 2010, Zeng et al. 2003a).

Table 1 below has all researched kinetic rates of dPAO P uptake and release. In 1993, an early anaerobic-anoxic batch reactor study tested nitrate as an electron acceptor in the anoxic phase, and a P release rate of 0.02-0.03 g P VSS^{-1} $h^{-1}$and a P uptake rate of 0.02-0.03 g P VSS^{-1}

h^{-1} were reported (Kuba et al. 1993). In the 2001 study of an anaerobic-aerobic-anoxic-aerobic sequencing batch reactor by Lee et al., the rates of P uptake were recorded at 3.0 and 26.8 mg P g VSS^{-1} h^{-1} for the anoxic and aerobic phases, respectively (Lee et al. 2001). Zeng et al. ran a 2003 lab-scale sequencing batch reactor to determine if simultaneous denitrification and phosphorous removal were possible with alternating anaerobic and low DO aerobic conditions. Batch tests from this study identified a P release rate of 1.55 mmol P g^{-1} VSS h^{-1} and a P uptake rate of 0.56 mmol P g^{-1} VSS h^{-1} (Zeng et al. 2003a). During the 2006 anaerobic/oxic/anoxic granular sludge lab reactor operation by Kishida et al., the kinetic rate of P release was 0.72 mmol P g^{-1} VSS h^{-1} and uptake was 0.12 mmol P g^{-1} VSS h^{-1} (Kishida et al. 2006). These rates were much lower than previously published data, which studied activated sludge and not granules. Monclus et al. found a P uptake rate for dPAOs of 5.6 mg P g^{-1} VSS h^{-1} in the 2009 study of a membrane bioreactor pilot plant after 150 days of operation (Monclús et al. 2010). More recently in 2014, the year-long batch study by Jabari et al. of two integrated fixed-film activated sludge bench-scale reactors compared dPAO activity based on electron acceptors, nitrate (20 mg NO_3-N L^{-1}) and nitrite (40-60 mg NO_2-N L^{-1}). This study found a maximum specific P uptake rate of 13.9 mg P h^{-1} g^{-1} VSS at a dose of 20 mg NO_2-N L^{-1}, and a rate of 4.9 mg P h^{-1} g^{-1} VSS at a dose of 40-60 mg NO_2-N L^{-1} (Jabari et al. 2014). They also found a maximum specific P uptake rate of 3.3 mg P h^{-1} g^{-1} VSS at a dose of 40 mg NO_3-N L^{-1}, and a rate of 8.5 mg P h^{-1} g^{-1} VSS at a dose of 60 mg NO_3-N L^{-1} (Jabari et al. 2014). Zhang et al. published an anoxic P uptake rate of 14.9 mg g VSS^{-1} h^{-1} from batch tests conducted on sludge from their benchtop membrane bioreactors (Zhang et al. 2009).

Table 1: Researched Kinetic Rates of dPAO P Uptake and Release.

	P Anerobic Release Rate (mg P g^{-1} VSS h^{-1})	P Aerobic Uptake Rate (mg P g^{-1} VSS h^{-1})	P Anoxic (NO_3) Uptake Rate (mg P g^{-1} VSS h^{-1})	P Anoxic (NO_2) Uptake Rate (mg P g^{-1} VSS h^{-1})	Notes
Kuba et al. 1993	20	30	N/A	N/A	Batch reactor study with units per gram of SS, not VSS
Lee et al. 2001	N/A	26.8	3.0	N/A	Anaerobic-aerobic sequencing batch reactor
Lee et al. 2001	N/A	14.9	9.5	N/A	Anaerobic-aerobic-anoxic-aerobic sequencing batch reactor
Zeng et al. 2003	48	N/A	17.34	N/A	Lab-scale sequencing batch reactor
Kishida et al. 2006	22.29	N/A	3.72	N/A	Anaerobic/oxic/anoxic granular sludge lab reactor
Vollertsen et al. 2006	1.15	N/A	N/A	N/A	Activated sludge side stream EBPR with anaerobic return
Gu et al. 2008	5.6-31.9	2.4-9.7	N/A	N/A	Six full-scale EBPR WWTPs in the US
He et al. 2008	11.2-19.2	1.9-11.0	N/A	N/A	Five Different Fullscale EBPR WWTPs
Zhang et. al. 2009	N/A	17.3	14.9	N/A	Activated sludge from benchtop membrane bioreactors
Monclús et al. 2010	5.01	13.60	5.6	N/A	Membrane bioreactor plant day 150
Jabari et al. 2014	N/A	N/A	8.5	13.9	Batch study of two integrated fixed-film activated sludge bench-scale reactors

2.3.4 Competitors

Well-researched competitors of PAOs and dPAOs are glycogen-accumulating organisms (GAOs) and denitrifying GAOs (dGAOs). GAOs and dGAOs compete with PAOs and dPAOs for carbon substrate during the anaerobic feast phase of EBPR (Oehmen et al. 2007, Oehmen et al. 2005). GAOs are capable of anaerobic VFA uptake and compete with PAOs in these basins for rbCOD (Mino et al. 1998, Oehmen et al. 2007, Oehmen et al. 2005). The bacteria with a GAO phenotype are *Candidatus Competibacter phosphatis* (*Competibacter*) (Oehmen et al. 2005). GAOs are unwanted within an EBPR configuration because they do not contribute to P removal from the system. Undesirably, GAOs compete for limited amounts of substrate with those organisms that do remove P (Oehmen et al. 2007, Oehmen et al. 2005). In the 2003 study, Zeng et al. found dGAOs outcompeting dPAOs. This study used an aerobic-anoxic batch reactor test to determine the activity for dGOAs and dPAOs in the system. The relative activities of the bacteria were determined by measuring acetate and glycogen consumption. Their results from modeling showed dGAOs contributed a majority of the reduction of nitrate and nitrite in their lab-scale sequencing batch reactor, limiting the amount of P removal in the system. These results were obtained without using microbial analysis (Zeng et al. 2003a).

2.3.5 Criticism of dPAOs

The existence of a polyphosphate accumulating organism capable of using nitrate or nitrite as an electron acceptor in addition to oxygen (dPAO) is still a debated topic amongst the scientific community. In the 2007 review paper of EBPR, Oehmen et al. dedicated an entire section to explaining reasons why PAOs and dPAOs are different organisms. They cited recent studies that show the existence of sub-clades within the *Accumlibacter* group (He et al. 2007). This review also referenced two sequencing batch reactor (SBR) studies (Carvalho et al. 2006

and Kerrn-Jespersen and Henze 1993) that operated under anerobic-aerobic conditions, then transitioned and stabilized under anerobic-anoxic conditions, suggesting the presence of two different organisms (PAOs and dPAOs) responsible for P removal (Oehmen et al. 2007). Without the ability to obtain a pure culture of dPAO using current laboratory techniques, their existence is still debated among scientists. In the 2019 study, Rubio-Rincon et al. concluded that *Ca. Accumulibacter delftensis* could not use nitrate as an electron acceptor. The authors were unable to show a significant anoxic P-uptake on nitrate, and as a result, it was impossible for Rubio-Rincon et al. to classify *Ca. Accumulibacter delftensis* as a dPAO (Rubio-Rincón et al. 2019). Despite aforementioned criticisms, dPAO are expected to be a part of the bacterial community in EBPR WWTPs, because many studies have been able to capture activity rates for organisms responsible for P uptake under anoxic or aerobic conditions suggesting the presence of dPAOs (Carvalho et al. 2007, Kishida et al. 2006, Kuba et al. 1993, Monclús et al. 2010, Zeng et al. 2003a).

2.4 Conditions for dPAO growth in EBPR

There are many operating conditions for municipal wastewater treatment that must be monitored closely to maximize the efficiency of EBPR without the use of any additional chemicals (Barnard et al. 2017, Mulkerrins et al. 2004). Based on previously published literature, this section will focus on four of these operating conditions to improve the selection of dPAOs within an EBPR system at a municipal wastewater treatment plant. These conditions are rbCOD/TP ratio, ORP, SRT of the fermenter, and VFAs present in the wastewater.

2.4.1 rbCOD/TP ratio

The ratio of readily biodegradable chemical oxygen demand (rbCOD) to total phosphorus (TP) rbCOD/TP in mg rbCOD mg^{-1} TP in the influent is paramount to the success of EBPR

plants. Readily biodegradable COD is one of two subfractions of biodegradable COD in municipal wastewater, slowly biodegradable particulate and readily biodegradable soluble, which are classified based on their biological response rate of biodegradation (Ekama et al. 1986). Papers on EBPR discuss the importance of the rbCOD/TP ratio and a minimum value that must be achieved for P to be biologically removed. As published by both Barnard et al. and Kobylinski et al., an rbCOD/TP ratios of 15 or higher are considered the threshold for the success of the EBPR process (Barnard et al. 2017, Kobylinski et al. 2008).

When there is a lack of rbCOD in the form of VFAs during the anaerobic feast phase, PAOs and dPAOs cannot take up enough substrate to store PHA or release orthophosphate. Without the release of orthophosphate in the anaerobic phase, the subsequent aerobic or anoxic phase will not see the take-up of phosphate by PAOs or dPAOs because they will not need to reestablish their storage needs (Houweling et al. 2010). Since plant operators can do little to affect change in their influent ratio, operators must closely monitor and adjust operation of the fermenter and RAS to produce VFAs within the treatment configuration of a wastewater treatment plant to maintain EBPR (Houweling et al. 2010).

2.4.2. ORP

Oxidation-reduction potential (ORP) shows the states of oxidation and reduction in biological systems. To enrich the dPAO community within a biological nutrient removal (BNR) plant, the ORP of the anaerobic zone should be lower than 180 mV, and ideally between -200 mV and -300 mV (Barnard et al. 2017, Yu et al. 1997). These low ORPs favor *Tetrasphaera* over *Ca. Accumulibacter* because they have the ability to ferment higher carbon compounds (Barnard et al. 2017). The other benefit of using an ORP probe is the ability to receive real-time, cost-effective feedback from basins in the wastewater treatment train (Yu et al. 1997). The Lee

et al. study in 2001 used the readings from the ORP probe to help adjust the duration of each phase in a sequencing batch reactor (SRB) to adapt to the changing conditions of the influent wastewater (Lee et al. 2001). The ORP probe, when monitored by a trained and empowered operator, has the potential to be used as a tool to provide instantaneous feedback to help make adjustments to improve the success of EBPR in a BNR plant (Barnard et al. 2017).

2.4.3 SRT in the Fermenter

The SRT is the length of time for which the sludge stays in a system. The SRT can be calculated in each separate basin or for the complete treatment process by taking the mass of organisms in the system and dividing that by the mass of organisms removed from the system each day, giving an average time the microorganisms are in the system (Mulkerrins et al. 2004). This calculation is performed daily by plant operators to assess the age of the sludge. The SRT of the fermenter is an essential operating condition of EBPR because it controls the acid-production phase of anaerobic degradation, fermentation. In the 2010 review, Houweling et al. describe the importance of controlling the SRT, so only the first phase of anaerobic digestion occurs in the fermenter. The first phase of anaerobic digestion is fermentation, which occurs in pre-fermenters by two processes, hydrolysis and acidogenesis (Houweling et al. 2010). The second phase of anaerobic digestion produces harmful consequences for the EBPR process, the conversion of VFAs to methane. Since this process requires a longer SRT for acetogenesis and methanogenesis to occur, operators must closely monitor the SRT of the fermenter and keep a long enough SRT to produce VFAs but short enough to wash out methanogenesis organisms (Houweling et al. 2010). Longer anaerobic SRTs are also favorable to *Tetrasphaera* over *Accumlibacter,* because *Tetrasphaera* has the ability to ferment (Nguyen et al. 2011).

The SRT of a fermenter depends on many factors, including load, temperature, and the configuration of the EBPR plant. Scientific literature has published guidelines for fermenter SRT ranges. For his 2017 review, Barnard et al. found the ideal SRT for RAS fermentation to be between 30-40 hours as confirmed in two previous studies (Barnard et al. 2017, Vale et al. 2008, Vollertsen et al. 2006). Barnard et al. also published the ideal side stream mixed liquor fermenter (SSMLF) SRT should be between 1.5-2.0? days (Barnard et al. 2017).

2.4.4 VFAs

In an EBPR plant, the anaerobic zone serves to ferment rbCOD down to VFAs (Barnard et al. 2017, Ekama et al. 1986). Literature that describes the EBPR process supports the need for VFAs, specifically acetic and propionic acid as a substrate in the anaerobic zone to feed PAOs and dPAOs, which create PHA and release orthophosphate (Comeau et al. 1986, Houweling et al. 2010, Mino et al. 1998). Barnard et al. in 2017 showed how PAOs and dPAOs can survive deeper anaerobic conditions in the EBPR treatment train while other heterotrophs die in this zone and instead were fermented to VFAs to help PAOs and dPAOs thrive (Barnard et al. 2017).

As discussed previously, controlling the amount of VFAs in the anaerobic zone is done through fermentation in either side stream reactors, RAS fermenters, or inline fermenters (Barnard et al. 2017, Barnard et al. 2012, Houweling et al. 2010). These processes can be controlled by switching on mixers in the fermentation zone to replace and resuspend the sludge blanket and controlling the flow in and out of the fermenters (Barnard et al. 2012, Houweling et al. 2010). The fermenter SRT directly affects the abundance of VFAs in an EBPR plant.

3.0 Methods and Procedures

A graphical representation of the methods used in this study is presented in Figure 1 below, and methods are described in this section.

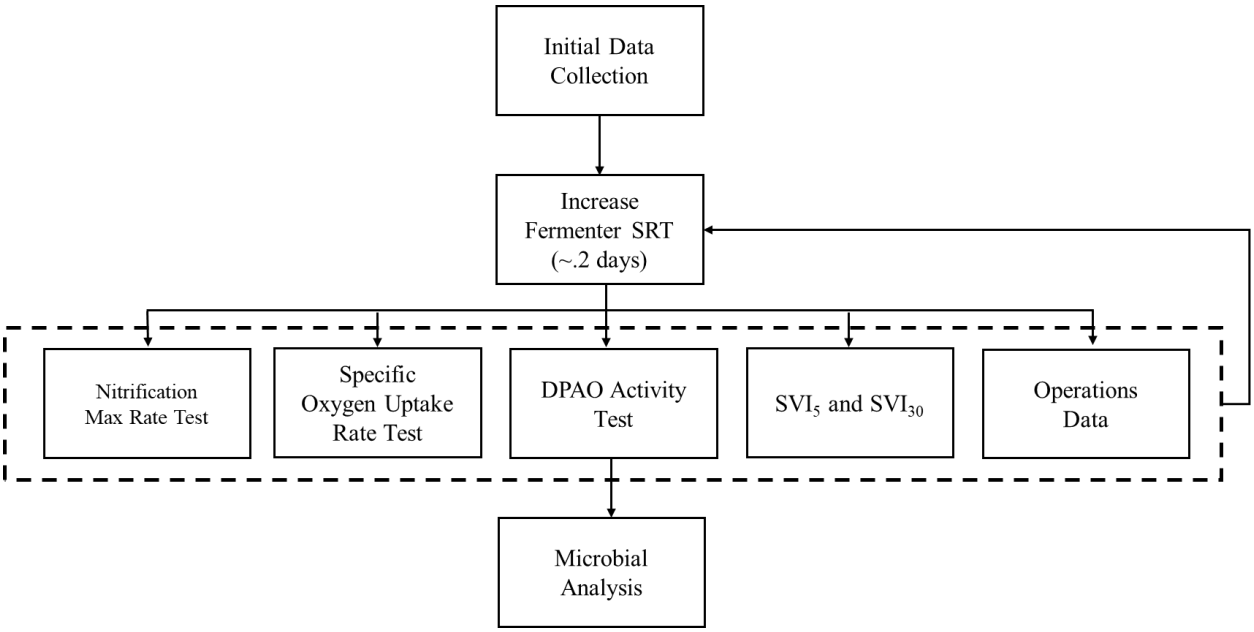

Figure 1: Methods Used in This Study

3.1 Wakarusa EBPR WWTP.

The EBPR WWTP used in this research is a modification of the Bardenpho configuration. The wastewater treatment plant is a three-stage Bardenpho system with an enhanced sidestream MLSS fermenter (S2EBPR), which was first proposed by Dr. James Barnard in 2017. Dr. Barnard served as a process engineer for the design of the full-scale Wakarusa Wastewater Treatment Plant participating in this study (Kobylinski et al. 2019). The purpose of the S2EBPR is to produce soluble carbon to increase the rbCOD/TP ratio, which averages 14.4 mg L^{-1} COD/mg L^{-1} TP in the raw influent. This ratio cannot reliably support BNR (Kobylinski et al. 2019).

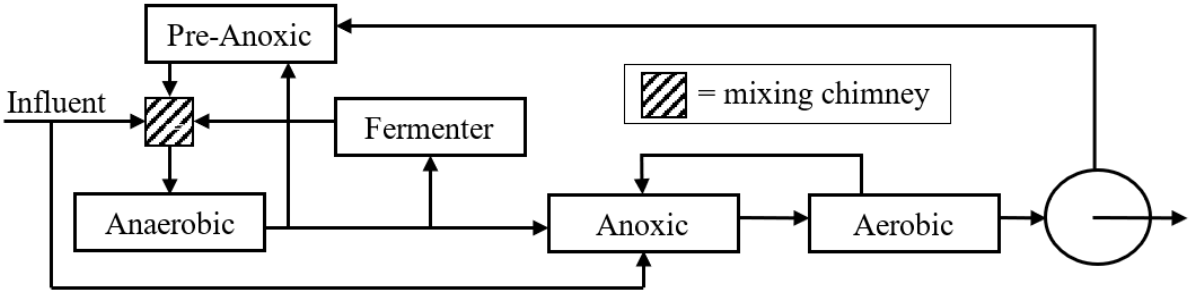

Figure 2: Wakarusa Treatment Plant Flow Diagram

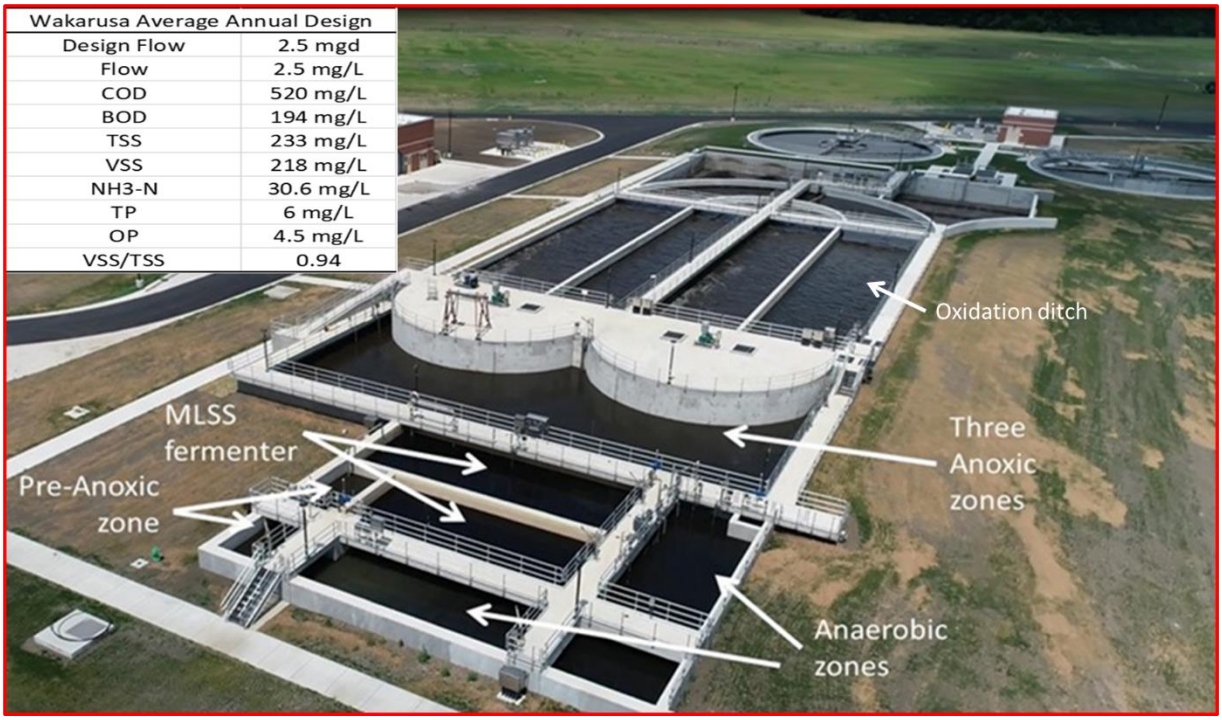

shows a schematic of the flow at the Wakarusa Wastewater Treatment plant. The S2EBPR configuration has the influent, fermenter MLSS, and RAS all flowing into a mixing chimney that empties into the anaerobic zone. From the anaerobic zone, flow moves into the anoxic cell, with a portion recycled either back to the fermenter or the pre-anoxic zone. A portion of the influent is also fed directly into the anoxic zone, to meet the carbon demand for denitrification. From the anoxic zone the flow moves into the oxidation ditch (Kobylinski et al. 2019). The composition of

the influent for the Wakarusa plant, which was used as the average annual design basis, is also shown in Figure 2.

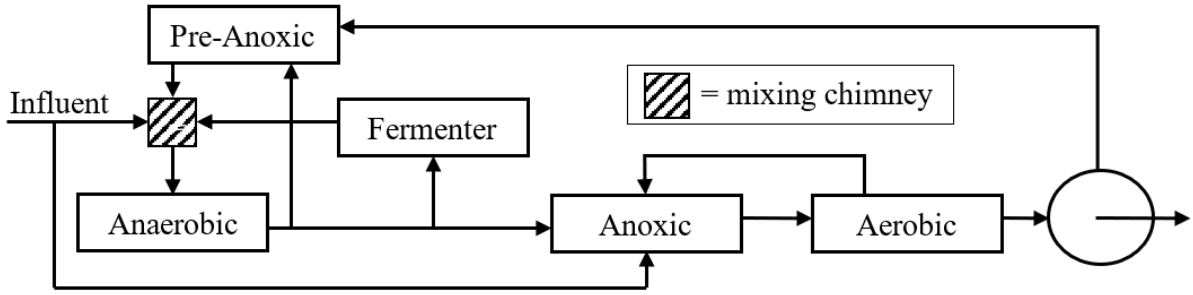

Figure 2: Wakarusa Treatment Plant Flow Diagram

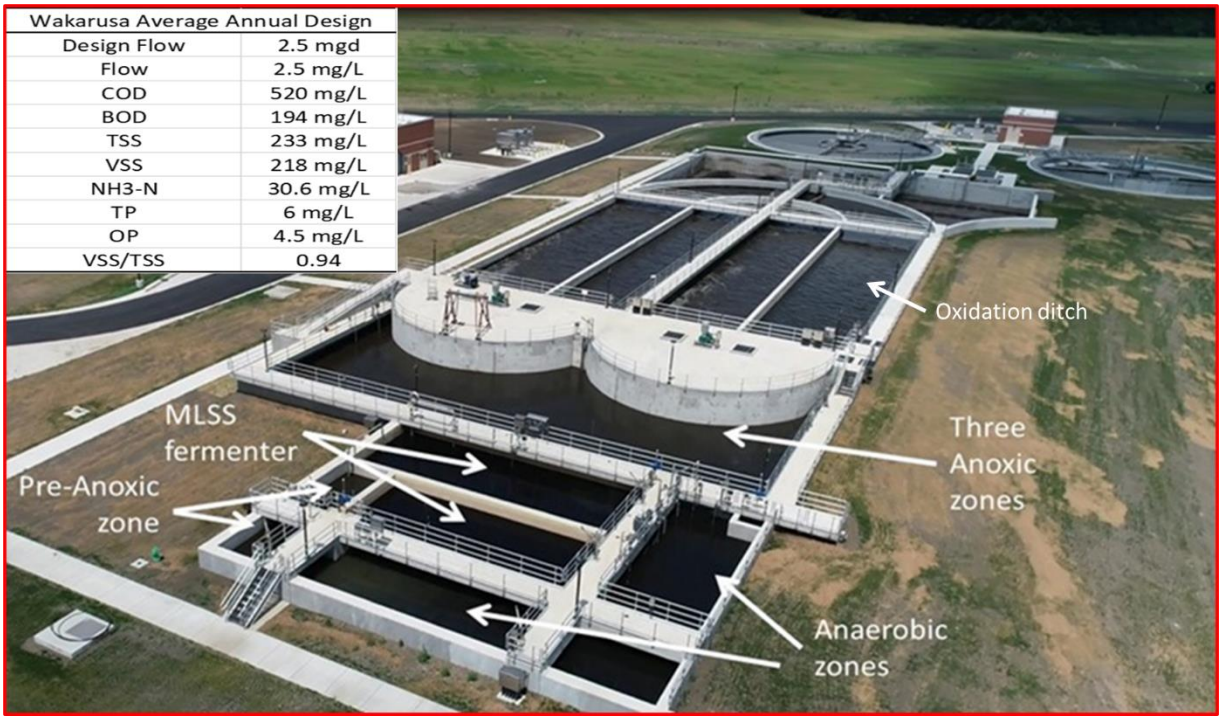

Figure 3:Wakarusa Wastewater Treatment Plant Flow Diagram and Aerial Photo Reproduced from (Kobylinski, E.A 2019)3.2 Initial Data Collection and Processing

The first step of this project was to collect all of the operational data recorded for the plant's first 477 days of operation. This data set included 38 different operational parameters and

25 nutrient parameters of the influent, effluent, and treatment basins. This data was collected using the probes installed along the treatment train and from daily operational analyses by the operators.

Data was transferred from the City of Lawrence in excel and imported into R, where data cleaning and calculations were performed. New data elements were calculated for parameter averages, the SRT of the fermenter, and total VFAs. The data collected by the probes (fermenter TSS, effluent temperature, Aerobic Zone 9 DO, Aerobic Zone 4 DO) was collected every hour, but for use in R, all data had to be given in daily averages, which were calculated in R for all 477 days of data collection. The SRT of the fermenter was derived from this data by adding an element for average TSS in the fermenter > 100 to account for "mixer on". The mass in the fermenter was calculated from this data. Mass wasted from the fermenter was calculated for a 24 hour period from the average TSS for the hours off plus the average TSS for the hours on, multiplied by the total volumetric flow during each mixer condition. A blank row was inserted for all days on the VFA tab which did not have data collected for a total of 173 missing days during the first 477 days of operation.

3.2.1 Correlation Matrix in R

To determine the parameters of the wastewater treatment plant that have a strong association, a correlation matrix was run in R using open source code provided by two packages corrplot and ggpubr (Kassambara 2019, R Core Team 2019, Wei 2017). This correlation matrix was run excluding blanks, meaning only days with a data entry for every parameter of the correlation matrix were used. Once blanks were removed for the correlation matrix, there were 168 useable days for the correlation matrix out of 477, or 35.2% of the data. For the nutrient comparison matrix, there were 229 days useable out of 477, or 48% of the data.

3.3 Stepwise Increase of Fermenter SRT

The correlation matrixes and a literature review of sidestream fermentation suggested that the fermenter's SRT was the highest correlated parameter that could easily be manipulated by wastewater treatment operators. Over 15 weeks, the SRT of the plant was increased from 1.1 days, where it had been averaging since the plant's inception, to 2.4 days. This increase was accomplished by adding approximately 0.2 days to the SSMLF's SRT every three weeks. This increase allowed the plant to operate in the Barnard et al. published ideal SSMLF SRT range between 1.5-2 days (Barnard et al. 2017).

The 15 weeks were subdivided into five three-week segments, each with a week-long adjustment period when the SRT of the SSMLF would be changed, followed by two weeks of testing. The five SRT phases were 1.1, 1.3, 1.5, 2.0, and 2.4 days. The mixer run time was decreased by 30 min for each of the two 12 hour cycles every other day during the adjustment week to change the SSMLF's SRT slowly enough not to shock the system and allow the bacterial community to adjust. Over the entire 15 weeks of the study, the mixer run time decreased from 1,320 min/day to 600 min/day.

The SRT of the SSMLF was calculated as shown below in Equation 1**Error! Reference source not found.**.

$$SRT = \frac{\text{Mass in System}}{\text{Mass Wasted per -day}} = \frac{(M \times V) \times 24 \text{ hours}}{(M_{\text{mixer on}} \times t_{on} \times Q) + (M_{\text{mixer off}} \times t_{off} \times Q)} \qquad \text{Equation 1}$$

M= The average TSS in the fermenter (mg L^{-1})
V= Volume of the fermenter (gallons)
Q= Pumping rate of the fermenter (gallons $hour^{-1}$)
$M_{mixer\ on}$ = The average TSS fermenter effluent probe readings during a 24-hour period while the mixers in the fermenter were turned on (mg L^{-1})
$M_{mixer\ off}$ = The average TSS fermenter effluent probe readings during a 24-hour period while the mixers in the fermenter were turned off (mg L^{-1})
t_{on}= Time mixers in the fermenter are on (hours)
t_{off}= Time mixers in the fermenter are off (hours)

The SRT is the mass in the system divided by the mass wasted per day. The TSS and pumping rates were recorded by probes installed in the SSMLF and accessed on the supervisory control and data acquisition (SCADA) system. The mass of TSS with the mixer off was calculated using only the recordings of the TSS while the mixers within the basin were off.

3.4 Nitrification Max Rate Test

The first of the three activity tests performed on the wastewater sludge was the Nitrification Max Rate Test. This test measures the maximum ammonia oxidation and nitrite oxidation rates of activated sludge from the oxic basin (van Loosdrecht et al. 2016).

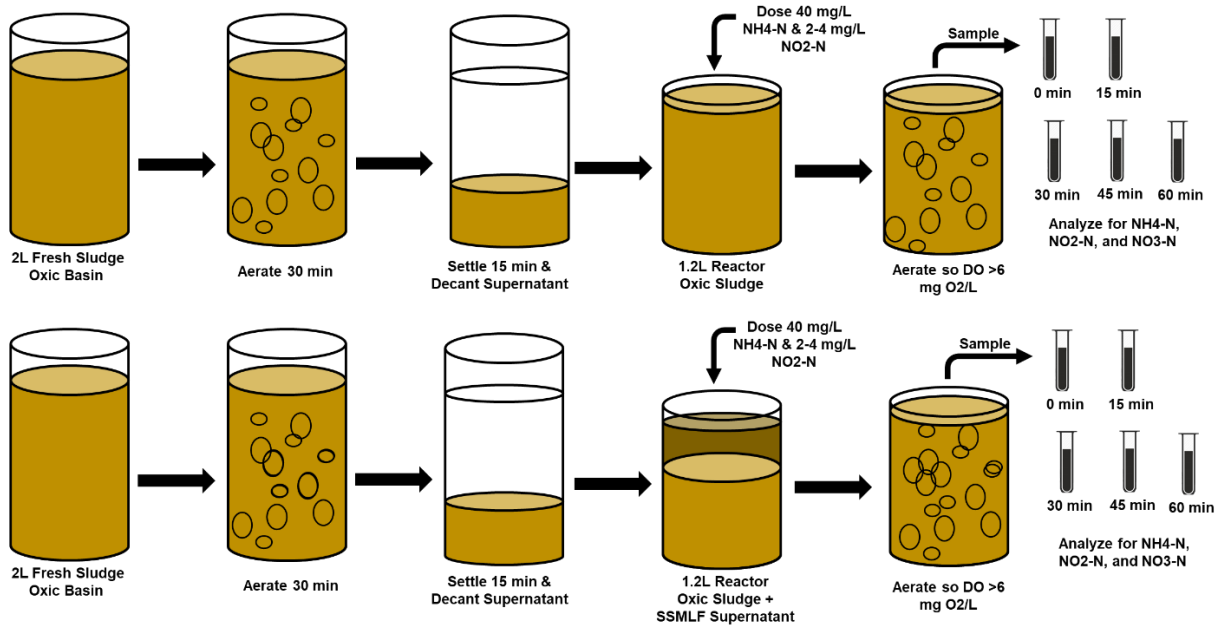

Figure 4: Nitrification Max Rate Test Design

These methods are based on those found in experimental methods of wastewater treatment. A diagram of the experiment posted above in Figure 4: Nitrification Max Rate Test Design shows the design and setup. First, two separate 2 L samples from the oxic basin were collected and

aerated for 30 minutes to oxidize excess COD. Samples were then settled, supernatant removed, and sludge was poured into two 1.2 L polycarbonate reactors. The complete setup design can be seen in Figure 5. One of the reactors was given the SSMLF supernatant in addition to oxic basin activated sludge to test for inhibition. Within each reactor, mixing was provided by a magnetic stirring bar, and the dissolved oxygen was maintained >6 mg O_2L^{-1}. The two reactors were each spiked with 30 to 40 mg L^{-1} NH_4-N (as ammonium chloride) and 2 - 4 mg L^{-1} NO_2-N (as sodium nitrite), respectively, and sampled continuously for 1 hour at 15-minute intervals. All collected samples were analyzed for NH_4-N, NO_2-N, and NO_3-N using HACH kits TNT832, TNT840, TNT835. The AOB and NOB rates were calculated as the slope of NOx-N produced and NO_3-N produced, respectively. The VSS and TSS concentrations of the mixed liquor sample were also measured to normalize the rates across all 15 weeks of testing.

Figure 5: 1.2L Polycarbonate Sealed Reactors with YSI 5500D Multi DO Optical Monitoring and Control Instrument Set Up for Nitrification Max Rate Test.

3.5 Specific Oxygen Uptake Rate Test

The specific oxygen uptake rate test (SOUR) was based on Standard Methods for the Examination of Water and Wastewater (APHA et al. 2017). This method measures the oxygen consumption rate of a sample of wastewater sludge. The microorganisms' oxygen uptake rate indicates the level of activity of the sludge. A complete diagram of the experimental methods is posted below in Figure 6.

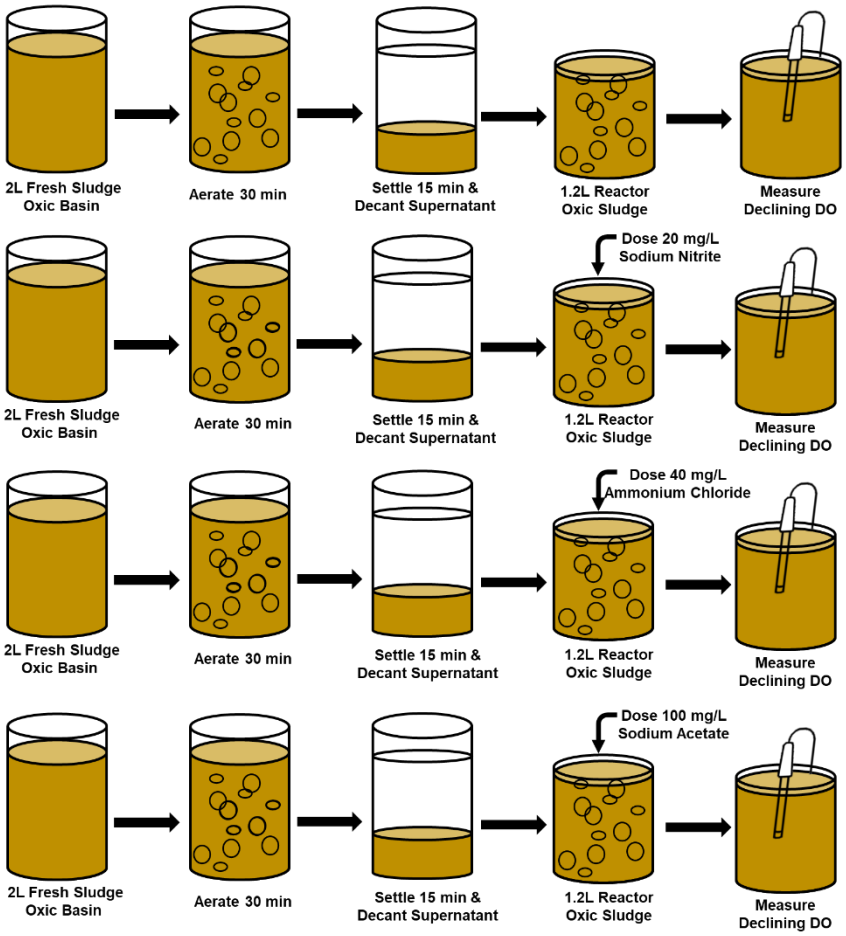

Figure 6: Specific Oxygen Uptake Rate Test Design

During the first step in the procedure, four 2 L samples were collected from the oxic basin and aerated for 30 min. The sludge was then settled, and the supernatant removed. The sludge was transferred into four 1.2 L polycarbonate reactors with sealed lid, see Figure *7*: 1.2L Polycarbonate Sealed Reactors with YSI 5500D Multi DO Optical Monitoring and Control Instrument set up for SOUR.. For this experiment, four SOURs were tested with different substrate additions: endogenous, nitrite spike, ammonium spike, and acetate spike. The endogenous sample was not spiked with any chemical additions. The ammonium reactor was spiked with ammonium chloride (40 mg-N L^{-1}) to measure the activity of the aerobic AOB (ammonia-oxidizing bacteria). The nitrite sample was spiked with sodium nitrite (20 mg-N L^{-1})

to measure the activity of the NOBs (nitrite-oxidizing bacteria). Finally, the acetate sample was spiked with sodium acetate (100 mg L^{-1}) to measure the activity of the heterotrophic bacteria. Each sample was aerated until DO reached >7.0 mg L^{-1} and then spiked with its respective chemical addition. The aeration was turned off, and the declining DO was recorded by a YSI 5500D MultiDO Optical Monitoring and Control Instrument until the DO no longer decreased at a steady rate. The OUR was calculated as the slope of declining DO. The VSS and TSS concentrations of the mixed liquor sample were measured to normalize the OUR across the entire study and give the specific oxygen uptake rates (SOURs).

Figure 7: 1.2L Polycarbonate Sealed Reactors with YSI 5500D Multi DO Optical Monitoring and Control Instrument set up for SOUR.

3.6 dPAO Activity Test

The final of the three activity tests was the dPAO activity test based on methods adapted from the? STOWA Report: Biological Phosphorus Removal (Janssen et al. 2002). This activity test was executed in two phases after set-up to mimic the metabolic processes of dPAO. Four 2 L samples of wastewater sludge were collected from the anoxic zone and aerated for one hour to allow the sludge to take back up any endogenously released PO_4 as poly-P. As in previous tests, the sludge was then settled, supernatant removed, and sludge poured into 1.2 L polycarbonate reactors. The goal of the first phase is to measure the maximum rate of phosphate release by PAOs/dPAOs when VFA in the form of acetate is in excess. A schematic for the first phase can be seen in Figure 8: Schematic of the feast (anaerobic) phase of the dPAO activity test.. In the feast phase, sludge is kept in anaerobic conditions (DO below 0.3 mg L^{-1}) through the addition of N_2 gas. The DO was monitored with the YSI 5500D MultiDO Optical Monitoring and Control Instrument. Then 10 mL of the 24.0 g L^{-1} NaAc solution was added to each of the four reactors for a final acetate concentration in the reactors at 200 mg L^{-1}. Four-mL samples were taken from the reactors after 0, 30, 60, 75, 90, 105, and 120 minutes and filtered through a 0.45 µM nylon syringe filter. MLSS and VSS were also measured on all four reactors. All samples were analyzed for PO_4-P, NO_2-N, and NO_3-N using the Dionex ICS-2000 IC with an AS40 autosampler, Chromeleon Software, a Dionex IonPac AS18 4 × 250 mm column, and a Dionex IonPac AG18 4 × 250 mm guard column. The activity rates of dPAOs present were calculated as the slope of PO_4-P released during the first phase.

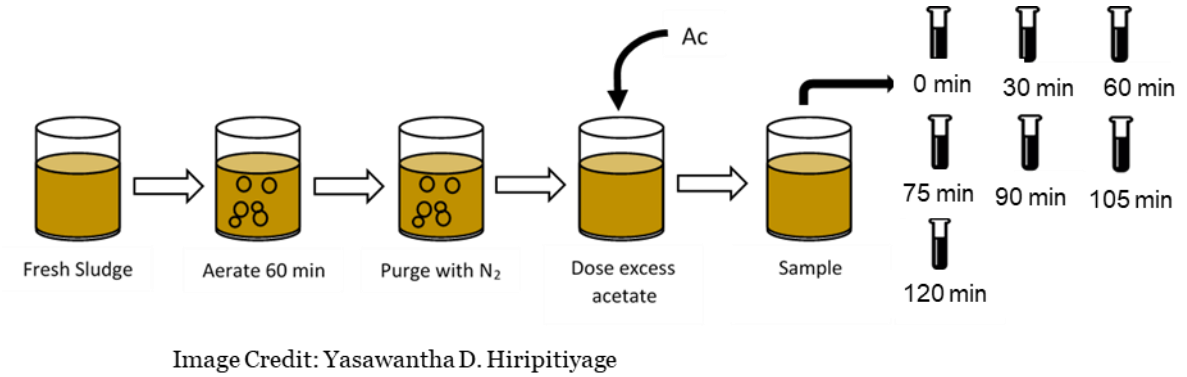

Image Credit: Yasawantha D. Hiripitiyage

Figure 8: Schematic of the feast (anaerobic) phase of the dPAO activity test.

The second phase, the famine phase of the experiment, introduces different electron acceptors (O_2, NO_2, NO_3) into each of the reactors to measure the phosphate uptake rate of both the PAOs and dPAOs. A schematic of this phase can be seen below in Figure 9. The purpose of the aerobic reactor (O_2) of the famine phase is to measure the maximum rate of phosphate uptake by PAOs. The purpose of the anoxic reactors (NO_2, NO_3) is to measure the maximum rate of phosphate uptake by dPAOs. After sampling is complete in the feast phase, and all acetate has been taken up and polyphosphate released, one reactor is supplied with oxygen, and DO is maintained at 6 mg L^{-1} O_2. The other reactors are maintained under anoxic conditions while one is spiked with NO_2-N at 15mg L^{-1}, one is spiked with NO_3-N at 15mg L^{-1}, and the last reactor is left as a control not receiving a terminal electron acceptor. Four-mL samples were taken from the reactors after 0, 30, 60, 75, 90, 105, and 120 minutes and filtered through a 0.45 µM nylon syringe filter. MLSS and VSS were also tested on all four reactors. All samples were analyzed for PO_4-P, NO_2-N, and NO_3-N using the Dionex ICS-2000 IC described above. The activity rates of dPAOs were calculated as the slope of PO_4-P taken up in the nitrate and nitrite reactors during the second phase. All concentrations of phosphate and acetate were measured on the Dionex ICS-2000 IC using a standard curve of known concentrations based on samples analyzed at both

the beginning and end of each IC run for each experiment. The P concentrations used to establish the standard curve were 0.0, 0.5, 1, 2, 4, 8, 10, 20 mg-L^{-1}; and the acetate concentrations were 0, 6, 12.5, 25, 50, 100, 250, 500 $^{-1}$.

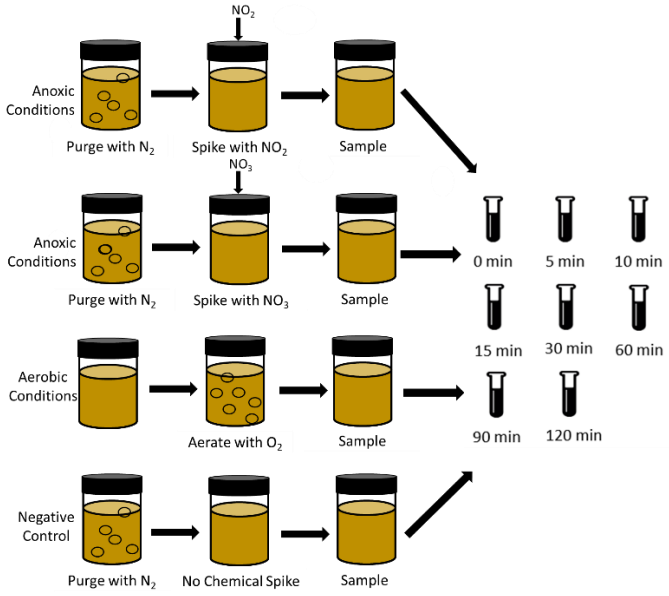

Figure 9: Schematic of the famine phase of the dPAO activity test.

3.7 SVI_5 and SVI_{30}

The sludge volume index (SVI) is the volume (mL) occupied by 1 g activated sludge after 30 minutes of settling (Mohlman 1934) For this experiment SVI_5 is defined as the volume (mL) occupied by 1 g activated sludge after 5 minutes of settling, while SVI_{30} is defined as Mohlman described SVI in 1934. SVI_5 and SVI_{30} were tested during each stage of the 15-week study as a measure of how well the sludge from the oxic basin settles and compacts. This method was based on those published in both Standard Methods (APHA et al. 2012) and Experimental Methods in Wastewater Treatment 6.2.1.3 (APHA et al. 2017, van Loosdrecht et al. 2016). Sludge was collected from the oxic basin, well mixed, and poured into a settleometer (Raven Environmental C-10202). After 5 and 30 minutes, the sludge volume was observed and recorded in mL L^{-1}. The MLSS of the sample was also taken from the collected sludge per method 2540 D

of standard methods, and the SVI_5 and SVI_{30} were calculated per **Error! Reference source not found.** below (APHA et al. 2017).

$$SVI_5 = \frac{SV_5}{MLSS} \quad or \quad SVI_{30} = \frac{SV_{30}}{MLSS} \qquad \text{Equation 2}$$

SVI_5= Sludge volume after 5 min (mL/g)
SVI_{30}= Sludge volume after 30 min (mL/g)
MLSS= mixed liquor suspended solids (g L^{-1})

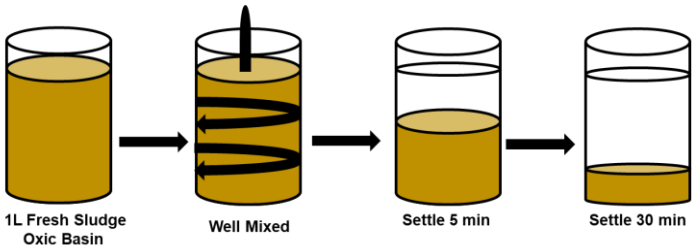

Figure 10: Schematic of SVI_5 and SVI_{30} determination

3.8 Operations Data Collection

Operational data from the plant was collected daily throughout the 15-week study. Just as the initial data collection was described in section 3.2 data was gathered from probes recorded to the SCADA system and daily wastewater operator experiments. The data collected by operators included influent VFAs, fermenter VFAs, influent TP, effluent TP, anoxic influent nitrate, anoxic effluent nitrate, fermenter supernatant floc filtered chemical oxygen demand (ffCOD), anaerobic effluent ffCOD, anoxic effluent ffCOD, influent ffCOD, effluent ffCOD, and fermenter ffCOD. All samples labeled as influent and effluent were composites while the rest were grab samples. Some of the data were not available every day during the 15-weeks, and the values on those days were counted as missing in all averages and not as zeros. Data collected through SCADA included fermenter TSS, temperatures throughout the treatment train, anaerobic

effluent Ortho-P, length of time mixer is on in fermenter, pumping rates throughout treatment train, and the fermenter Ortho-P all reported in hourly increments. The probe for the fermenter Ortho-P failed and came offline during this study and data was not available during SRT 2.0-2.4. All collected data were recorded on an Excel spreadsheet and uploaded as a .csv file into R, version 3.6.1 "Action of the Toes" (R Core Team 2019).

3.9 Microbial Community Testing and Visualization

The microbial community structure was investigated using culture-independent methods, including qPCR and FISH. All samples used in the following three sections of DNA testing were collected on days of the dPAO activity testing from the end of the anaerobic basin. Ten 50-mL samples were collected, two for each SSMLF SRT set point over the 15-week experiment. All samples were stored in the -20°C freezer before use. In this section, HyClone Water (Fisher Scientific), molecular biological grade was used as the reagent water.

3.9.1 FISH

Fluorescent in situ hybridization (FISH) is a microscopy protocol that allows for the visualization of specific bacteria under an epifluorescence (EPI) microscope by hybridizing fluorescently-labeled probes made up of short strands of DNA (oligonucleotides) to ribosomal rRNA in bacterial cells (Nielsen et al. 2009). The protocol used in this study for FISH is based on methods published in Experimental Methods in Wastewater Treatment(van Loosdrecht et al. 2016) and the FISH Handbook for Biological Wastewater Treatment (Nielsen et al. 2009). All probes used in this experiment can be seen in Table 2. Three different PAO probes were chosen for their specificity to detect *Ca. Accumulibacter* (PAO 462, PAO 651, PAO 846), all of which were labeled with the Alexa 488 fluorophores (Crocetti et al. 2000). These three probes have been used to study the presence of PAOs within an EBPR WWTP (Carvalho et al. 2007, He et al.

2007, Nguyen et al. 2011, Yun et al. 2019). To compare PAOs to total bacteria, all samples were also stained with a mixture of eubacteria (EUB) probes: EUB 388, EUB 388 II, and EUB 388 III, all of which are labeled with CY5 fluorophores (Amann et al. 1990, Daims et al. 1999). This dual staining method is one commonly used throughout the literature (Carvalho et al. 2007, Yun et al. 2019).

Table 2: Oligonucleotide Probes Used in This Study.

Probe	Sequence (5'-3')	Specificity	FA (%)	Fluorophore	Reference
EUB338	GCTGCCTCCCGTAGGAGT	Most Bacteria	50	CY5	Amann et al. 1990
EUB338 II	GCAGCCACCCGTAGGTGT	Planctomycetes	50	CY5	Daims et al. 1999
EUB338 III	GCTGCCACCCGTAGGTGT	Verrucomicrobiales	50	CY5	Daims et al. 1999
PAO 462	CCGTCATCTACWCAGGGTATTAAC	Most *Accumulibacter*	35	Alexa 488	Crocetti et al. 2000
PAO651	CCCTCTGCCAAACTCCAG	Most *Accumulibacter*	35	Alexa 488	Crocetti et al. 2000
PAO846	GTTAGCTACGGCACTAAAAGG	Most *Accumulibacter*	35	Alexa 488	Crocetti et al. 2000

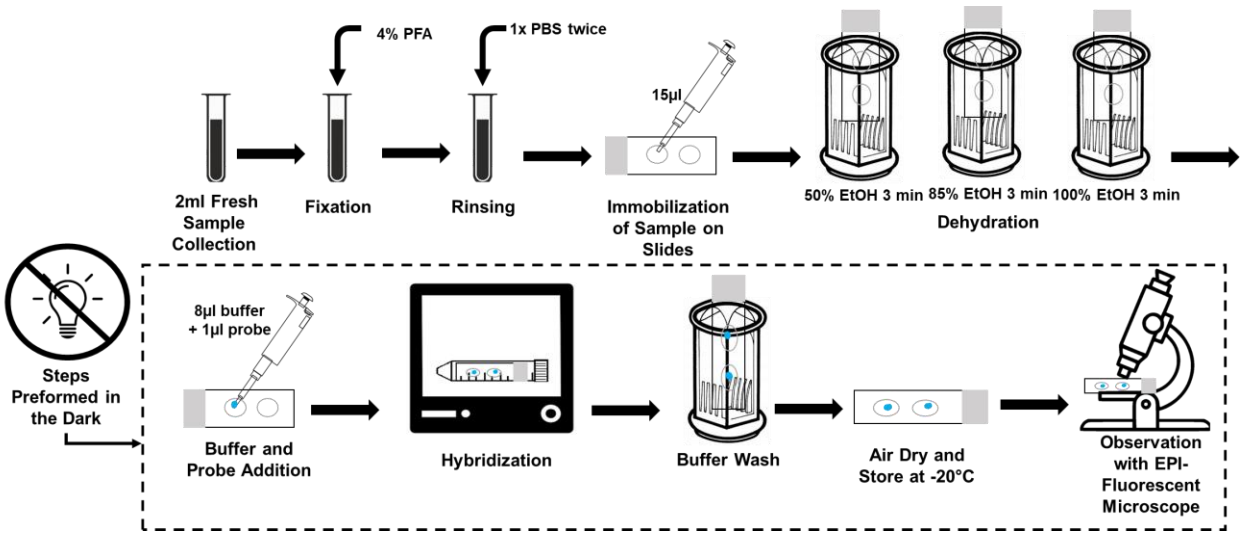

Figure 11: Schematic of FISH Protocol

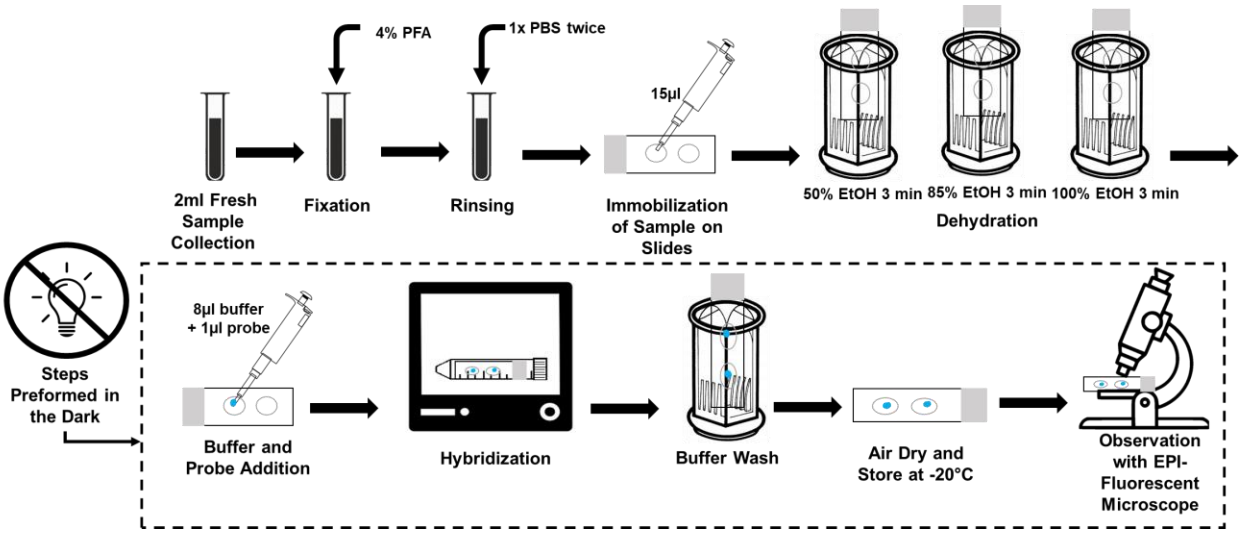

Figure *11* above depicts a diagram of the FISH protocol used in this study. Samples were collected on the days of the dPAO activity tests from the anaerobic basin and stored at -20°C until fixed in 4% paraformaldehyde, washed in 1x phosphate-buffered saline (PBS) and then stored at -20°C in 1xPBS until applied to the slide. Slides were prepared for use in FISH protocol by creating a hydrophilic surface by first acid washing them in 1M HCL for 8 hours, then coating them with 0.01% poly-L-lysine. The next step was immobilization of sample on the slides by adding 15 µL of sample to each etched circle on the slide and allowing sample to dry onto the pretreated slide in the fume hood for 30 min. To reduce excess water and increase the resolution of the sample under the EPI microscope, immobilized slides were dehydrated in 50% (ethanol) EtOH, 80% EtOH, and 100% EtOH for three min each before air drying in a fume hood.

Hybridization buffer was created based on probe-prescribed formamide concentrations: 50% formamide for EUB probes, 35% formamide for PAO probes. Eight µL of the 50% formamide buffer were pipetted to the slide directly on the dried sample, then 1 µL of each EUB probe requiring the same formamide concentration was added into the buffer. Hybridization was carried out by wetting tissue with hybridization buffer and adding that under a slide inside a 50 mL test tube placed inside a Fisher Biotech Hybridization Incubator Model FBHI-10 at 46 °C for

1.5 hours. During hybridization, 50 mL of a washing buffer were prepared based on the formamide concentration and containing a mixture of 1M Tris, 5 M NaCl, 10% SDS, 0.5 M EDTA. After hybridization, a few drops were applied to the slide, to remove excess probe solution before submerging the slide in the washing buffer in a 48 °C water bath for 15 min and the slide was rinsed with cold reagent water and allowed to vertically air dry in a fume hood. Hybridization steps were then repeated with the 35% formamide concentration hybridization buffer and the PAO probes. Slides were stored in the dark at -20°C until ready for observation under EPI microscope.

Slides were observed in the dark on a laser scanning confocal upright microscope, Leica TCS SPE Laser Scanning Confocal DM6-Q upright microscope (Leica Microsystems, Buffalo Grove, IL). EUB fluorescence was observed under the CY5 (635) laser at 50% strength, gain 650, and between wavelengths 650-700 nm. PAO fluorescence was observed under the GFP (488) laser, with a gain of 650, and between wavelengths 500-540 nm. Quantification of observed results was performed using Fiji, a distribution of the open-source software ImageJ (Schindelin et al. 2012). The method used to determine the relative abundance of PAOs was adapted from Bouchez et al. 2000. In this study, twenty images were obtained for each SRT spread out over two sampling days during each SRT. This method of quantification of FISH has been cited throughout literature (Carvalho et al. 2007, Crocetti et al. 2000). The area of bacteria hybridized by the PAO probes was divided by the total area of bacteria stained by the EUB probes using image analysis in FIJI (Bouchez et al. 2000).

3.9.2 Neisser Staining

The next step for microbial analysis was Neisser staining in which a working mixture of crystal violet and methylene blue bind to negatively charged polar bodies (poly-P) at high pH

within a cell to aid in the visualization of PAOs under the microscope within activated sludge (van Loosdrecht et al. 2016). Neisser staining has been used to visualize PAOs in EBPR sludges (Crocetti et al. 2000, Kong et al. 2005, Mino et al. 1998, Welles et al. 2015). This includes Crocetti et al 2000, who used Neisser staining to help validate their FISH results by removing the mounting agent after FISH was performed on a sample and then stained the sample using Neisser Staining techniques to validate that the cells that fluoresce with the PAO mix also contained poly-P (Crocetti et al. 2000). The methods used in this study were based on those explained in Experimental Methods of Wastewater Treatment (van Loosdrecht et al. 2016). An overview of this method can be seen below in Figure 12: Neisser Staining Method. First, a fixed smear was used to adhere the activated sludge to the slide. Then, a working solution of two parts methylene blue and one part crystal violet was added to the slide for 15 seconds then washed off with reagent water. Second, a counter stain of 0.2% Bismark brown was added to the slide for 1 minute before being washed off in the same manner with reagent water. After air drying, the results were observed using mineral oil immersion at 100x magnification under bright field. The microscope used for visualization was a Leica DM 2500 (Leica Microsystems, Buffalo Grove, IL) with a Leica DFC 500 camera attached (Leica Microsystems, Buffalo Grove, IL).

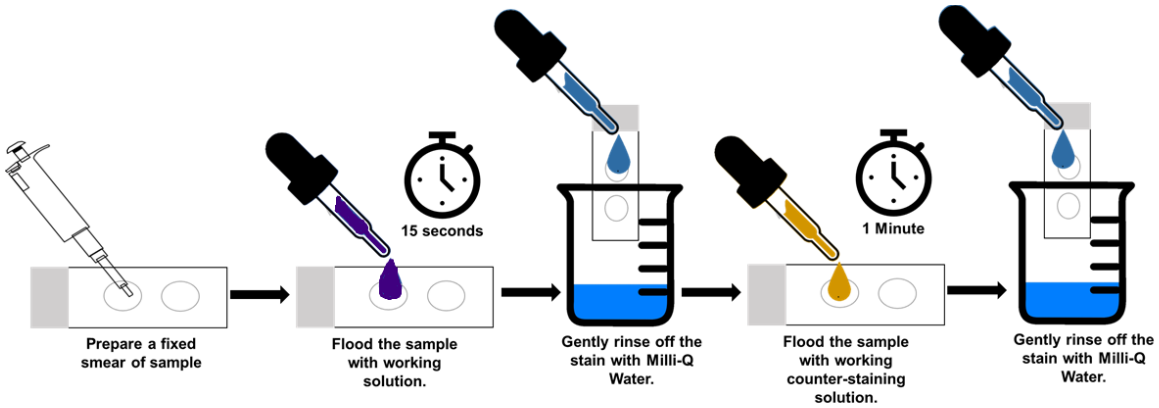

Figure 12: Neisser Staining Method

3.9.3 qPCR

Quantitative polymerase chain reaction (qPCR) was used to help quantify the PAOs and GAOs present in the anaerobic basin throughout the duration of the experiment. A complete list of all primers used in this experiment can be seen in Table *3* (He et al. 2007, Kong et al. 2002). To estimate the relative abundance of PAOs and GAOs, qPCR was also performed on 16S rRNA genes to quantify total bacteria.

qPCR was run on the iCycler (Bio-Rad, Hercules, CA) using the iCycler software. The total reaction volume was 20 µL with 5 µL of sample diluted either 1:10 or 1:100 and 15 µL of master mix created from iQ SYBR green super mix (Bio-Rad, Hercules, CA). All qPCR started with a 3 min. denaturation step at 95 °C followed by 45 cycles of a 30s denaturing step at 94 °C, then an annealing step for 45 s at temperatures specified in Table 3, and an elongation step at 72°C for 30 s (He et al. 2007).

Primer	Sequence	Target	Annealing temperature (T_a)	Amplicon size (bp)	Reference
518f	CCAGCAGCCGCGGTAAT	Acc 16S rRNA genes (PAOs)	65	351	(He et al. 2007)
PAO846 r	GTTAGCTACGGCACTAAAAGG				
341f	CCTACGGGAGGCAGCAG	Bacterial 16S rRNA genes	60	194	(He et al. 2007)
534r	ATTACCGCGGCTGCTGG				
GB612f	CGATCCTCTAGCCCACT	Gammaproteobacteria (GAOs)	60	377	(Kong et al. 2002)
GAOQ989r	TTCCCCGGATGTCAAGGC				

Table 3: Primers Used For qPCR

Amplification efficiencies along with starting concentrations were calculated according to the procedure outlined by Ruijter et al. 2009 and the accompanying software, LinRegPCR. First the total bacteria for each well were calculated with the bacterial 16s qPCR results. Then, to obtain the relative gene copies of PAOs and GAOs present in the basin, the total PAO and GAO

starting concentrations for each well were calculated and divided by total bacteria present (Ruijter et al. 2009).

4.0 Results and Discussion

4.1 Initial Correlation Matrices in R

The first phase of this study, before the stepwise increase of the fermenter, was the creation of correlation matrices with the data from the WWTP's first 477 days of operation. The data was processed as described in the Section 3.0: Methods and Procedures. The results of the first correlation matrix across 38 operational parameters can be seen in Figure 13: Correlation Matrix of Initial 477 Days of Data. In this correlation matrix, each parameter was compared to all others only when all parameters had a data point in that row, eliminating all rows with missing data (blanks). So, if there were days when not all parameters had a data point collected, the data for that day was removed from the comparison. For this correlation matrix there were 168 usable rows out of 477, meaning this matrix excluded 35% of the data collected.

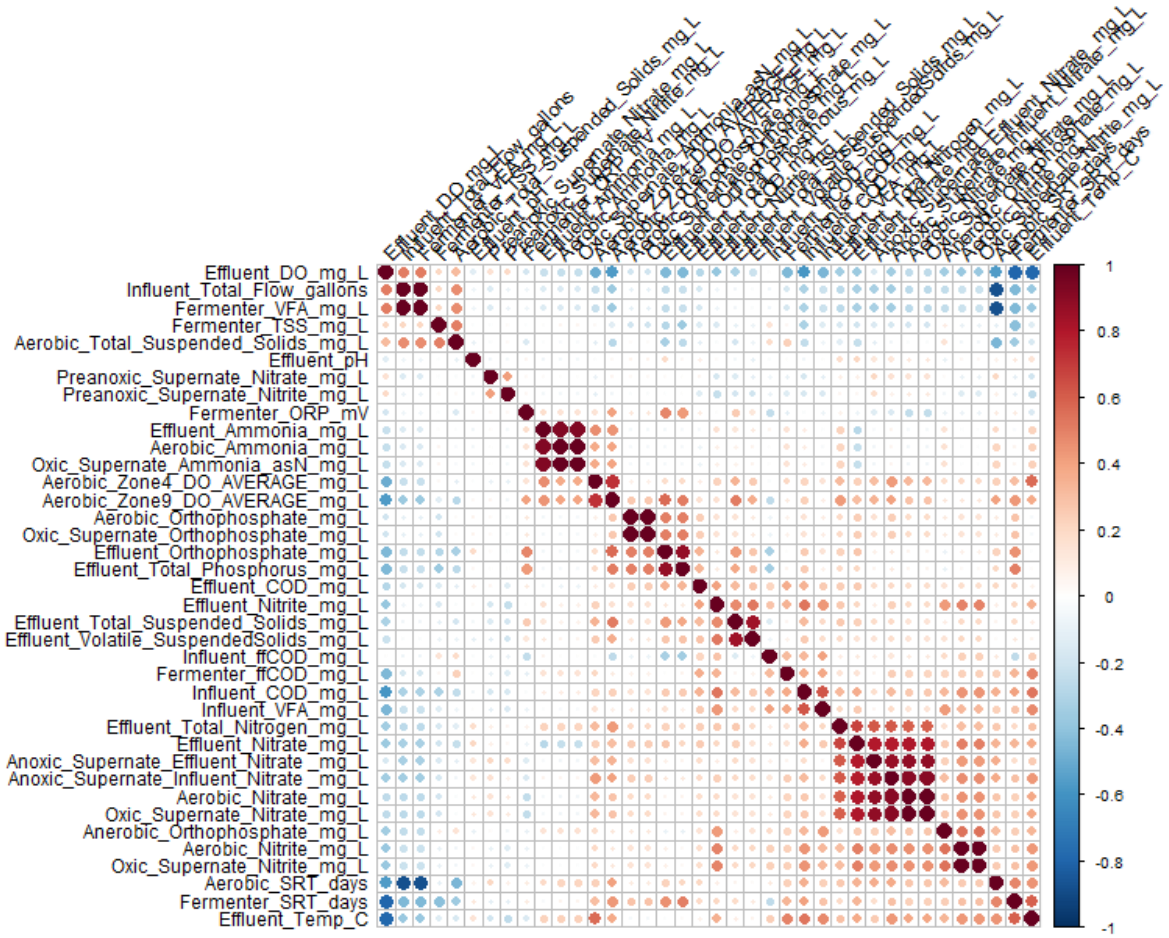

Figure 13: Correlation Matrix of Initial 477 Days of Data.

The colors of Figure 13 relate to the correlation between data parameters. Blue equals a negative relationship, and red equals a positive relationship. The size and saturation of the colored circle graphically represent the correlation coefficient. The large and more saturated the dot the closer the correlation coefficient is to 1 or -1 for positive or negative correlation respectively. The diagonal of the correlation matrix will always have a relationship of 1 by design, because each parameter is compared to itself. The results of this correlation matrix confirmed many known patterns of this wastewater treatment plant, where the effluent from one basin that flows into another have a high correlation with a coefficient > 0.85 and p-value of <

0.001. An example of this is in the Anoxic Basin Effluent Nitrate and the Aerobic Basin Nitrate having a correlation coefficient of 0.88 and p-value of < 0.001.

This initial correlation matrix was then refined to focus on 25 parameters highlighted in the literature that control EBPR, including all nutrient and sidestream fermenter data. The results of this refined correlation matrix can be seen below in Figure 14: Revised Initial Correlation Matrix.

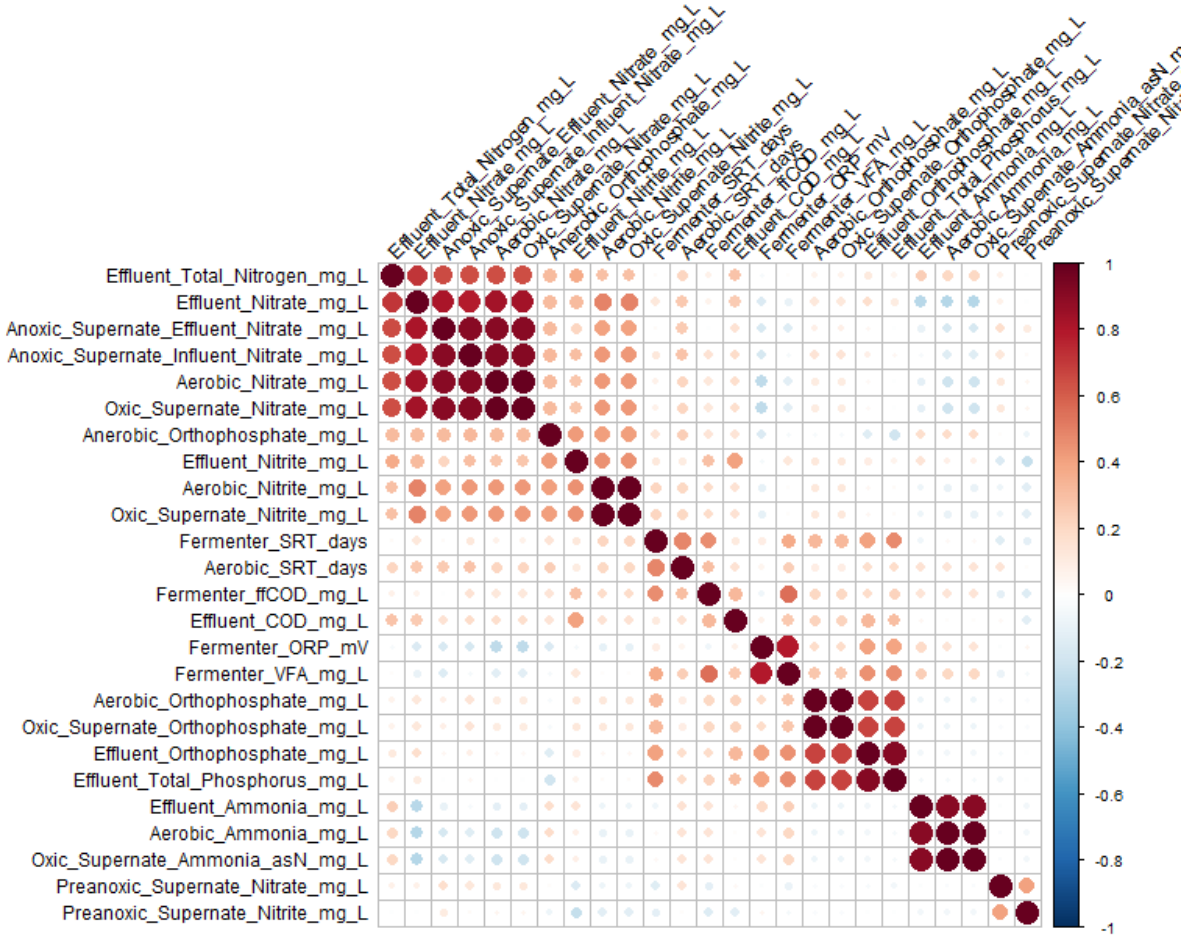

Figure 14: Revised Initial Correlation Matrix

From this correlation, it became apparent that the fermenter SRT, fermenter VFA, fermenter ORP, fermenter ffCOD, and effluent total phosphorous were strongly correlated. To further investigate these relationships, a Pearson correlation was performed for normalized data.

Fermenter SRT vs. fermenter ffCOD had a correlation coefficient of 0.48 and a p-value < 0.05, indicating a positive correlation between the two. Fermenter SRT vs. fermenter ffCOD had a correlation coefficient of 0.59 and a p-value > 0.05, meaning the fermenter's SRT and rbCOD/TP ratio had a strong positive correlation. Finally, the fermenter SRT and fermenter ORP had a correlation coefficient of 0.52 and a p-value < 0.05. These results helped progress this experiment out of the preliminary phase of research. First, the findings assisted in narrowing down what operational conditions would be affected once the SRT in the SSMLF began to change. Based on the prior literature review, SRT was expected to change the VFAs, rbCOD/TP ratio, and ORP. All three of these parameters correlated with fermenter SRT. Their strong relationships indicate these operational conditions are most closely related and therefore their combined impact could have the most significant effect contributing to the selection of dPAOs in the WWTP bacterial community. Finally, these results also provided information on how the plant has been operating for its first year and what baseline conditions of operation existed before the experiment started.

4.2 Stepwise Fermenter SRT Increase

The results of the 15-week stepwise increase of the SSMLF can be seen in Figure 15: Stepwise Increase of SSMLF . There were five different SRT phases of this study: 1.1 days, 1.3 days, 1.5 days, 2.0 days, and 2.4 days.

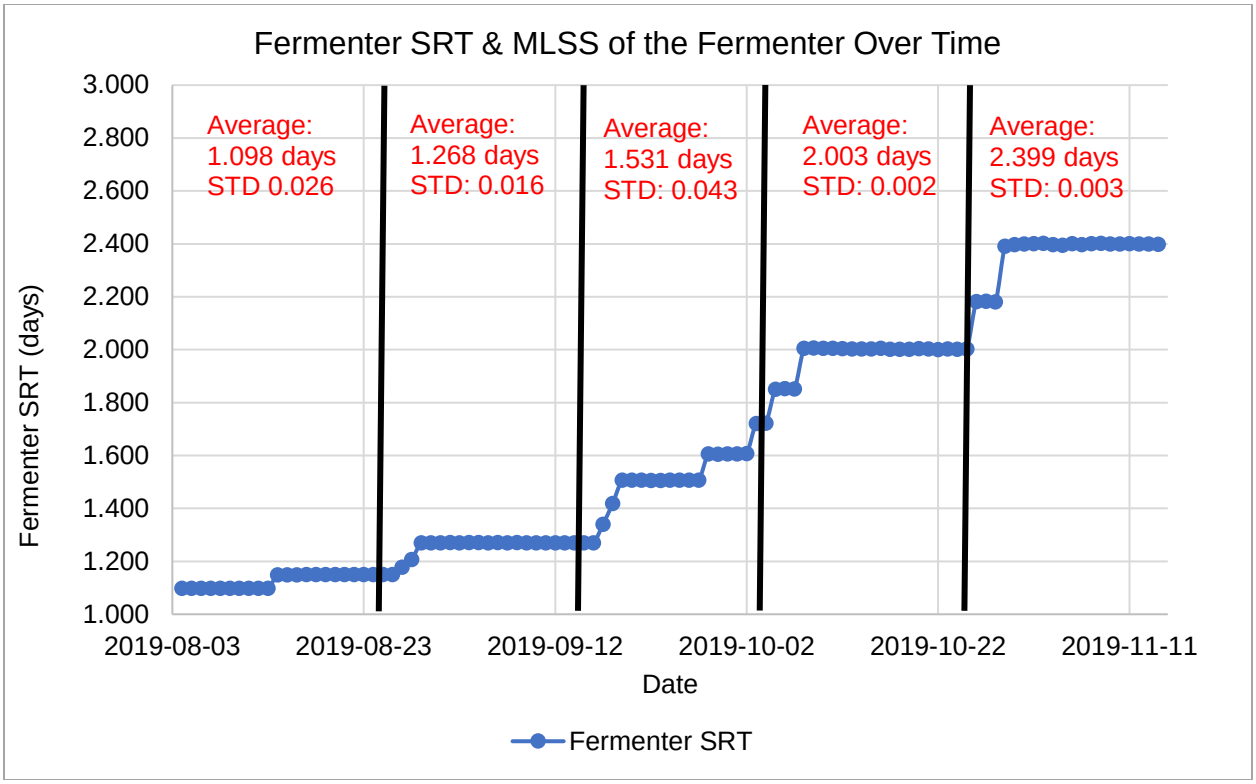

Figure 15: Stepwise Increase of SSMLF

Figure 15: Stepwise Increase of SSMLF shows the calendar date of the recorded SSMLF SRT along the x-axis and the SRT in days along the y-axis. The SRT was recorded each day of the study and the SRT of each stepwise increase can be seen at the top of the figure. The standard deviation was calculated during the two weeks of stabilization and not during the increase in SRT. The rise from SRT 1.53 days and 2.003 days took the most amount of time and can be seen in three increments in the chart above. Once raised the SRT was never lowered throughout the course of this study to allow for stabilization at each increased SRT.

4.2.1 SRT Increase vs. MLSS

After the SRT of the experiment was calculated, it was compared to the MLSS of the SSMLF throughout the duration of the study. The results can be seen below in Figure 16: SSMLF SRT and MLSS. This figure is similar to Figure 15: Stepwise Increase of SSMLF

above, with the addition of MLSS given in mg L^{-1} along the secondary Y-axis. Throughout the experiment, the MLSS of the SSMLF continued to increase from an average of 3,690 ± 250 mg L^{-1} at an SRT of 1.1 days, almost doubling to an average of 6,150 ± 420 mg L^{-1} at an SRT of 2.4 days. This increase in MLSS meant all activity test data throughout the experiment needed to be normalized to give specific rates. The normalized rates help to minimize the impact of the increase in MLSS and provide results that could be compared across the duration of the experiment.

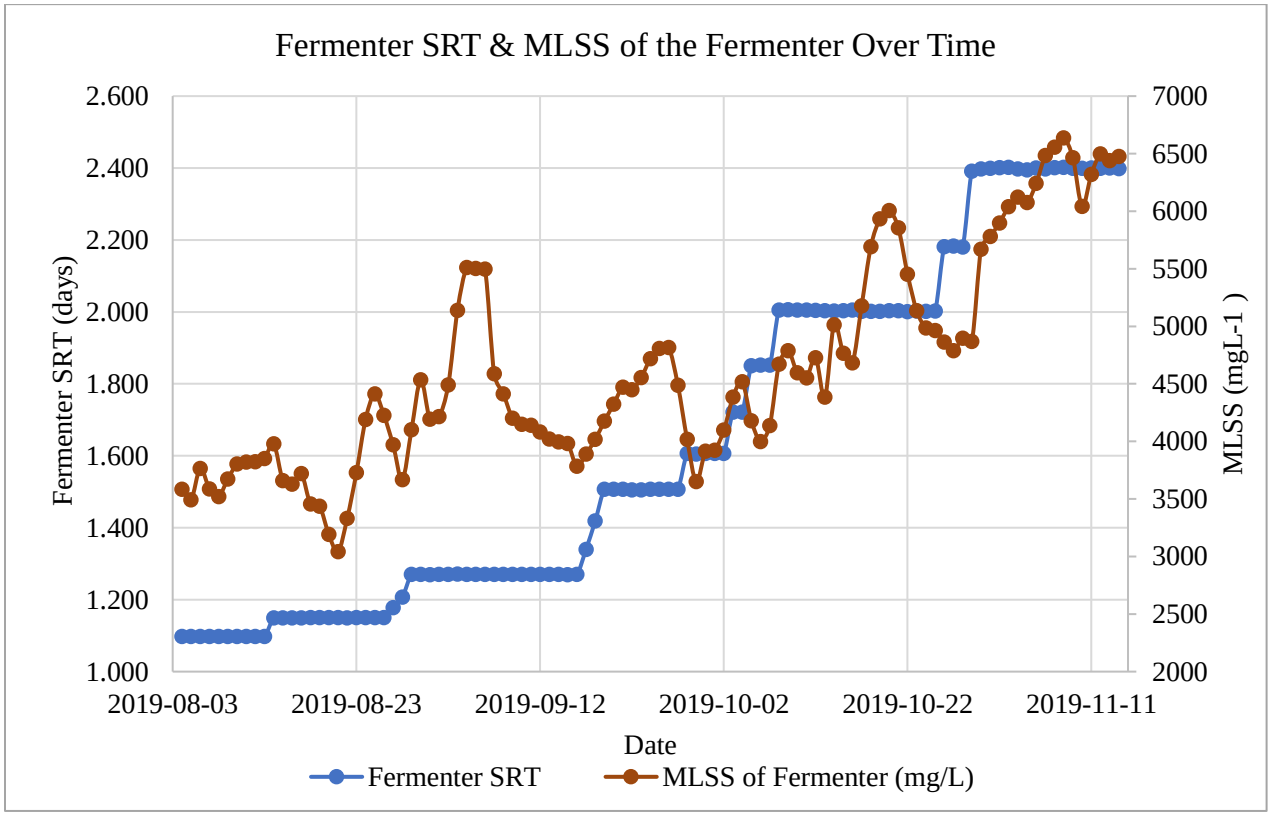

Figure 16: SSMLF SRT and MLSS

4.2.2 SRT Increase vs. Temperature of Basins

After the calculations of MLSS vs. SRT, it was also essential to look at temperatures in all of the basins throughout the study. Heat is known to affect the kinetic rates of PAOs to include both P release in the anaerobic phase and P uptake in the aerobic period (Brdjanovic et

al. 1997, Meijer et al. 2002). Temperature has also been shown to play a role in PAO-GAO competition within EBPR systems. Higher temperatures around 30°C have been shown to favor GAOs, allowing them to outcompete and become the dominant population within a system (Lopez-Vazquez et al. 2009, Whang and Park 2006, Winkler et al. 2011). Temperatures around 20°C have been shown to select for PAOs to be more abundant than GAOs in an EBPR system (Lopez-Vazquez et al. 2009, Whang and Park 2006, Winkler et al. 2011). This experiment was conducted from August to November when water temperatures in all of the basins were expected to remain relatively constant without any adverse effects on PAO population competition or kinetic rates.

The results of graphing SRT vs. time and the temperature of the EBPR basins can be seen below in Figure 17. This graph has the date across the x-axis, SSMLF SRT along the primary y-axis, and the temperature of the basins in units of °C along the secondary y-axis. Throughout the experiment, the temperature averages for all five phases of the trial saw a fluctuation of only 4.6°C or 20% from an average of 22.6 ± 0.2 °C at 1.1 days SRT to 18.0 ± 0.2°C at 2.4 days SRT. Based on literature, these temperatures should favor growth of PAOs over GAOs within the WWTP (Lopez-Vazquez et al. 2009, Whang and Park 2006, Winkler et al. 2011). However, with temperatures averaging below 20°C in the last phase of SRT 2.4 days, the effect of temperature on the activity rates during this time cannot be discounted. These average temperatures could be causing adverse effects within the microbial community in the WWTP. To help overcome these issues, all activity tests were performed in the lab in a temperature-controlled environment. .

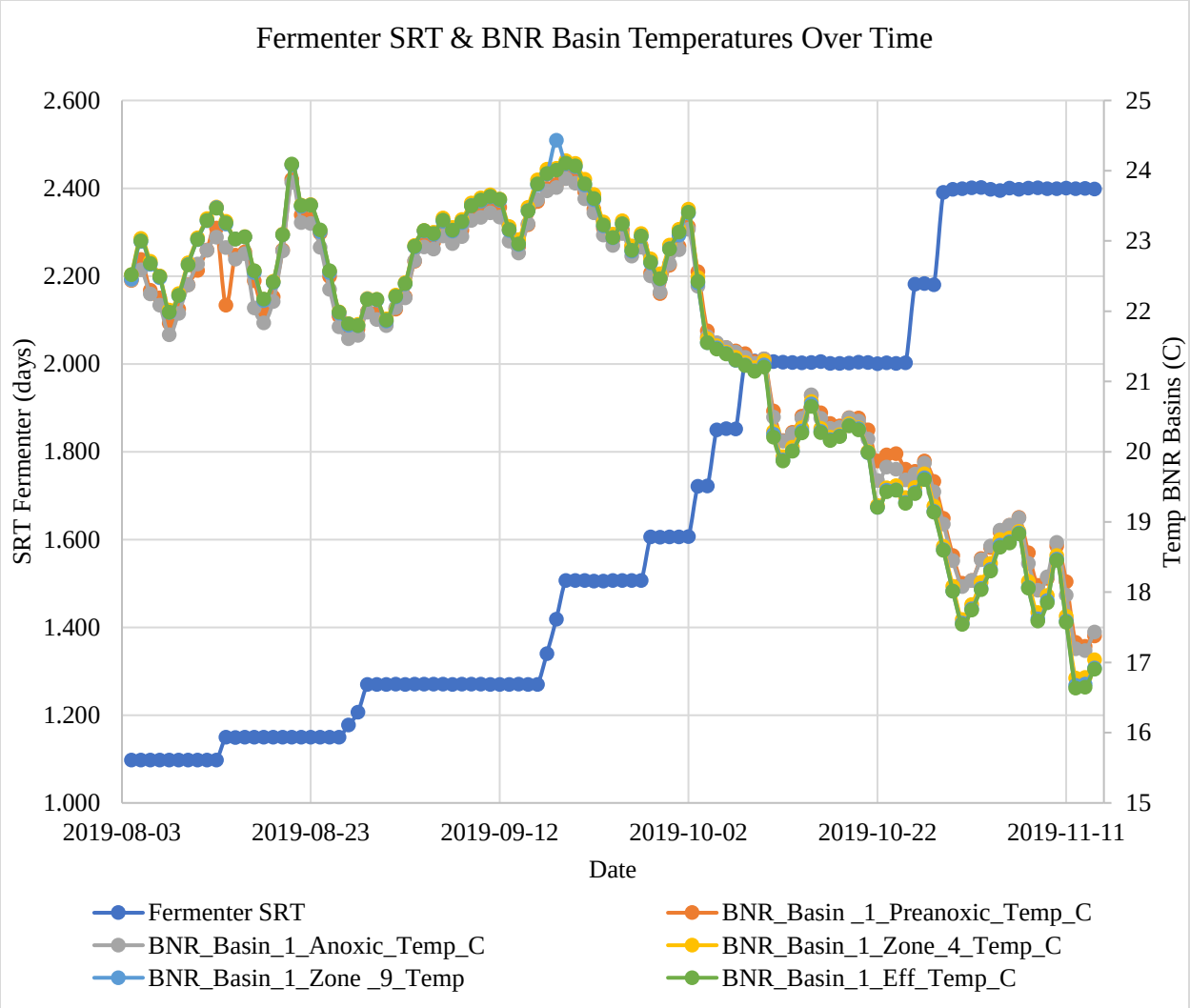

Figure 17: SSMLF SRT vs. Time vs. Temperature

4.3 Operator Data Results and Discussion

Based on the literature review and results of the initial data collected from the wastewater treatment plant's first year of operation, the following parameters were tracked throughout the experiment to see how their changes correlated to a selection of dPAOs within the wastewater sludge. These parameters included VFAs, ffCOD, rbCOD/TP, and ORP. In general, all of these parameters increased with an increase in SRT up until SRT 2.4 days when some began to decline.

4.3.1 VFAs

The VFAs created in the SSMLF throughout this experiment can be seen below in Figure 18. This figure illustrates that not only did the amount of VFAs created by the fermenter increase as SRT increased but the diversity of VFAs also increased. Figure 18 shows a 289%, or threefold, increase in the mg L^{-1} of VFAs created by the sidestream fermenter from 1.10 days SRT to 2.00 days SRT. However, by the time the fermenter had reached an SRT of almost 2.40 days there was decrease in the amount of VFA production. This is not strong enough evidence to say methanogenesis had begun to occur, but it indicates that had the fermenter continued to operate at higher SRTs its performance and production of VFAs would decline as methanogenesis was reached. At an SRT of 1.54 days the fermenter started the formation of butyric acid, isobutyric acid, propionic acid, and valeric acid. These had not been previously present in measurable quantities at lower SRTs. At SRTs of 1.54 days and higher, the SSMLF was consistently producing acetic and propionic acid, which PAOs take up in anaerobic conditions making EBPR possible (Comeau et al. 1986, Houweling et al. 2010, Mino et al. 1998). This increase in volume and assortment of VFAs within the fermenter leads to the EBPR WWTP being able to support a more diverse microbial population and stable microbial community.

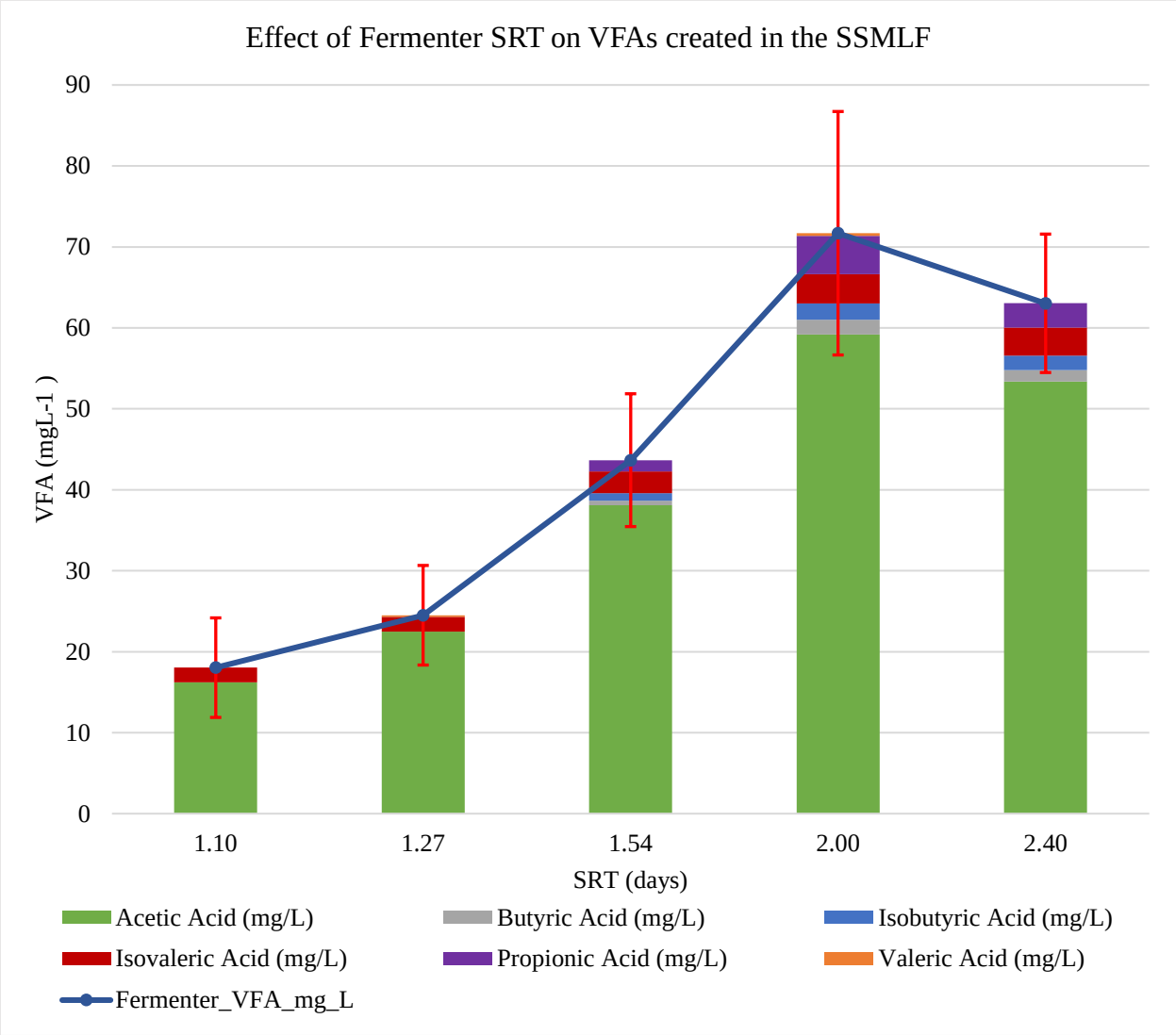

Figure 18: Effect of Fermenter SRT on VFAs Created in the Fermenter

4.3.2 ffCOD

The ffCOD created by the SSMLF was also monitored throughout the experiment because of its high correlation to SRT in the fermenter. The results of the ffCOD created by the SSMLF can be seen below in Figure *19*. This figure reveals an increase in ffCOD created by the fermenter of 118% at an SRT of 2.00 days compared to 1.10 days. The rise in ffCOD directly correlates to the increase of rbCOD in the SSMLF. This increase will be further discussed in the next section.

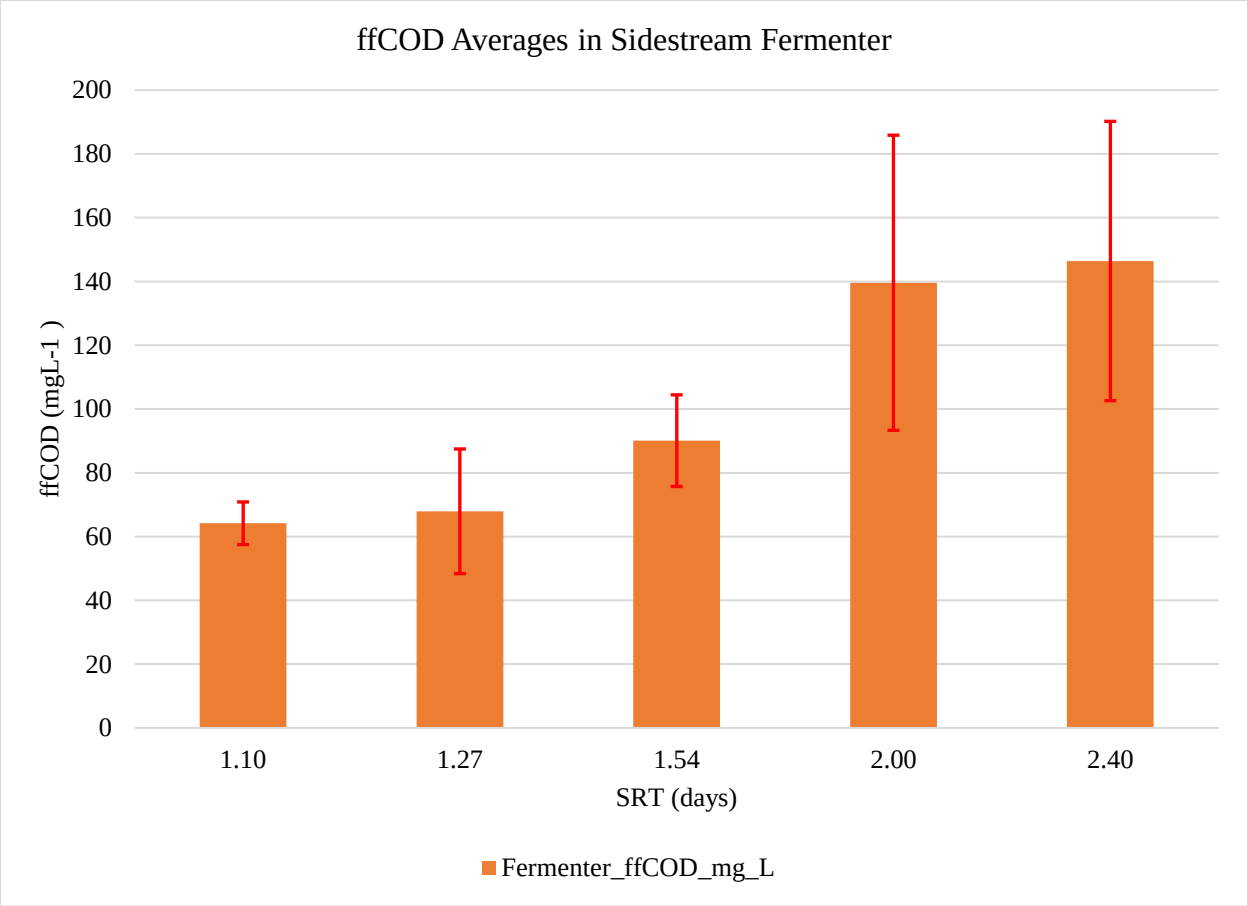

Figure 19: Effect of Fermenter SRT on the Average ffCOD Created

4.3.3 rbCOD/TP

The increase in the rbCOD:TP ratio throughout the experiment can be seen below in Figure 20: Influent and Fermenter effluent rbCOD:TP Ratios. Yellow bars indicate influent rbCOD:TP while blue bars indicate the fermenter's rbCOD:TP.. Wakarusa operates with an average influent rbCOD:TP ratio of 14 which is below 15, the design threshold necessary for consistent phosphorous removal at an EBPR WWTP (Barnard et al. 2017, Kobylinski et al. 2008). Figure *20*: Influent and Fermenter effluent rbCOD:TP Ratios. Yellow bars indicate influent rbCOD:TP while blue bars indicate the fermenter's rbCOD:TP. shows the average rbCOD:TP ratio created by the sidestream fermenter as compared to just the influent rbCOD:TP ratio at each stepwise increase of the SSMLF SRT throughout the experiment. This ratio

improved by an average of 35% throughout the study, with an increase of 79% to 25.9 ± 5.2 at SRT 2.0 days. The increase in rbCOD:TP ratio supports the selection of PAOs because the COD within the fermenter becomes the VFAs necessary for phosphate removal in EBPR.

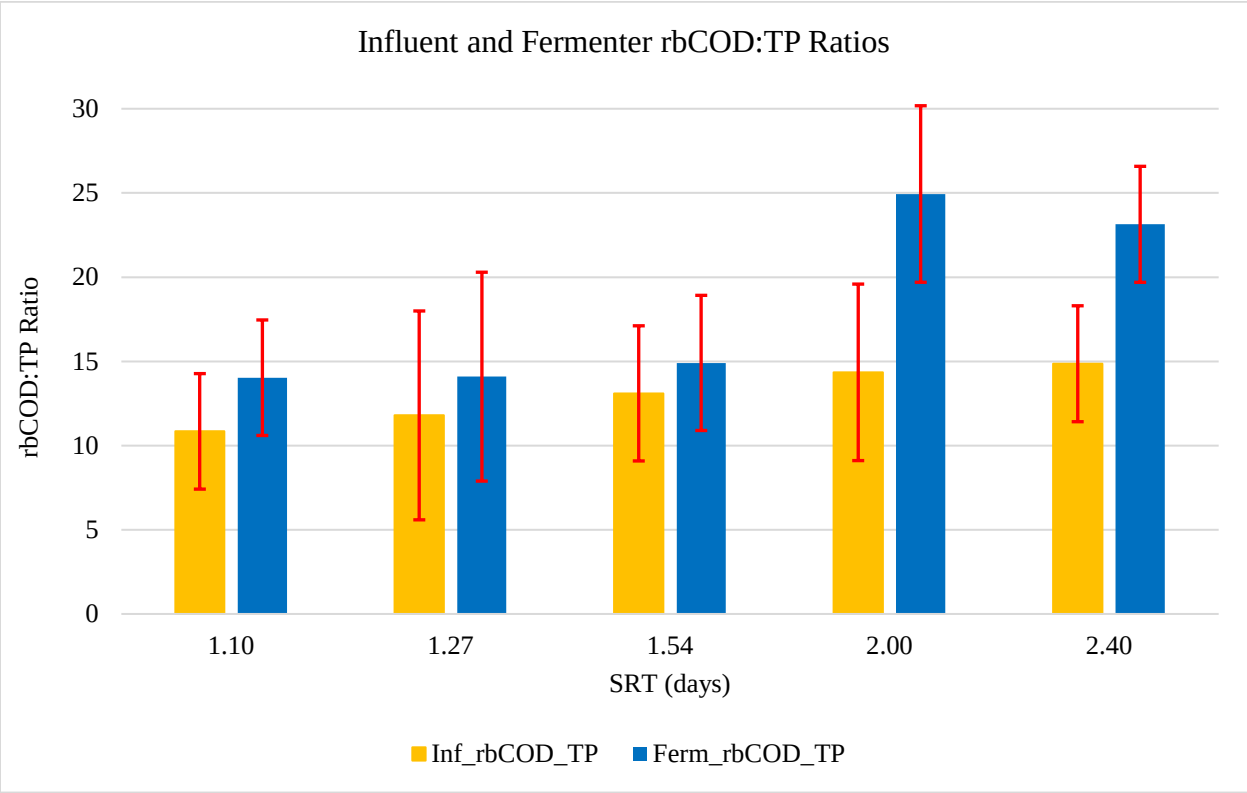

Figure 20: Influent and Fermenter effluent rbCOD:TP Ratios. Yellow bars indicate influent rbCOD:TP while blue bars indicate the fermenter's rbCOD:TP.

4.3.4 ORP

The ORP of the WW in the WWTP was tracked via an inline probe, which, as stated above had the added benefit of providing real-time feedback during the duration of this experiment (Yu et al. 1997). Unfortunately, the probe went offline during the study, and it was determined that the data collected before going offline was unreliable and could not be used in this report. This unforeseen issue stopped the testing of the hypothesis that the ORP of the anaerobic zone should be lower than -180 mV but ideally between -200 mV and -300 mV to enrich the dPAO community within a BNR plant (Barnard et al. 2017, Yu et al. 1997).

4.3.5 Percent Phosphorous Removal

To see the overall performance of the EBPR WWTP, the total percent of P removed was tracked throughout the experiment, and these results can be seen in Figure *21*: Effect of Fermenter SRT on Percent Phosphate Removal. The grey bars represent the % P removal based on influent and effluent concentrations at each stepwise increase of the Fermenter SRT.. This figure reveals an increase in the overall percent phosphorus removal from 96% to 98%, meaning the plant continued to see high phosphorus removal throughout the experiment. This indicates a robust PAO population within the WWTP as it continued to maintain excellent P removal throughout the entirety of the study despite changes to the SRT of the fermenter, which has the potential to shift the bacterial community within the plant. A linear regression of this data yields an R^2 value of 0.93. Running a Pearson correlation on percent P removal and SRT of the fermenter shows a statistically significant correlation with a p value of 0.013.

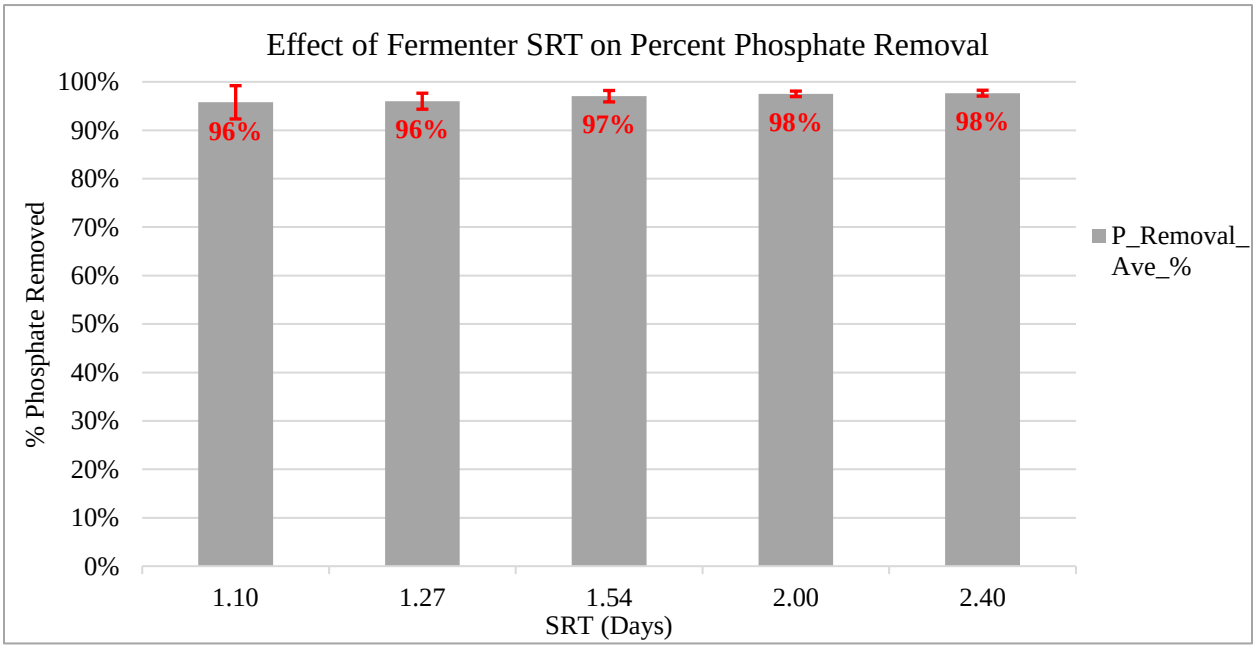

Figure 21: Effect of Fermenter SRT on Percent Phosphate Removal. The grey bars represent the % P removal based on influent and effluent concentrations at each stepwise increase of the Fermenter SRT.

4.3.6 Statistical Significance of Operational Data

Statistical analysis was completed on the operational data set collected during this experiment. The Shapiro-Wilk test was used to test for the normality of each variable tracked throughout the study. The resulting p-value from the Shapiro-Wilk test was used to identify any variables that have a non-normal distribution, p-value < 0.05. On variables determined to have a normal distribution, a Pearson correlation was run with the fermenter SRT set against a normally distributed variable. The results of this statistical test were visualized with a plot. Of the normally distributed operational dataset, two variables (fermenter VFAs and fermenter acetic acid concentration) had a statistically significant correlation with fermenter SRT. The fermenter SRT vs. VFAs created by the fermenter was significantly correlated with a p-value < 0.05 and a correlation coefficient of 0.817 (Appendix A). The fermenter SRT vs. acetic acid produced by the fermenter was significantly correlated with a p-value < 0.05 and a correlation coefficient of 0.541 (Appendix A). This suggests that as the SRT of the fermenter increased, the amount of VFAs created by the fermenter also increased. Specifically, acetic acid increased, which is critical for the metabolism of PAOs and the complete biological removal of phosphorous in the WWTP.

4.4 Activity Test Results and Discussion

The next section describes the results of the three batch activity tests performed at each of the five different SSMLF SRTs. Each of the batch tests was performed in duplicate on two separate days within each tested SRT as described above in the methods section. Duplicate testing was performed to create biological replicates. The average of the duplicate activity tests was used to generate the data points, while the differences between duplicates were used to calculate the standard deviation. Overall, these results show low activity when compared to other

rates presented in literature, although the bacteria in the system had achieved consistently high P removal.

4.4.1 Maximum Nitrification Rate Test

The maximum nitrification rate is an indicator of AOB and NOB health within the WWTP (Monti and Hall 2008). The reaction rates were calculated through linear regression to find the slope of NH_4-N consumption and NO_x-N production. The slopes were then divided by the VSS gL^{-1} of the batch test reactors to calculate the specific NH_4-N consumption and NO_x-N production rates for each SSMLF SRT as described in Experimental Methods for Wastewater Treatment (van Loosdrecht et al. 2016). The results for the maximum nitrification rate test can be seen below in Figure 22: Maximum Nitrification Rate Test. WW represents samples with just oxic basin sludge, while WWF represents samples with oxic basin sludge and SSMLF supernatant. .

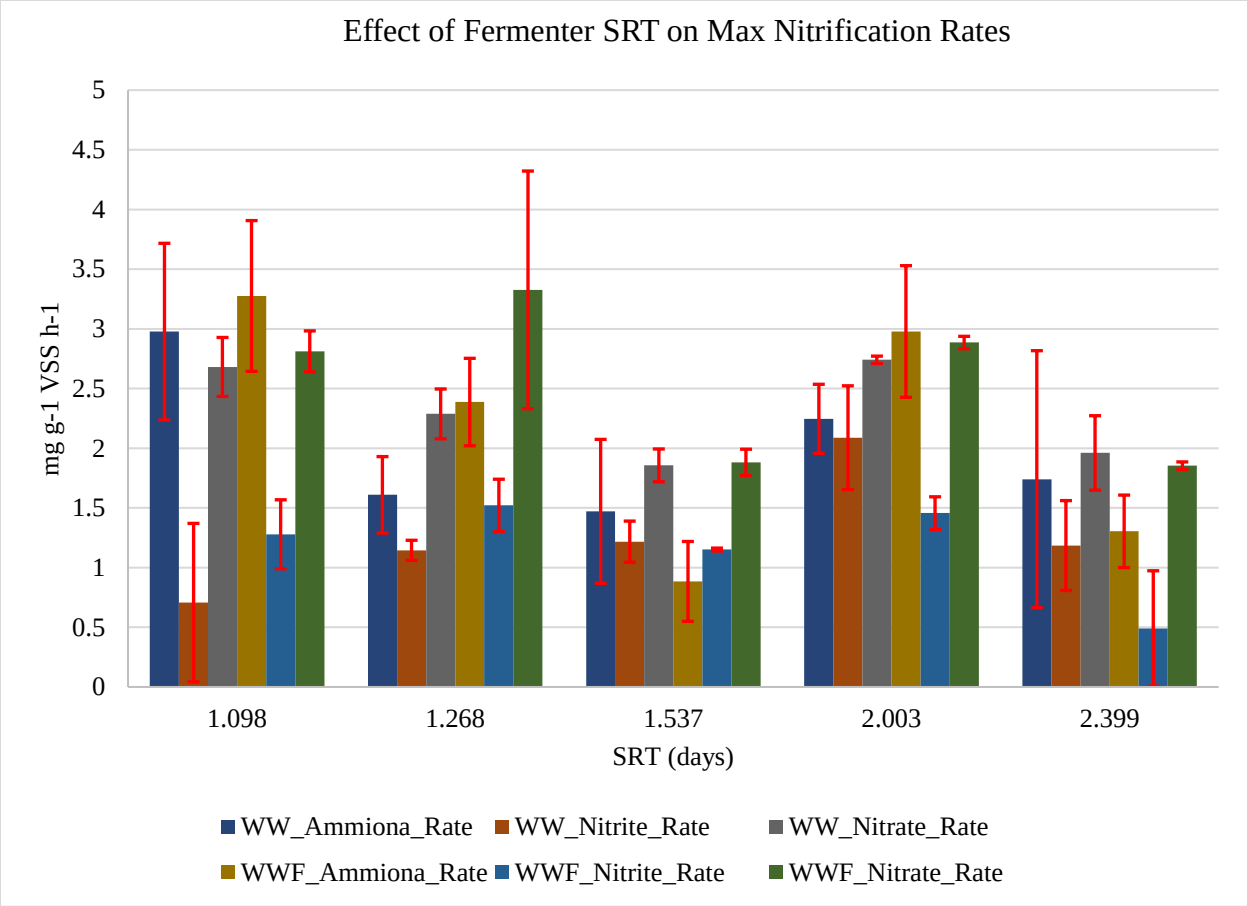

Figure 22: Maximum Nitrification Rate Test. WW represents samples with just oxic basin sludge, while WWF represents samples with oxic basin sludge and SSMLF supernatant.

Throughout the experiment, the maximum specific ammonium oxidation rate stayed between 1.47 and 2.98 mg N/gVSS-h for sludge collected from the oxidation ditch and varied slightly more, between 0.88 and 3.28 mg N/gVSS-h, for sludge from the oxidation ditch mixed with fermenter supernatant. The fermenter supernatant was added to a second reactor to test for inhibition of nitrification. The rates from this study were lower than specific nitrification rates found in literature for EBPR activated sludge, around 2-5 mg N/gVSS-h (Monti and Hall 2008, Onnis-Hayden et al. 2011). For three out of the five tested SRTs, there was a higher maximum specific ammonium oxidation rate for the fermenter supernatant plus oxidation ditch sludge

(mixed liquor) than there was for just oxidation ditch sludge, suggesting that the SSMLF supernatant was not inhibiting nitrification.

Since the duration of this test did not allow for the full oxidation of spiked ammonium to nitrate, there was an accumulation of nitrite during the experiment (van Loosdrecht et al. 2016). For the first two SRTs tested, the maximum specific nitrite accumulation rate was higher for the fermenter supernatant plus mixed liquor than there was for mixed liquor only. After an SRT of 1.3 days, the maximum specific nitrite accumulation rate was higher for the oxidation ditch sludge. The maximum specific nitrate production rate was higher for oxidation ditch sludge at each SRT than the fermenter supernatant plus oxidation ditch sludge.

4.4.2 Specific Oxygen Uptake Rate Test

The results of the Specific Oxygen Uptake Rate Tests (SOUR) used to indicate biomass activity in the WWTP can be seen below in Figure 23: Effect of Fermenter SRT on Specific Oxygen Uptake Rates. The blue bars represent the average endogenous SOUR at each stepwise increase of the fermenter SRT. The orange bars represent the average ammonia SOUR at each stepwise increase of the fermenter SRT. The grey bars represent the average nitrite SOUR at each stepwise increase of the fermenter SRT. The yellow bars represent the average acetate SOUR at each stepwise increase of the fermenter SRT. . The rate of oxygen uptake is stoichiometrically related to the rate of substrate removal, giving an indication of activity. These results show a general stability in all measured SOURs no matter the chemical spiked at each increased SRT except for SRT 2.4 days, which showed an increase from the rates obtained previously. The endogenous SOURs ranged from 1.69 ± 0.23 mg O_2 g^{-1} VSS h^{-1} at SRT 1.1 days to 2.44 ± 0.04 mg O_2 g^{-1} VSS h-1 at SRT 2.4 days. These numbers are lower than those reported in literature for EBPR activated sludge at 5.5 mg O_2 g^{-1} VSS h^{-1} or traditional activated sludge in

a BNR WWTP, between 3-5 mg O_2 g^{-1} VSS h^{-1} (Kristensen Holm et al. 1992, Zafiriadis et al. 2017). The SOUR results from the ammonia spike stayed the most stable between SRT 1.1 days and SRT 2.0 days than any of the other substrates tested with an average rate of 3.34 ± 0.19 mg O_2 g^{-1} VSS h^{-1}. This indicates the AOB population did not shift much over this duration of the experiment because their activity rates had little variation. The nitrite substrate spike resulted in a SOUR increase from 2.46 ± 0.23 mg O_2 g^{-1} VSS h^{-1} to 6.17 ± 2.23 mg O_2 g^{-1} VSS h^{-1} throughout the experiment. The nitrite SOUR gradually rose at each increased SRT before sharply rising at an SRT of 2.40 days, indicating greater activity from NOBs at each increased SRT. These results were confirmed by the maximum nitrification activity test which showed an increase in nitrite utilization at each increased SRT. The SOUR obtained from spiking 100mgL^{-1} sodium acetate to indicate the activity of heterotrophs within the WWTP ranged from 3.59 ± 1.81 mg O_2 g^{-1} VSS h^{-1} to 12.61 mg O_2 g^{-1} VSS h^{-1}. Again, these rates were consistently lower than those found in literature with an 100 mgL^{-1} acetate spike recording a SOUR of 16 mg O_2 g^{-1} VSS h^{-1} (Saad et al. 2016).

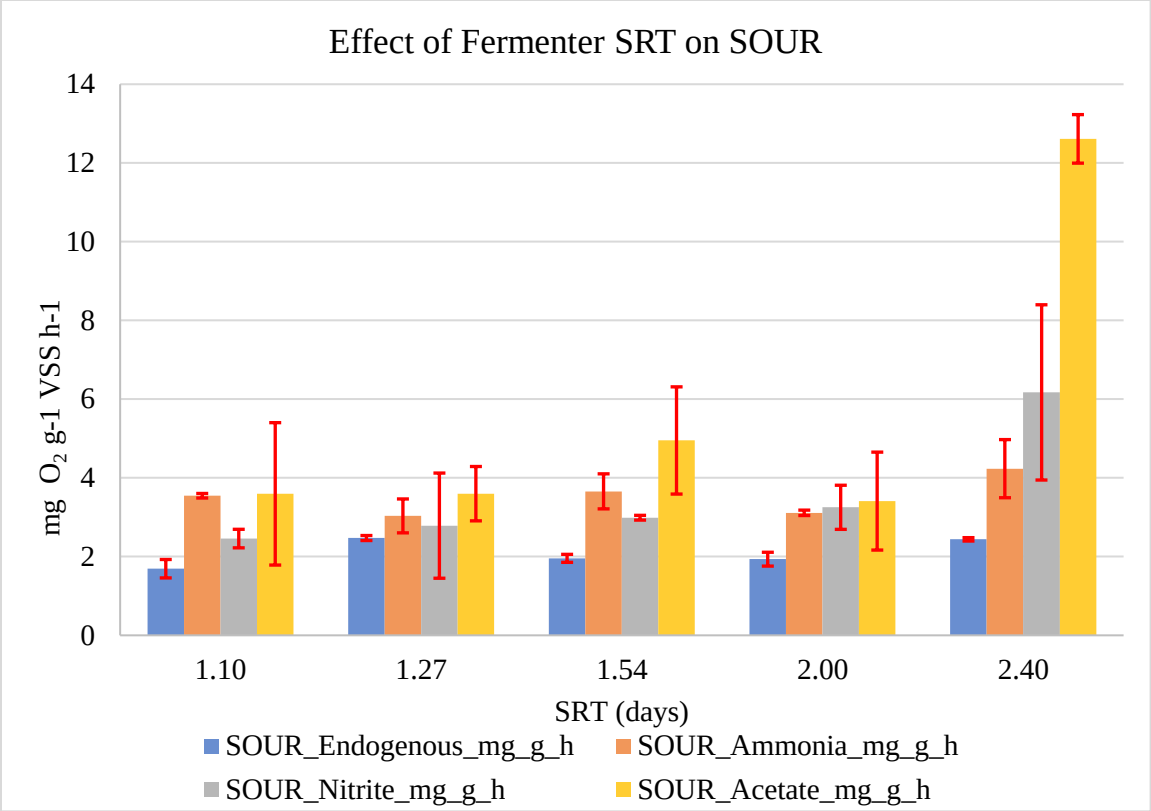

Figure 23: Effect of Fermenter SRT on Specific Oxygen Uptake Rates. The blue bars represent the average endogenous SOUR at each stepwise increase of the fermenter SRT. The orange bars represent the average ammonia SOUR at each stepwise increase of the fermenter SRT. The grey bars represent the average nitrite SOUR at each stepwise increase of the fermenter SRT. The yellow bars represent the average acetate SOUR at each stepwise increase of the fermenter SRT.

4.4.3. dPAO Activity Test

The dPAO activity test measures the activity of the dPAOs and PAOs within the WWTP bacterial community by calculating the rates of P release under anaerobic conditions and P uptake under both anoxic and aerobic conditions. The complete results of this test can be seen below in Figure 24.

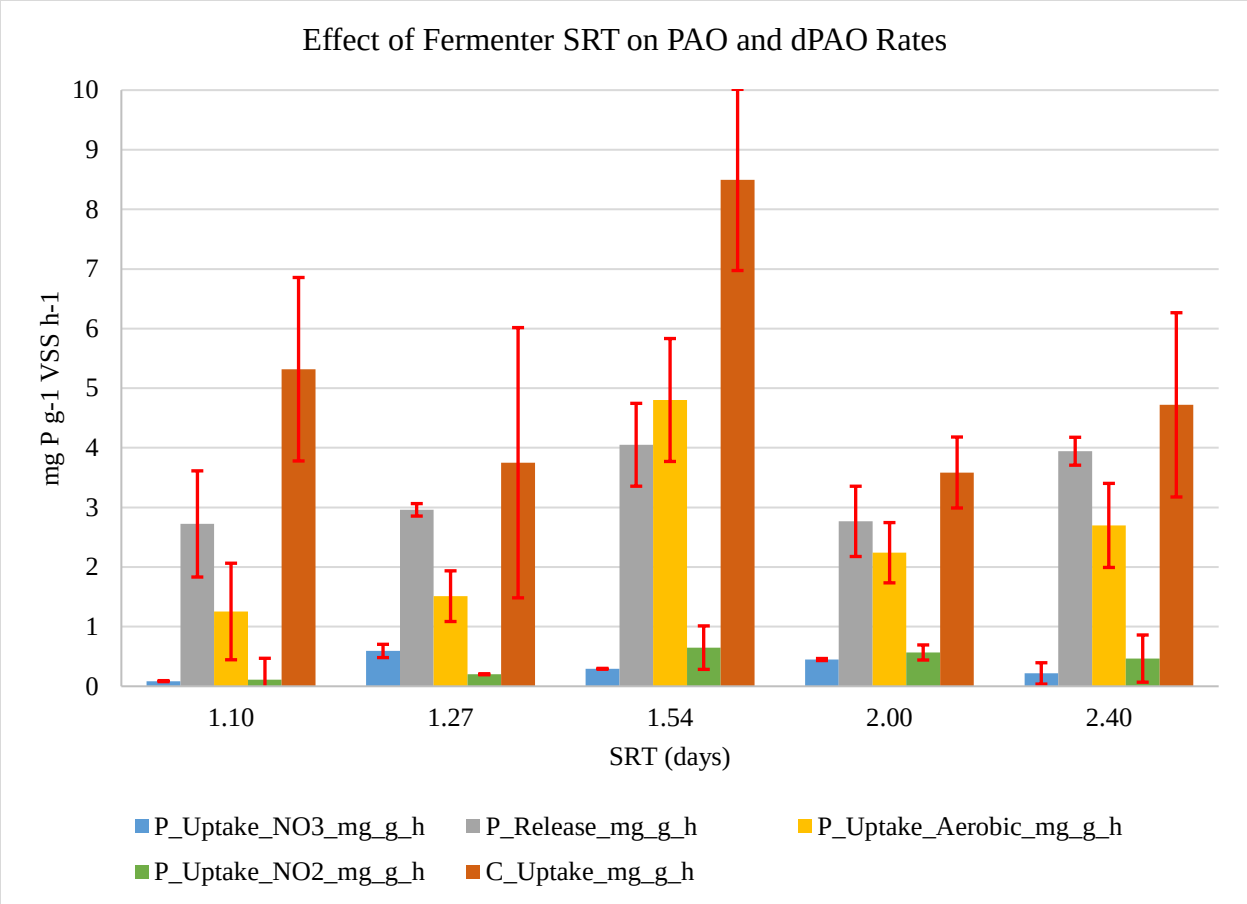

Figure 24: Effect of Fermenter SRT on dPAO and PAO Activity Rates

The phosphorus release rate was calculated in the famine phase of the batch activity test. These rates varied from 2.72 ± 0.89 mg P g^{-1} VSS h^{-1} at SRT 1.1 days to the highest rate of 4.05 ± 0.69 mg P g^{-1} VSS h^{-1} at the1.54-day SRT. These release rates showed low activity compared to literature values as has been the trend throughout the study's activity tests. Results in literature have many examples of higher P uptake ratios; see Table 1. However, a study by Vollertsen et al. 2006 testing activated sludge in an EBPR WWTP using a side stream fermenter with anerobic return found a P uptake rate consistent with this research at 1.15 mg P g^{-1} VSS h^{-1} (Vollertsen et al. 2006). Two different studies in 2008 looking at a combined total of 11 different EBPR WWTPs showed a great variability in both P uptake and release ratios ranging from 5.6 to 31.9

mg P g^{-1} VSS h^{-1} across all plants with good phosphorus removal (Gu et al. 2008, He et al. 2008). This shows that low activity rates are not always an indicator of poor P removal.

As mentioned in the literature section of this paper, P release/C uptake ratios are also a highly discussed result of activity tests. The P release/ C uptake ratio results can be seen below in Figure 25: Effect of Fermenter SRT on P Release:Ac Uptake Ratio. During the first two SRTs the P:Ac (mg L^{-1} P: mg L^{-1} Ac) ratio indicated the presence of GAOs within the sludge because the reported ratio was below 0.5 (Gu et al. 2008, Schuler and Jenkins 2003). For the remainder of this experiment (SRTs > 1.54 d), the ratio indicates that PAOs are more prevalent than GAOs in the WWTP. At SRTs 1.54 days and 2.40 days, the ratio was between 0.5 - 0.7, which has indicates PAOs are using the glycolytic pathway (Acevedo et al. 2012, Welles et al. 2015, Zhou et al. 2008). This is because the PAOs need to make up for the lack of ATP formed from poly-P hydrolysis when there is a low amount of poly-P available. At SRT 2.0 days, the ratio of P:Ac was 0.80, which indicates the PAOs within the WWTP changed their dominant metabolic pathway to the TCA cycle. This happens under conditions where poly-P is not limiting, and as a result have a much higher P release/ C uptake (P:Ac) ratio greater than 0.7 (Acevedo et al. 2012, Welles et al. 2015).

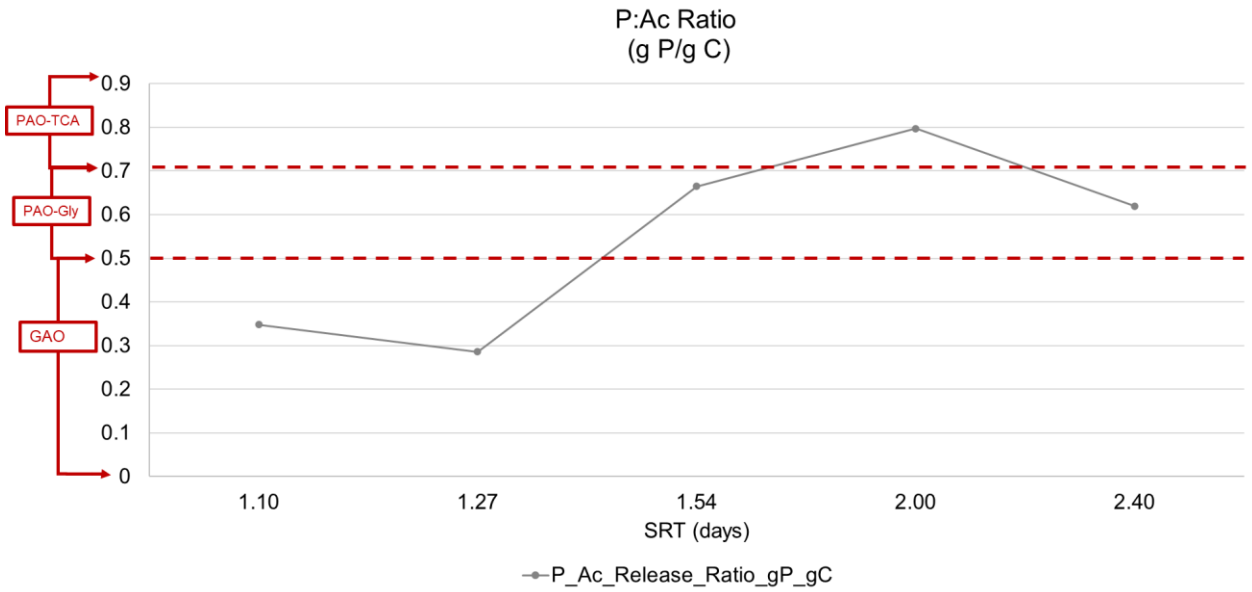

Figure 25: Effect of Fermenter SRT on P Release:Ac Uptake Ratio

Finally, the rate of P uptake was also measured under both aerobic and anoxic conditions, for PAO and dPAO activity, respectively. Since the anoxic reactor did not have O_2 available as a terminal electron acceptor, all the P uptake in this reactor is assumed to be performed by dPAOs only and not PAOs. The results of the different P uptake rates can be seen below in Figure 26. The highest P aerobic uptake rates were at the 1.54-day SRT, recording 4.80 ± 1.03 mg P g^{-1} VSS h^{-1}, while the lowest, at an SRT of 1.1 days, was 1.25 ± 0.81 mg P g^{-1} VSS h^{-1}. The SRT for the greatest P uptake aerobically corresponded to the highest uptake rate under anoxic conditions with NO_2 as the terminal electron acceptor. The P uptake rate under anoxic conditions ranged from 0.65 ± 0.37 mg P g^{-1} VSS h^{-1} to 0.09 ± 0.01 mg P g^{-1} VSS h^{-1}. The P uptake rates of this study are in the lower range of previously published rates ranging from 1.9 - 30 mg P g^{-1} VSS h^{-1} for aerobic uptake to 3.0 - 17.3 mg P g^{-1} VSS h^{-1} for anoxic uptake (He et al. 2008, Kuba et al. 1993, Lee et al. 2001, Zeng et al. 2003b). These low rates could be an indicator of an older, more inactive sludge, or it could also be a result of not all of the acetate being taken up in the anaerobic phase. This means both an electron donor (acetate) and a terminal electron acceptor

(either O_2, NO_2 or NO_3) were present during the P uptake phase (Zafiriadis et al. 2017). The IC data of each run indicated that approximately 100 mgL^{-1} of acetate remained in the reactors at the start of either the aerobic or anoxic phase, which could have caused lower P uptake rates. To help minimize this issue, uptake rates were calculated from samples collected between 60-120 min.

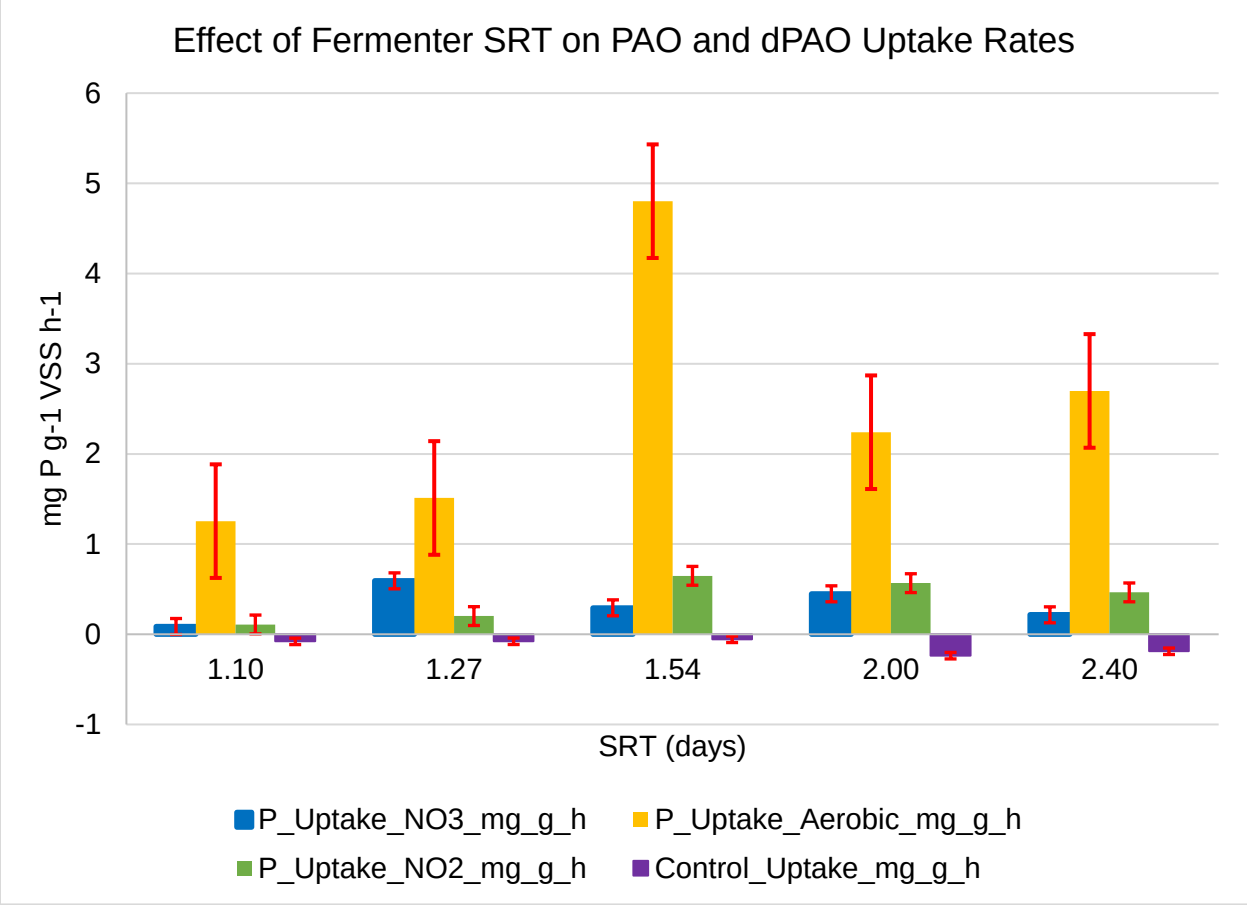

Figure 26: Effect of Fermenter SRT on P Uptake Rates

4.4.4 Sludge Volume Index

Sludge Volume Index (SVI) was used to determine settleability at each SRT during this experiment. As described earlier, SVI was recorded at both the 5 min and 30 min mark. The results from the SVI tests throughout this study can be seen below in Figure 27, while an example of the test set up and results can be seen in Figure *28*.

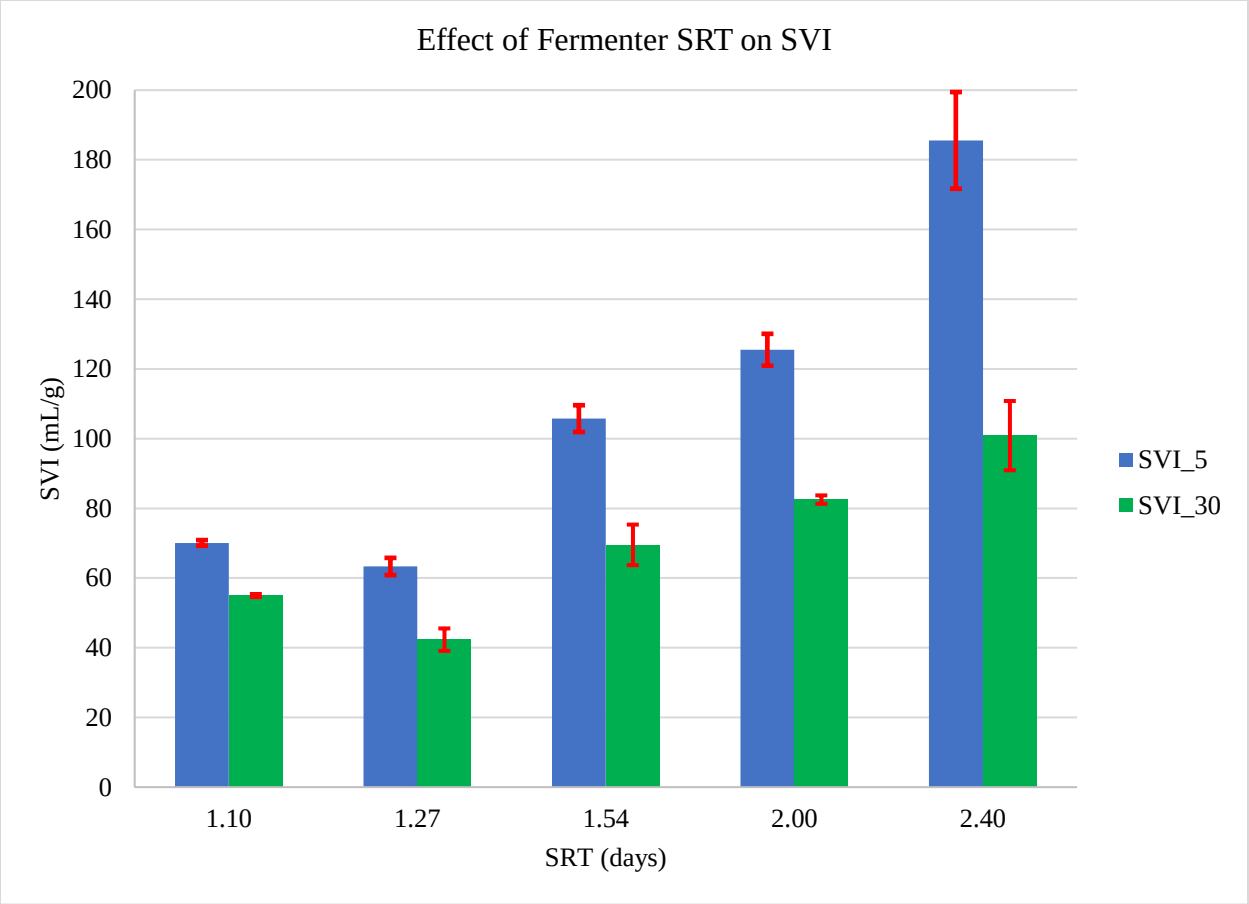

Figure 27: Effect of Fermenter SRT on SVI

The SVI_5 in this study ranged from 63 ± 3 mL/g to 186 ± 14 mL/g, while SVI_{30} varied from 42 ± 3 mL/g to 101 ± 10 mL/g. Traditionally good settling sludge is below 150 mL/g, while less than 80 mL/g is desirable (Metcalf et al. 2003). Since the SVI_{30} was below 100 mL/g throughout the experiment, it was concluded the sludge maintained good settling at all tested SRTs. The SVI_{30} found in this experiment is lower than values found in literature for EBPR activated sludge systems. In an extensive study of nine EBPR plants, Schuler and Jang 2007 cited the average EBPR plant's SVI_{30} at 130 ± 49 mgL^{-1} (Schuler and Jang 2007). In general, activated sludge from EBPR plants is expected to have better settleability, lower SVI_{30}, because of the contribution of phosphate density within PAOs and dPAOs present in EBPR sludges compared to non-EBPR sludges (Schuler and Jang 2007, Winkler et al. 2011).

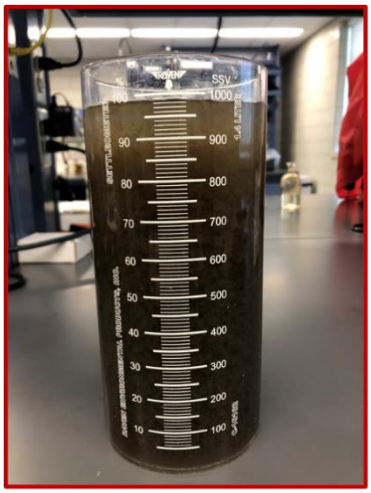

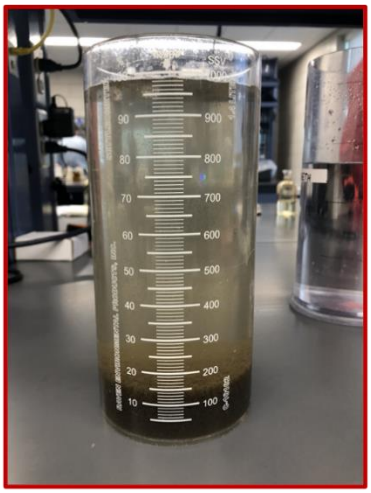

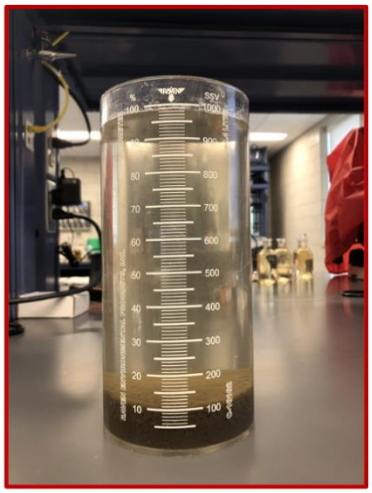

Figure 28: SVI Example Results

4.5 Microbial Results

Obtaining the microbial results was not without its fair share of unforeseen obstacles, including a global pandemic. Despite these hurdles, the results in this section correlate an increase in the PAO population throughout the WWTP with an increase in SRT from 1.1 to 2.4 days. Statistical analysis of the microbial results revealed both datasets from the qPCR and FISH experiments were positively correlated with SRT. The FISH dataset was significantly positively correlated with the SRT of the SSMLF with a correlation coefficient of 0.79 and a p-value less than 0.05. The qPCR dataset had a positive correlation coefficient of 0.46 with SRT, and a p-value less than 0.05. The microbial results show a stronger relationship with fermenter SRT when compared to the activity dataset, but not as strong a correlation as VFAs generated.

4.5.1 FISH

FISH revealed a steady increase in the abundance of PAOs in the anaerobic basin throughout the experiment,

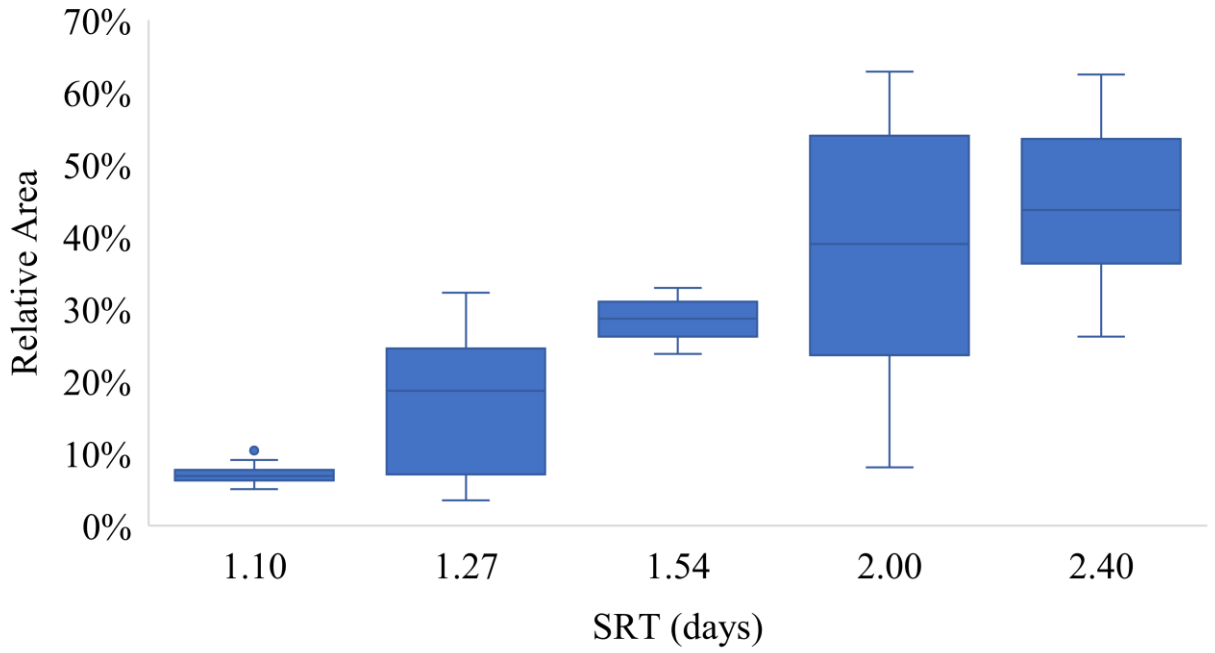

Figure 29

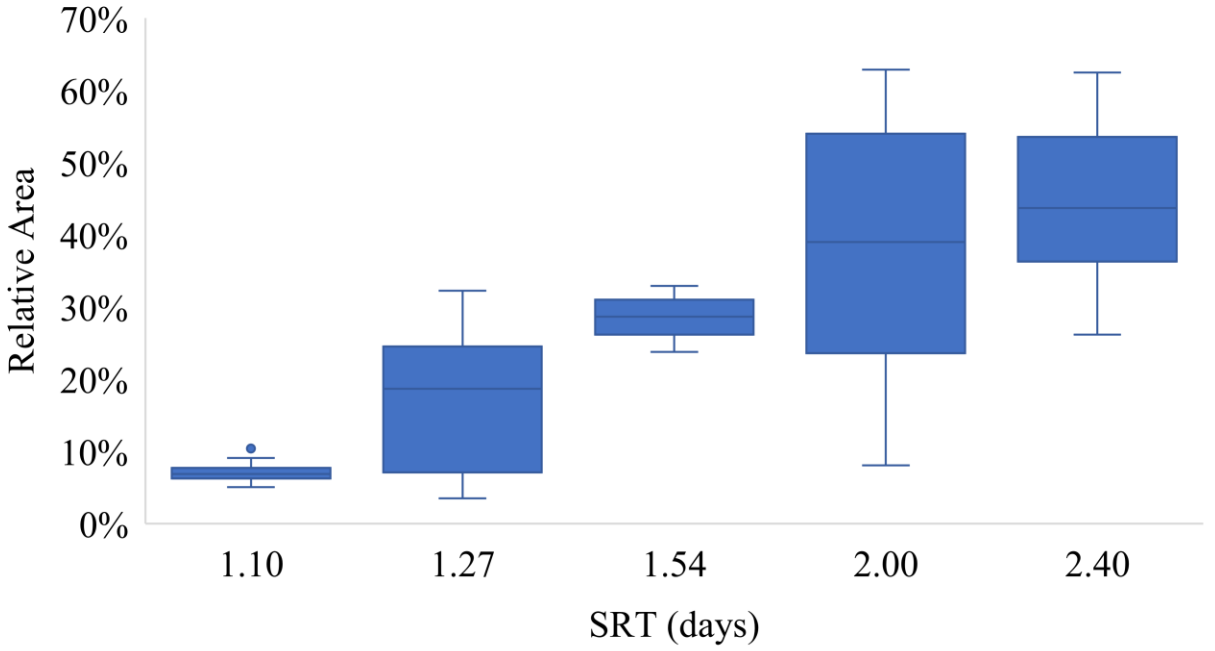

Figure 29: FISH Results Showing Impact of Fermenter SRT on Abundance of PAOs SRT 1.1 days had 7.1 ± 1.2% mean relative area of PAOs/EUB compared to a mean area of 44.7 ± 9.7% for an SRT of 2.4 days. This was an increase of 37% across the duration of the experiment, indicating that as the SRT in the fermenter increased so did the amount of PAOs available to perform EBPR.

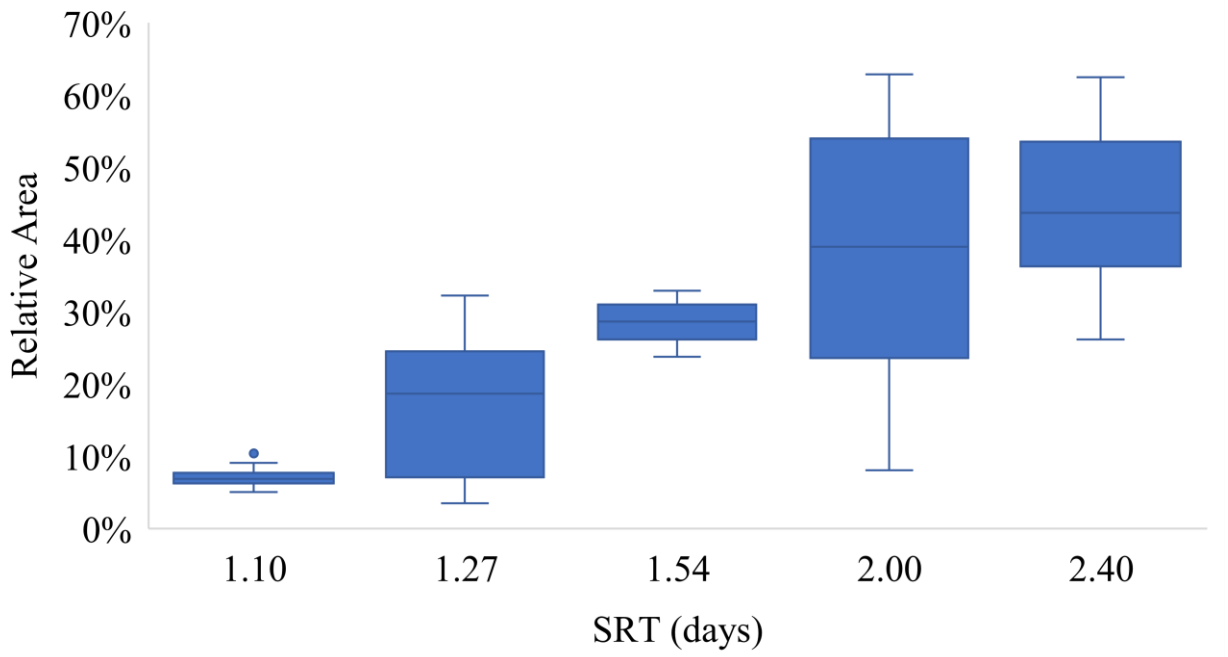

Figure 29: FISH Results Showing Impact of Fermenter SRT on Abundance of PAOs

In Figure 30 below, you can see the increase in the number of bacteria hybridized by the PAO probes from 1.1-day SRT (panel a) to 2.4-day SRT (panel d). Previous studies found the relative abundance of PAOs to be between 5 - 24% of all bacteria (Gu et al. 2008, He et al. 2008, Mielczarek et al. 2013). Studies of SBRs using FISH have shown a higher percentage of PAOs. A study by Carvalho et al. 2007 with acetate as the only carbon source found the PAO relative abundance to be 37 ± 2%, similar to the results of this study at an SRT of 2 days (Carvalho et al. 2007). These results suggest that the increase in the SRT of an SSMLF could increase the PAO population within a WWTP above percentages typically seen in a traditional configuration of

EBPR WWTP. In this study, the relative percentage of PAOs approached levels seen previously only by enriched sludges in SBRs.

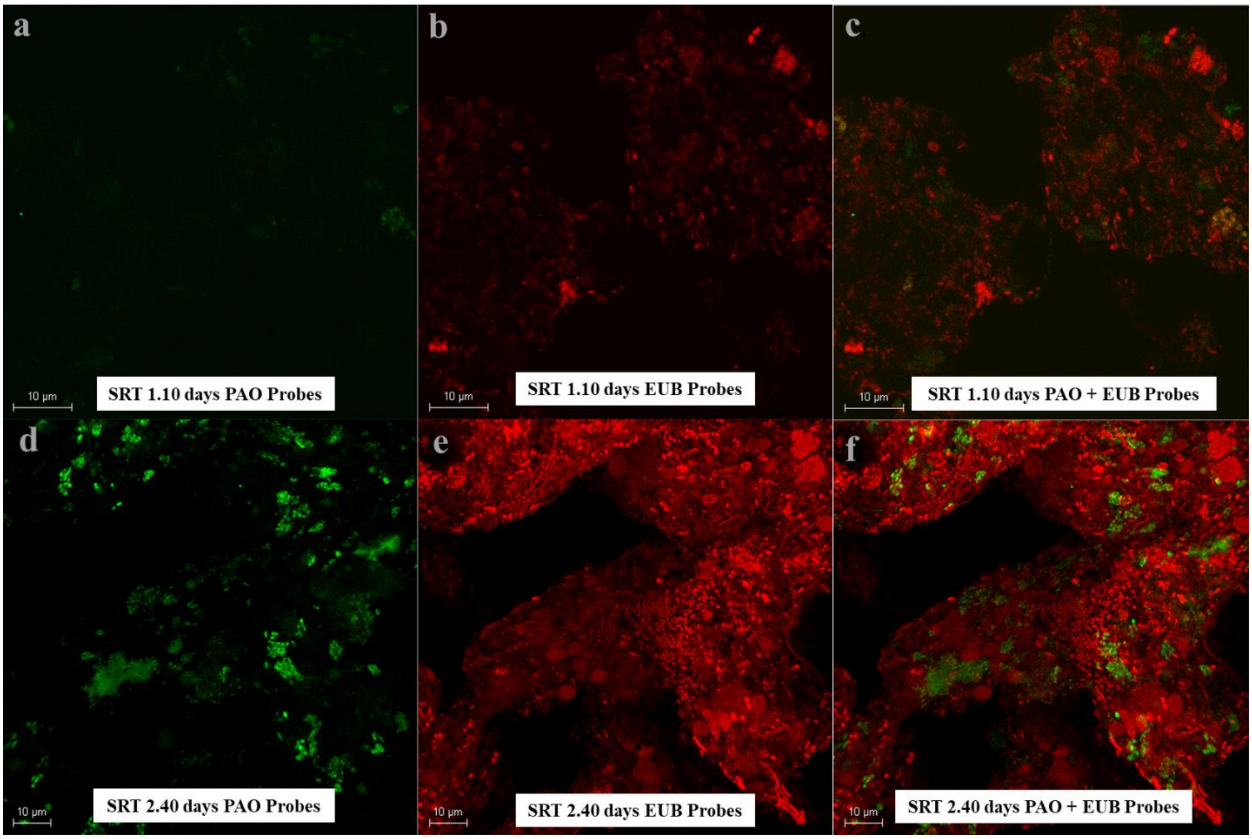

Figure 30: FISH Results observed under LSCM with 100x objective, scale bar represents 10 µm in all panels. a. PAOs hybridized at 1.1 days SRT; b. All bacteria hybridized with EUB probes at 1.1 days SRT; c. Overlay of images a and b; d. PAOs hybridized at 2.4 days SRT; e. All bacteria hybridized with EUB probes at 2.4 days SRT; f. Overlay of images d and e

4.5.2 qPCR

The qPCR results can be seen below in Figure 31. These results show a similar trend to those from the FISH results. As SRT in the SSMLF increased, so did the abundance of PAOs, normalized to all bacteria as measured by the 16s rRNA gene. To determine the relative abundance of PAOs, the LinRegPCR program first calculated the quantification cycle (Cq) or number of cycles needed to reach the fluorescence threshold (Ruijter et al. 2009). From the Cq value, a starting concentration (N0) is calculated for either the PAOs or GAOs. This number is given in

arbitrary units and must be divided by the N0 of the 16S reference genes to determine the gene expression ratio (Ruijter et al. 2009). From an SRT of 1.1 days to an SRT of 2.4 days, there was an increase of 8% from 5 ± 1% to 13 ± 10%. These results estimate a lower abundance of PAOs than FISH but still report an increasing trend (Ruijter et al. 2009). These results are similar to those obtained by Islam et al. in 2017, which found PAOs to be 8.7% of total bacteria by qPCR in a sidestream EBPR WWTP (Islam et al. 2017). When compared to smaller-scale reactors for EBPR, the relative abundance of PAOs reported in this study was lower than those obtained in the pilot and bench-scale reactors (Camejo et al. 2016).

As shown in Figure *31*, the abundance of GAOs throughout the experiment remained below one percent throughout this experiment at every SRT. The qPCR 96 well plate with the GAO primers in the supermix did have some significant evaporation in 10 wells, and those were excluded from quantification analysis. Nevertheless, there is a clear trend that GAOs throughout this experiment did not make up a significant percentage of the bacterial population in the WWTP. These results confirm those found in pilot and full-scale EBPR plant studies of microbial communities in EBPR, finding GAOs to be in similarly low relative abundance or not detected (Camejo et al. 2016, Islam et al. 2017).

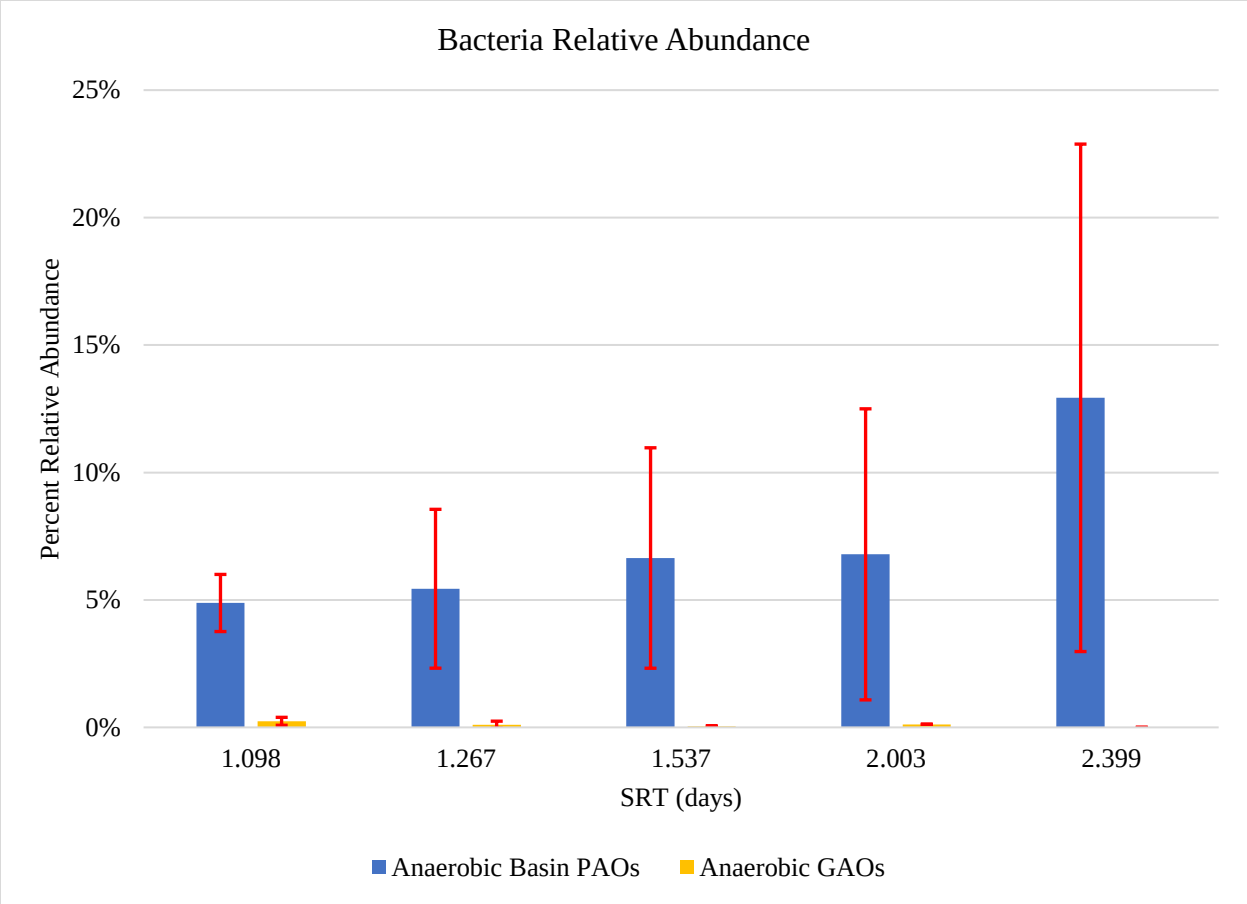

Figure 31: Results of qPCR

4.5.3 Neisser Staining

Neisser staining was performed on ten samples collected from the anaerobic basin on the same days of the PAO activity test. Most available protocols on Neisser staining recommend staining fresh samples, but since the samples for this experiment were stored at -20°C, an additional analysis was carried out to test the effects of freezing a sample on Neisser staining results. The results in this experiment did not show a noticeable difference in the amount of staining between the fresh sample and those kept at -20°C before staining. These results, that Neisser staining can be successful without the use of fresh samples, are consistent with results from Crocetti et al. 2000, who completed Neisser staining on samples that had previously undergone FISH and still showed Neisser-positive results on poly-p containing bacteria (Crocetti et al. 2000).

All tested samples had colonies of Neisser-positive cells, which appeared a blue/purple color under bright field 100x oil immersion magnification. These results support the observation of PAOs increasing relative abundance with SRT. Neisser staining has been used throughout the literature to confirm the results obtained through FISH. While FISH targets RNA specific to PAOs, Neisser stains the intercellular storage of poly-P (Crocetti et al. 2000, Kong et al. 2005, Welles et al. 2015). Examples of these images are not included in this report because of technical issues with the microscope camera and labwork being halted due to the COVID-19 pandemic.

5.0 Conclusions

Although EBPR is common practice in municipal wastewater treatment to meet declining effluent TP limits, the sidestream fermenter in the Bardenpho configuration of a WWTP is a relatively new design. This configuration has proven challenging to model, and because of this, it is missing research on ideal operating conditions to maximize the selection of PAOs and dPAOs. The sidestream fermenter process contributes to an improved VFA:TP ratio necessary for EBPR within the WWTP without the cost of adding additional carbon essential to support an increased PAO and dPAO population for P removal.

This study aimed to optimize a three-stage Bardenpho WWTP with sidestream fermenter to select for dPAOs and PAOs through the stepwise increase of the SRT of the SSMLF from 1.1 to 2.4 days. The optimization of the performance of the nutrient removal plant was tracked and confirmed through collected operational data, batch activity tests, and microbial analysis. The dPAO activity indicated the presence of dPAOs, which used both nitrite and nitratenitrate as terminal electron acceptors in an anoxic reactor while taking up phosphorus. The FISH probes and qPCR primers showed evidence of a bacterial community of PAOs, which increased in abundance from an SRT of 1.1 days to an SRT of 2.4 days. These probes and primers, however,

were unable to quantify *Tetrasphaera* dPAOs. Operational data showed the increase of not only the amount but diversity of VFAs created by the SSMLF as SRT increased from 1.1 days to 2.0 days. There was a slight dip in VFA production at 2.4 days SRT, but this decrease was not reflected in total P removal performance by the plant. The average temperature of the basins decreased to 18.03 ± 0.219°C during this time, and this lower production of VFAs could not be solely attributed to the increased SRT, but also could have been due to the lower average temperature. The batch activity tests, SOURs, max nitrification rate tests, dPAO activity tests, and SVI results confirmed there is bacterial activity within the WWTP capable of removing nutrients at each stepwise increase of the SSMLF. However, the results of these tests showed lower activity rates than previous studies of EBPR WWTPs, pilot studies, and SBR studies. Despite the low activity, the population of bacteria remained resilient throughout the study and maintained P removal rates over 96% throughout the study. The P/Ac ratio between SRT 1.1 and 1.3 days indicated the presence of GAOs in the WWTP, however the presence of GAOs were not confirmed in qPCR. Since the precene of dPAOs was not accounted for by FISH or qPCR quantification dPAOs, which have always had lower published activity rates could have been responsible for a majority of P release at this time. Then as the PAO population increased as confirmed in FISH and qPCR analysis so did the P/Ac ratio.Most promising of all were the microbial analysis results, which showed an increase in the PAO population of 37% through quantitative FISH and a rise of 8% through qPCR. These results showed similar percentages of PAO populations in consistently high-performing EBPR WWTPs.

In this study, high P removal percentages can be achieved, without the added expense of supplemental carbon, in a WWTP with a low influent rbCOD:TP ratio by adjusting the SRT of the sidestream fermenter. The population of bacteria in a WWTP with a SSMLF in a three-stage

Bardenpho configuration in this study was robust and resilient and can achieve an increase in percent P removed over a range of SRTs. Over the duration of the experiment, the concentration of TP in the effluent averaged 0.134 mg L^{-1} TP ± 0.076 mg L^{-1}. TN in the effluent averaged 8.228 mg L^{-1}TN ± 2.038 mg L^{-1}, showing resiliency over the 15 weeks. Based on the results of this study, a sidestream fermenter should be operated around an SRT of 2.0 days to optimize VFA creation to select for PAOs that complete EBPR.

5.1 Future Research

Further research is necessary to explore the tipping point or methanogensis of an SSMLF in a Bardenpho EBPR WWTP. This study took the SRT of the SSMLF out to 2.4 days; however, methanogenesis was not reached. Finding the tipping point of this configuration would help WWTP operators by giving them high and low limits to operate within and allow them the flexibility to make adjustments based on current operating conditions. Additionally, further research is needed on the bacteria responsible for simultaneous denitrification and phosphorous removal (dPAOs) to create additional primer and probes for dPAOs. These developments will allow for higher quality qPCR and FISH analysis with an increased range of bacteria able to be quantified.

Works Cited

Acevedo, B., Oehmen, A., Carvalho, G., Seco, A., Borrás, L. and Barat, R. (2012) Metabolic shift of polyphosphate-accumulating organisms with different levels of polyphosphate storage. Water Research 46(6), 1889-1900.

Amann, R.I., Binder, B.J., Olson, R.J., Chisholm, S.W., Devereux, R. and Stahl, D.A. (1990) Combination of 16S rRNA-targeted oligonucleotide probes with flow cytometry for analyzing mixed microbial populations. Applied and Environmental Microbiology 56(6), 1919-1925.

Andreasen, K., Petersen, G., Thomsen, H. and Strube, R. (1997) Reduction of nutrient emission by sludge hydrolysis. Water Science and Technology 35(10), 79-85.

APHA, A.P.H.A., Association, A.W.W., Federation, W.P.C. and Federation, W.E. (2017) Standard methods for the examination of water and wastewater, American Public Health Association.

Barnard, J., Dunlap, P. and Steichen, M. (2017) Rethinking the Mechanisms of Biological Phosphorus Removal.

Barnard, J., Houweling, D., Analla, H. and Steichen, M. (2012) Saving phosphorus removal at the Henderson NV plant. Water Science and Technology 65(7), 1318-1322.

Barnard, J.L. (1976) A review of biological phosphorus removal in the activated sludge process. Water SA 2(3), 136-144.

Bouchez, T., Patureau, D., Dabert, P., Juretschko, S., Dore, J., Delgenes, P., Moletta, R. and Wagner, M. (2000) Ecological study of a bioaugmentation failure. Environmental microbiology 2(2), 179-190.

Brdjanovic, D., Loosdrecht, M.C.v., Hooijmans, C.M., Alaerts, G.J. and Heijnen, J.J. (1997) Temperature effects on physiology of biological phosphorus removal. Journal of environmental engineering 123(2), 144-153.

Camejo, P.Y., Owen, B.R., Martirano, J., Ma, J., Kapoor, V., Santo Domingo, J., McMahon, K.D. and Noguera, D.R. (2016) Candidatus Accumulibacter phosphatis clades enriched under cyclic anaerobic and microaerobic conditions simultaneously use different electron acceptors. Water Research 102, 125-137.

Carvalho, G., Lemos, P.C., Oehmen, A. and Reis, M.A.M. (2007) Denitrifying phosphorus removal: Linking the process performance with the microbial community structure. Water Research 41(19), 4383-4396.

Comeau, Y., Hall, K.J., Hancock, R.E.W. and Oldham, W.K. (1986) Biochemical model for enhanced biological phosphorus removal. Water Research 20(12), 1511-1521.

Comeau, Y., Oldham, W.K. and Hall, K.J. (1987) Biological Phosphate Removal from Wastewaters. Ramadori, R. (ed), pp. 39-55, Pergamon.

Cordell, D., Drangert, J.-O. and White, S. (2009) The story of phosphorus: Global food security and food for thought. Global Environmental Change 19(2), 292-305.

Crocetti, G.R., Hugenholtz, P., Bond, P.L., Schuler, A., Keller, J., Jenkins, D. and Blackall, L.L. (2000) Identification of Polyphosphate-Accumulating Organisms and Design of 16S rRNA-Directed Probes for Their Detection and Quantitation. Applied and Environmental Microbiology 66(3), 1175-1182.

Daims, H., Brühl, A., Amann, R., Schleifer, K.-H. and Wagner, M. (1999) The Domain-specific Probe EUB338 is Insufficient for the Detection of all Bacteria: Development and Evaluation of a more Comprehensive Probe Set. Systematic and Applied Microbiology 22(3), 434-444.

Egle, L., Rechberger, H., Krampe, J. and Zessner, M. (2016) Phosphorus recovery from municipal wastewater: An integrated comparative technological, environmental and economic assessment of P recovery technologies. Science of The Total Environment 571, 522-542.

Ekama, G., Dold, P. and Marais, G.v.R. (1986) Procedures for determining influent COD fractions and the maximum specific growth rate of heterotrophs in activated sludge systems. Water Science and Technology 18(6), 91-114.

Flowers, J.J., Cadkin, T.A. and McMahon, K.D. (2013) Seasonal bacterial community dynamics in a full-scale enhanced biological phosphorus removal plant. Water Research 47(19), 7019-7031.

Gu, A.Z., Saunders, A., Neethling, J., Stensel, H. and Blackall, L. (2008) Functionally relevant microorganisms to enhanced biological phosphorus removal performance at full-scale wastewater treatment plants in the United States. Water Environment Research 80(8), 688-698.

He, S., Gall, D.L. and McMahon, K.D. (2007) “Candidatus Accumulibacter” Population Structure in Enhanced Biological Phosphorus Removal Sludges as Revealed by Polyphosphate Kinase Genes. Applied and Environmental Microbiology 73(18), 5865-5874.

He, S., Gu, A.Z. and McMahon, K.D. (2008) Progress toward understanding the distribution of Accumulibacter among full-scale enhanced biological phosphorus removal systems. Microbial ecology 55(2), 229-236.

Hesselmann, R.P.X., von Rummell, R., Resnick, S.M., Hany, R. and Zehnder, A.J.B. (2000) Anaerobic metabolism of bacteria performing enhanced biological phosphate removal. Water Research 34(14), 3487-3494.

Houweling, D., Dold, P. and Barnard, J. (2010) Theoretical limits to biological phosphorus removal: rethinking the influent COD: N: P ratio. Proceedings of the Water Environment Federation 2010(9), 7044-7059.

Islam, M.S., Zhang, Y., Dong, S., McPhedran, K.N., Rashed, E.M., El-Shafei, M.M., Noureldin, A.M. and Gamal El-Din, M. (2017) Dynamics of microbial community structure and nutrient removal from an innovative side-stream enhanced biological phosphorus removal process. Journal of Environmental Management 198, 300-307.

Jabari, P., Munz, G. and Oleszkiewicz, J.A. (2014) Selection of denitrifying phosphorous accumulating organisms in IFAS systems: Comparison of nitrite with nitrate as an electron acceptor. Chemosphere 109, 20-27.

Janssen, P., Meinema, K. and Van der Roest, H. (2002) Biological phosphorus removal, IWA publishing.

Kassambara, A. (2019) ggpubr: 'ggplot2' Based Publication Ready Plots.

Kishida, N., Kim, J., Tsuneda, S. and Sudo, R. (2006) Anaerobic/oxic/anoxic granular sludge process as an effective nutrient removal process utilizing denitrifying polyphosphate-accumulating organisms. Water Research 40(12), 2303-2310.

Kobylinski, E., Van Durme, G., Barnard, J., Massart, N. and Koh, S.-H. (2008) How biological phosphorous removal is inhibited by collection system corrosion and odor control practices. Proceedings of the Water Environment Federation 2008(15), 1719-1735.

Kobylinski, E.A., Barnard, D.J.L., Harger, M., Morris, L., Sturm, D.B. and Keller, J. (2019) Start-up of a 3 Stage Bardenpho WWTP with a MLSS Sidestream Fermenter.

Kong, Y., Nielsen, J.L. and Nielsen, P.H. (2005) Identity and ecophysiology of uncultured actinobacterial polyphosphate-accumulating organisms in full-scale enhanced biological phosphorus removal plants. Appl. Environ. Microbiol. 71(7), 4076-4085.

Kong, Y., Ong, S.L., Ng, W.J. and Liu, W.-T. (2002) Diversity and distribution of a deeply branched novel proteobacterial group found in anaerobic–aerobic activated sludge processes. Environmental microbiology 4(11), 753-757.

Kristensen Holm, G., Elberg Jørgensen, P. and Henze, M. (1992) Characterization of functional microorganism groups and substrate in activated sludge and wastewater by AUR, NUR and OUR. Water Science and Technology 25(6), 43-57.

Kristiansen, R., Nguyen, H.T.T., Saunders, A.M., Nielsen, J.L., Wimmer, R., Le, V.Q., McIlroy, S.J., Petrovski, S., Seviour, R.J., Calteau, A., Nielsen, K.L. and Nielsen, P.H. (2012) A metabolic model for members of the genus Tetrasphaera involved in enhanced biological phosphorus removal. The Isme Journal 7, 543.

Kuba, T., Smolders, G., van Loosdrecht, M.C.M. and Heijnen, J.J. (1993) Biological Phosphorus Removal from Wastewater by Anaerobic-Anoxic Sequencing Batch Reactor. Water Science and Technology 27(5-6), 241-252.

Lee, D.S., Jeon, C.O. and Park, J.M. (2001) Biological nitrogen removal with enhanced phosphate uptake in a sequencing batch reactor using single sludge system. Water Research 35(16), 3968-3976.

Levin, G.V. (1971) Phosphorus Removal by Luxury Uptake Communication. Jour. Water Poll. Control Fed 43, 1972.

Lopez-Vazquez, C.M., Oehmen, A., Hooijmans, C.M., Brdjanovic, D., Gijzen, H.J., Yuan, Z. and van Loosdrecht, M.C. (2009) Modeling the PAO–GAO competition: effects of carbon source, pH and temperature. Water Research 43(2), 450-462.

Marques, R., Santos, J., Nguyen, H., Carvalho, G., Noronha, J.P., Nielsen, P.H., Reis, M.A.M. and Oehmen, A. (2017) Metabolism and ecological niche of Tetrasphaera and Ca. Accumulibacter in enhanced biological phosphorus removal. Water Research 122, 159-171.

Meijer, S.C.F., van Loosdrecht, M.C.M. and Heijnen, J.J. (2002) Modelling the start-up of a full-scale biological phosphorous and nitrogen removing WWTP. Water Research 36(19), 4667-4682.

Melia, P.M., Cundy, A.B., Sohi, S.P., Hooda, P.S. and Busquets, R. (2017) Trends in the recovery of phosphorus in bioavailable forms from wastewater. Chemosphere 186, 381-395.

Metcalf, L., Eddy, H.P. and Tchobanoglous, G. (2003) Wastewater engineering: treatment, disposal, and reuse, McGraw-Hill New York.

Mielczarek, A.T., Nguyen, H.T.T., Nielsen, J.L. and Nielsen, P.H. (2013) Population dynamics of bacteria involved in enhanced biological phosphorus removal in Danish wastewater treatment plants. Water Research 47(4), 1529-1544.

Mino, T., Arun, V., Tsuzuki, Y. and Matsuo, T. (1987) Biological Phosphate Removal from Wastewaters. Ramadori, R. (ed), pp. 27-38, Pergamon.

Mino, T., van Loosdrecht, M.C.M. and Heijnen, J.J. (1998) Microbiology and biochemistry of the enhanced biological phosphate removal process. Water Research 32(11), 3193-3207.

Mohlman, F.W. (1934) The Sludge Index. Sewage Works Journal 6(1), 119-122.

Monclús, H., Sipma, J., Ferrero, G., Rodriguez-Roda, I. and Comas, J. (2010) Biological nutrient removal in an MBR treating municipal wastewater with special focus on biological phosphorus removal. Bioresource Technology 101(11), 3984-3991.

Monti, A. and Hall, E.R. (2008) Comparison of Nitrification Rates in Conventional and Membrane-Assisted Biological Nutrient Removal Processes. Water Environment Research 80(6), 497-506.

Moser-Engeler, R., Udert, K.M., Wild, D. and Siegrist, H. (1998) Products from primary sludge fermentation and their suitability for nutrient removal. Water Science and Technology 38(1), 265-273.

Mulkerrins, D., Dobson, A.D.W. and Colleran, E. (2004) Parameters affecting biological phosphate removal from wastewaters. Environment International 30(2), 249-259.

Nguyen, H.T.T., Le, V.Q., Hansen, A.A., Nielsen, J.L. and Nielsen, P.H. (2011) High diversity and abundance of putative polyphosphate-accumulating Tetrasphaera-related bacteria in activated sludge systems. FEMS Microbiology Ecology 76(2), 256-267.

Nielsen, P.H., Daims, H., Lemmer, H., Arslan-Alaton, I. and Olmez-Hanci, T. (2009) FISH handbook for biological wastewater treatment, Iwa publishing.

Oehmen, A., Lemos, P.C., Carvalho, G., Yuan, Z., Keller, J., Blackall, L.L. and Reis, M.A.M. (2007) Advances in enhanced biological phosphorus removal: From micro to macro scale. Water Research 41(11), 2271-2300.

Oehmen, A., Teresa Vives, M., Lu, H., Yuan, Z. and Keller, J. (2005) The effect of pH on the competition between polyphosphate-accumulating organisms and glycogen-accumulating organisms. Water Research 39(15), 3727-3737.

Onnis-Hayden, A., Majed, N., Schramm, A. and Gu, A.Z. (2011) Process optimization by decoupled control of key microbial populations: Distribution of activity and abundance of polyphosphate-accumulating organisms and nitrifying populations in a full-scale IFAS-EBPR plant. Water Research 45(13), 3845-3854.

Pereira, H., Lemos, P.C., Reis, M.A., Crespo, J.P., Carrondo, M.J. and Santos, H. (1996) Model for carbon metabolism in biological phosphorus removal processes based on in vivo13C-NMR labelling experiments. Water Research 30(9), 2128-2138.

Peterson, S.B., Warnecke, F., Madejska, J., McMahon, K.D. and Hugenholtz, P. (2008) Environmental distribution and population biology of Candidatus Accumulibacter, a primary agent of biological phosphorus removal. Environmental microbiology 10(10), 2692-2703.

R Core Team (2019) R: A Language and Environment for Statistical Computing, R Foundation for Statistical Computing, Vienna, Austria.

Romanski, J., Heider, M. and Wiesmann, U. (1997) Kinetics of anaerobic orthophosphate release and substrate uptake in enhanced biological phosphorus removal from synthetic wastewater. Water Research 31(12), 3137-3145.

Rubio-Rincón, F.J., Weissbrodt, D.G., Lopez-Vazquez, C.M., Welles, L., Abbas, B., Albertsen, M., Nielsen, P.H., van Loosdrecht, M.C.M. and Brdjanovic, D. (2019) "Candidatus Accumulibacter delftensis": A clade IC novel polyphosphate-accumulating organism without denitrifying activity on nitrate. Water Research 161, 136-151.

Ruijter, J.M., Ramakers, C., Hoogaars, W.M.H., Karlen, Y., Bakker, O., van den Hoff, M.J.B. and Moorman, A.F.M. (2009) Amplification efficiency: linking baseline and bias in the analysis of quantitative PCR data. Nucleic Acids Research 37(6), e45-e45.

Saad, S.A., Welles, L., Abbas, B., Lopez-Vazquez, C.M., van Loosdrecht, M.C.M. and Brdjanovic, D. (2016) Denitrification of nitrate and nitrite by 'Candidatus Accumulibacter phosphatis' clade IC. Water Research 105, 97-109.

Schindelin, J., Arganda-Carreras, I., Frise, E., Kaynig, V., Longair, M., Pietzsch, T., Preibisch, S., Rueden, C., Saalfeld, S. and Schmid, B. (2012) Fiji: an open-source platform for biological-image analysis. Nature methods 9(7), 676-682.

Schuler, A.J. and Jang, H. (2007) Causes of Variable Biomass Density and Its Effects on Settleability in Full-Scale Biological Wastewater Treatment Systems. Environmental Science & Technology 41(5), 1675-1681.

Schuler, A.J. and Jenkins, D. (2003) Enhanced biological phosphorus removal from wastewater by biomass with different phosphorus contents, part II: Anaerobic adenosine triphosphate utilization and acetate uptake rates. Water Environment Research 75(6), 499-511.

Schuler, A.J. and Xiao, Y. (2008) Predicted Distributed State Effects on Enhanced Biological Phosphorus Removal in a 5-Stage Bardenpho Wastewater Treatment Configuration. Water Environment Research 80(5), 454-463.

Slater, F.R., Johnson, C.R., Blackall, L.L., Beiko, R.G. and Bond, P.L. (2010) Monitoring associations between clade-level variation, overall community structure and ecosystem function in enhanced biological phosphorus removal (EBPR) systems using terminal-restriction fragment length polymorphism (T-RFLP). Water Research 44(17), 4908-4923.

Smolders, G., Van der Meij, J., Van Loosdrecht, M. and Heijnen, J. (1994) Model of the anaerobic metabolism of the biological phosphorus removal process: stoichiometry and pH influence. Biotechnology and Bioengineering 43(6), 461-470.

Vale, P., Barnard, J., Thomas, D. and Dold, P. (2008) RAS Fermentation to Enhance Biological Phosphorus Removal.

van Loosdrecht, M.C., Nielsen, P.H., Lopez-Vazquez, C.M. and Brdjanovic, D. (2016) Experimental methods in wastewater treatment, IWA publishing.

Vollertsen, J., Petersen, G. and Borregaard, V.R. (2006) Hydrolysis and fermentation of activated sludge to enhance biological phosphorus removal. Water Science and Technology 53(12), 55-64.

Wachtmeister, A., Kuba, T., Van Loosdrecht, M.C.M. and Heijnen, J.J. (1997) A sludge characterization assay for aerobic and denitrifying phosphorus removing sludge. Water Research 31(3), 471-478.

Wang, D., Tooker, N.B., Srinivasan, V., Li, G., Fernandez, L.A., Schauer, P., Menniti, A., Maher, C., Bott, C.B., Dombrowski, P., Barnard, J.L., Onnis-Hayden, A. and Gu, A.Z. (2019) Side-stream enhanced biological phosphorus removal (S2EBPR) process improves system performance - A full-scale comparative study. Water Research 167, 115109.

Wei, T.S., Viliam (2017) R package "corrplot": Visualization of a Correlation Matrix.

Welles, L., Tian, W.D., Saad, S., Abbas, B., Lopez-Vazquez, C.M., Hooijmans, C.M., van Loosdrecht, M.C.M. and Brdjanovic, D. (2015) Accumulibacter clades Type I and II performing kinetically different glycogen-accumulating organisms metabolisms for anaerobic substrate uptake. Water Research 83, 354-366.

Wentzel, G., Loewenthal, R. and Ekama, G. (1988) Enhanced polyphosphate organism cultures in activated sludge systems-Part 1: Enhanced culture development. Water SA 14(2), 81-92.

Wentzel, M., Lötter, L., Loewenthal, R. and Marais, G. (1986) Metabolic behaviour of Acinetobacter spp. in enhanced biological phosphorus removal- a biochemical model. Water S. A. 12(4), 209-224.

Whang, L.M. and Park, J.K. (2006) Competition between polyphosphate-and glycogen-accumulating organisms in enhanced-biological-phosphorus-removal systems: Effect of temperature and sludge age. Water Environment Research 78(1), 4-11.

Winkler, M.K.H., Bassin, J.P., Kleerebezem, R., de Bruin, L.M.M., van den Brand, T.P.H. and van Loosdrecht, M.C.M. (2011) Selective sludge removal in a segregated aerobic granular biomass system as a strategy to control PAO–GAO competition at high temperatures. Water Research 45(11), 3291-3299.

Winter, C.T. (1989) The Role of Acetate in Denitrification and Biological Phosphate Removal in Modified Bardenpho Systems. Water Science and Technology 21(4-5), 375-385.

Yu, R.-F., Liaw, S.-L., Chang, C.-N., Lu, H.-J. and Cheng, W.-Y. (1997) Monitoring and control using on-line ORP on the continuous-flow activated sludge batch reactor system. Water Science and Technology 35(1), 57-66.

Yuan, Z., Pratt, S. and Batstone, D.J. (2012) Phosphorus recovery from wastewater through microbial processes. Current Opinion in Biotechnology 23(6), 878-883.

Yun, G., Lee, H., Hong, Y., Kim, S., Daigger, G.T. and Yun, Z. (2019) The difference of morphological characteristics and population structure in PAO and DPAOgranular sludges. Journal of Environmental Sciences 76, 388-402.

Zafiriadis, I., Kapagiannidis, A.G., Ntougias, S. and Aivasidis, A. (2017) Inhibition of the respiratory chain reactions in denitrifying EBPR biomass under simultaneous presence of acetate and electron acceptor. New Biotechnology 36, 42-50.

Zeng, R.J., Lemaire, R., Yuan, Z. and Keller, J. (2003a) Simultaneous nitrification, denitrification, and phosphorus removal in a lab-scale sequencing batch reactor. Biotechnology and Bioengineering 84(2), 170-178.

Zeng, R.J., Yuan, Z. and Keller, J. (2003b) Model-based analysis of anaerobic acetate uptake by a mixed culture of polyphosphate-accumulating and glycogen-accumulating organisms. Biotechnology and Bioengineering 83(3), 293-302.

Zhang, H., Wang, X., Xiao, J., Yang, F. and Zhang, J. (2009) Enhanced biological nutrient removal using MUCT–MBR system. Bioresource Technology 100(3), 1048-1054.

Zhou, Y., Pijuan, M., Zeng, R.J., Lu, H. and Yuan, Z. (2008) Could polyphosphate-accumulating organisms (PAOs) be glycogen-accumulating organisms (GAOs)? Water Research 42(10), 2361-2368.

Appendix A

Normally Distributed operational data and activity test results correlated to SRT of Fermenter. Graphs show normally distributed variables with statistically significant correlation to SRT of the Fermenter.

Type	Variable	Distribution	Correlation Significance
Operational Data	Fermenter VFA (mg/L)	Normal	Significant
Operational Data	Acetic Acid (mg/L)	Normal	Significant
Operational Data	Influent rbCOD (mg/L)	Normal	Significant
Activity Test Data	SOUR Nitrite (mg-g/h)	Normal	Significant
Activity Test Data	SVI 5	Normal	Significant
Activity Test Data	SVI 30	Normal	Significant
Activity Test Data	WW Nitrite Rate	Normal	Significant
Activity Test Data	WW + Fermenter Nitrite Rate	Normal	Significant
Operational Data	Effluent Phosphate (mg/L)	Normal	Not Significant
Activity Test Data	SOUR Endogenous (mg-g/h)	Normal	Not Significant
Activity Test Data	SOUR Ammonia (mg-g/h)	Normal	Not Significant
Activity Test Data	WW Ammonia Rate	Normal	Not Significant
Activity Test Data	WW+ Fermenter Ammonia Rate	Normal	Not Significant
Activity Test Data	P Release (mg-g/h)	Normal	Not Significant
Activity Test Data	P Uptake Aerobic (mg-g/h)	Normal	Not Significant
Activity Test Data	P Uptake NO3 (mg-g/h)	Normal	Not Significant
Operational Data	Fermenter ffCOD (mg/L)	Non-Normal	Not Correlated
Operational Data	Fermenter TSS (mg/L)	Non-Normal	Not Correlated
Operational Data	Influent TP (mg/L)	Non-Normal	Not Correlated
Operational Data	Phosphate Removal (mg/L)	Non-Normal	Not Correlated
Operational Data	Percent P Removal (%)	Non-Normal	Not Correlated
Operational Data	Butyric Acid (mg/L)	Non-Normal	Not Correlated
Operational Data	Isobutyric Acid (mg/L)	Non-Normal	Not Correlated
Operational Data	Isocaleric Acid (mg/L)	Non-Normal	Not Correlated
Operational Data	Propionic Acid (mg/L)	Non-Normal	Not Correlated
Operational Data	Valeric Acid (mg/L)	Non-Normal	Not Correlated
Operational Data	Fermenter rbCOD (mg/L)	Non-Normal	Not Correlated
Operational Data	Influent rbCOD:TP	Non-Normal	Not Correlated
Operational Data	Fermenter rbCOD:TP	Non-Normal	Not Correlated
Activity Test Data	SOUR Acetate (mg-g/h)	Non-Normal	Not Correlated
Activity Test Data	WW Nitrate Rate	Non-Normal	Not Correlated
Activity Test Data	WW+Fermenter Nitrate Rate	Non-Normal	Not Correlated
Activity Test Data	P Uptake NO2 (mg-g/h)	Non-Normal	Not Correlated

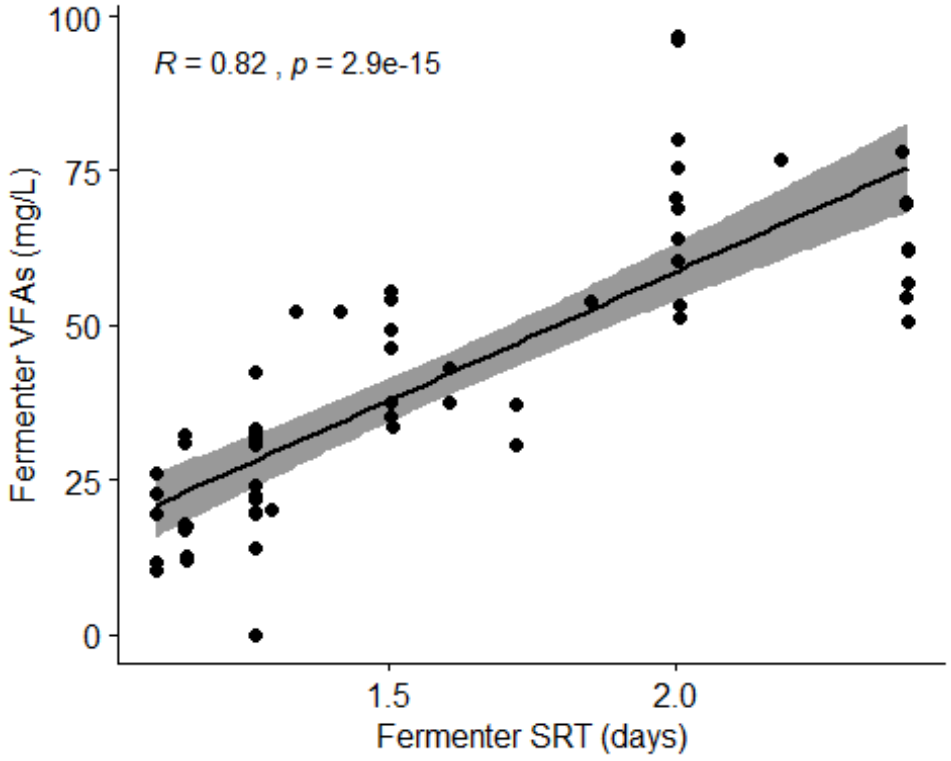
R = 0.82 , p = 2.9e-15
Fermenter VFAs (mg/L)
100
75
50
25
0
1.5
2.0
Fermenter SRT (days)

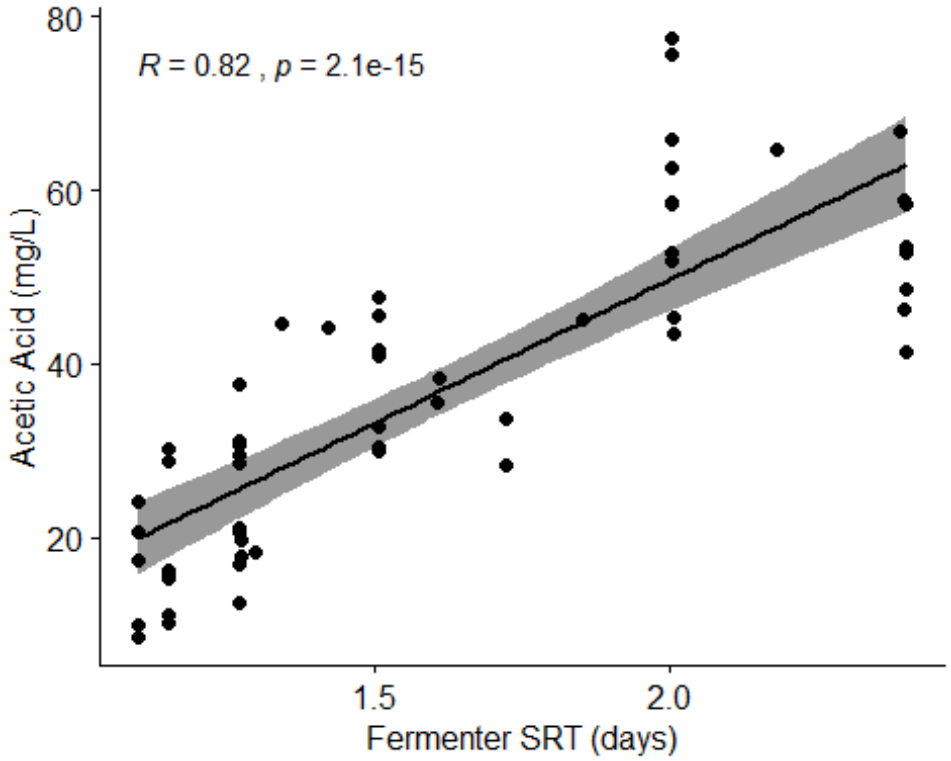
R = 0.82 , p = 2.1e-15
Acetic Acid (mg/L)
80
60
40
20
1.5
2.0
Fermenter SRT (days)

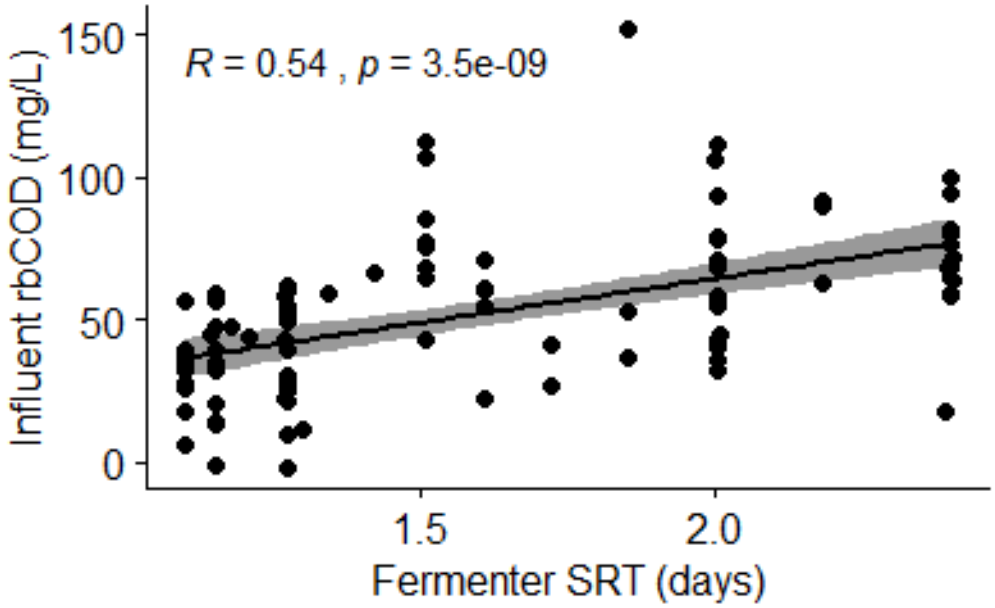
R = 0.54 , p = 3.5e-09
Influent rbCOD (mg/L)
150
100
50
0
1.5
2.0
Fermenter SRT (days)

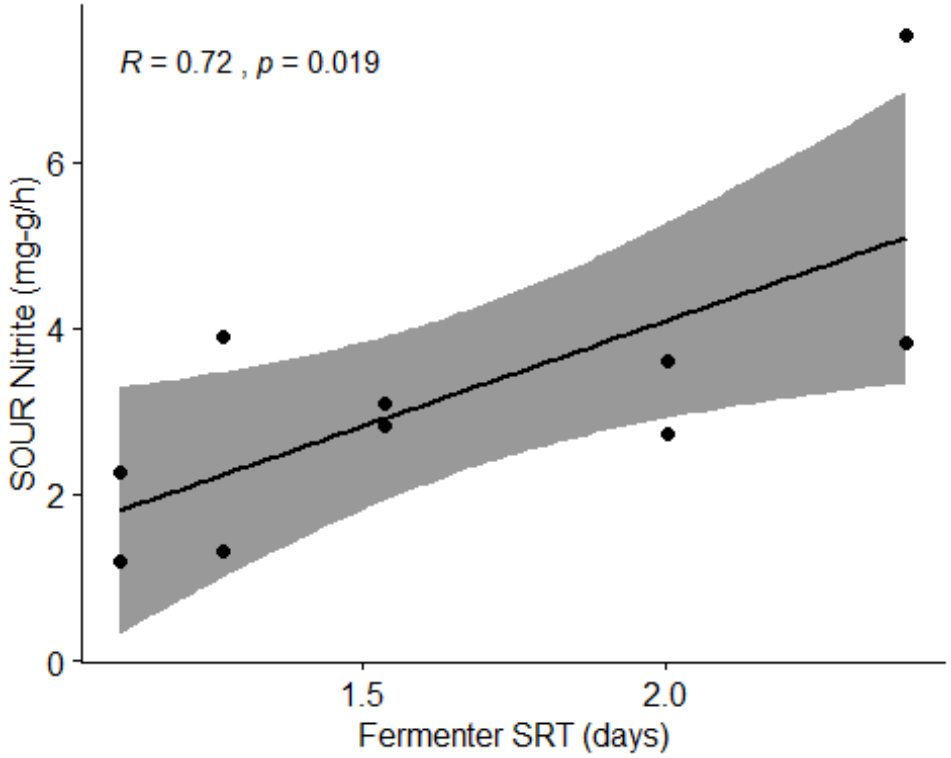
R = 0.72 , p = 0.019
SOUR Nitrite (mg-g/h)
6
4
2
0
1.5
2.0
Fermenter SRT (days)

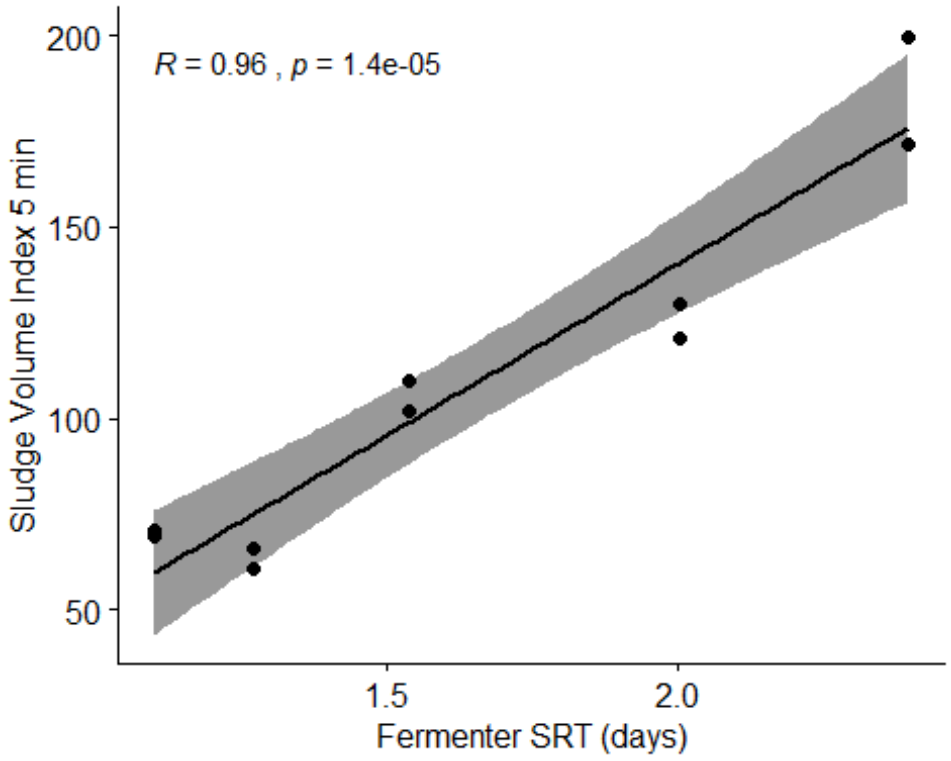
R = 0.96 , p = 1.4e-05
Sludge Volume Index 5 min
200
150
100
50
1.5
2.0
Fermenter SRT (days)

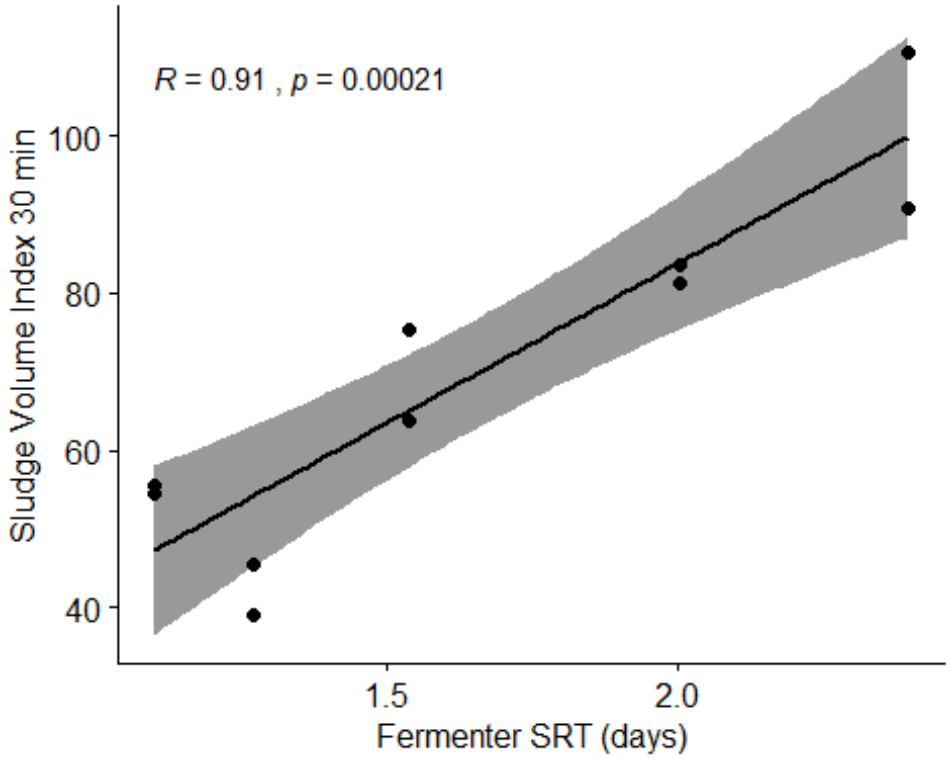
R = 0.91 , p = 0.00021
Sludge Volume Index 30 min
100
80
60
40
1.5
2.0
Fermenter SRT (days)

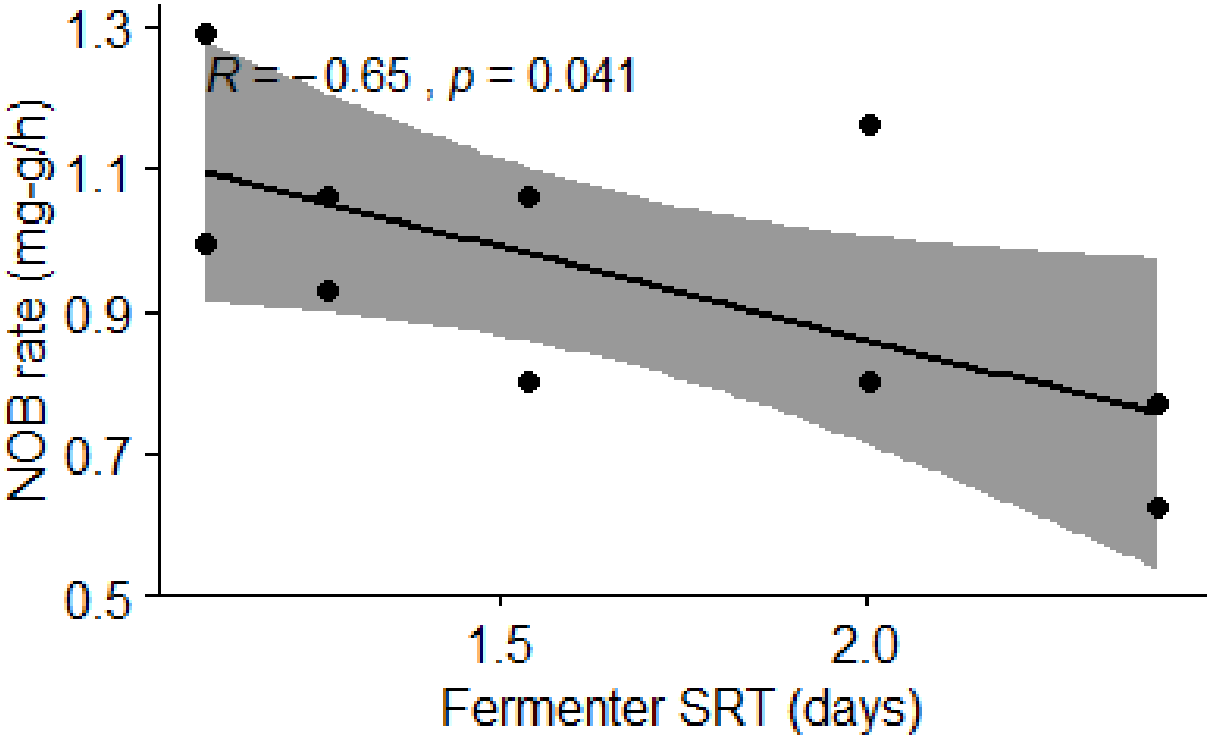
R = −0.65 , p = 0.041
NOB rate (mg-g/h)
1.3
1.1
0.9
0.7
0.5
1.5
2.0
Fermenter SRT (days)

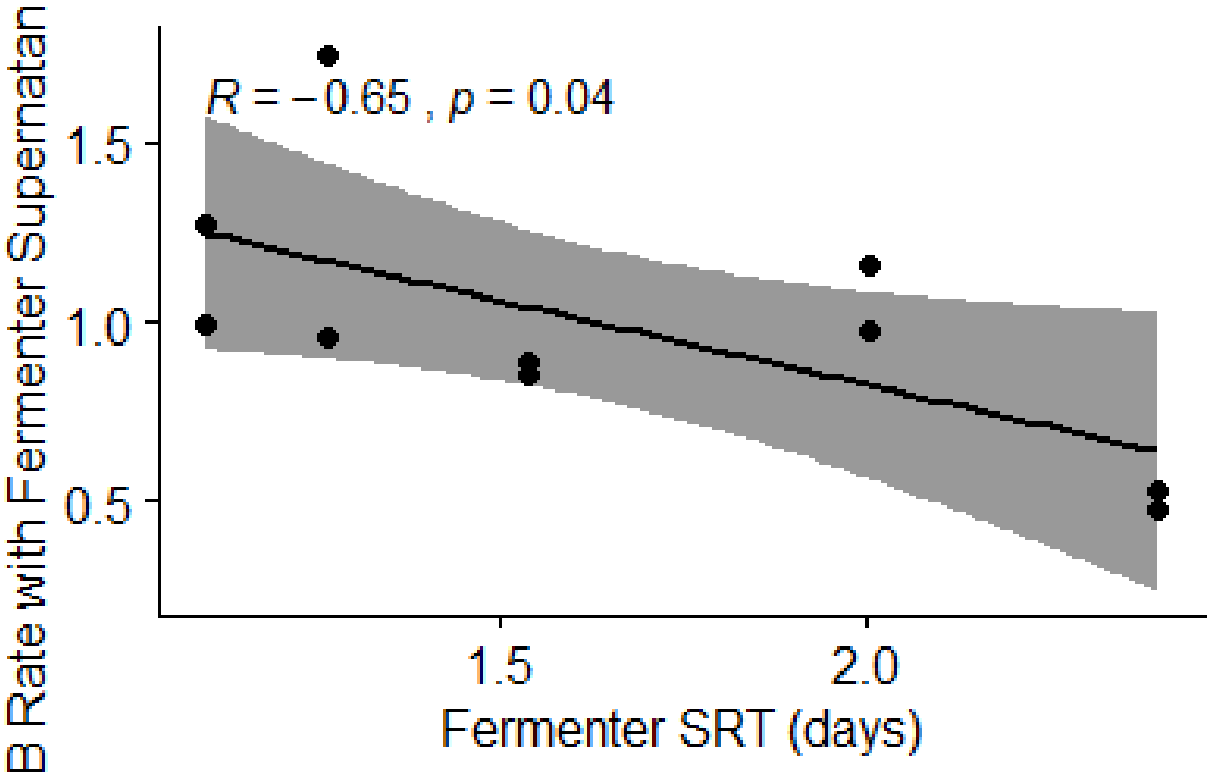
R = −0.65 , p = 0.04
B Rate with Fermenter Supernatan
1.5
1.0
0.5
1.5
2.0
Fermenter SRT (days)

Appendix B.

Table of influent and effluent conditions of the WWTP during this experiment.

Fermenter SRT (Days)	Influent Ammonia (mg/L)	Effluent Ammonia (mg/L)	Influent COD	Influent Total (mg/L)	Effluent COD	Effluent Total (mg/L)	Influent Total N (mg/L)	Effluent Total N (mg/L)	Effluent Nitrate (mg/L)	Effluent Nitrite (mg/L)	Influent Total P (mg/L)	Effluent Total P (mg/L)
1.10	15.54	0.32		261.18		17.09	23.32	7.09	6.10	0.35	3.01	0.07
1.27	17.28	0.01		265.56		21.44	23.34	8.43	8.11	0.03	3.57	0.13
1.54	21.85	0.03		364.23		21.38	26.93	7.94	7.81	0.07	4.66	0.13
2.00	25.33	0.18		370.12		24.00	31.81	10.95	9.99	0.18	4.69	0.12
2.40	29.59	0.26		414.24		26.35	35.69	9.08	8.09	0.48	5.16	0.12